



National Library  
of Canada

Bibliothèque nationale  
du Canada

Canadian Theses Service

Service des thèses canadiennes

Ottawa, Canada  
K1A 0N4

## NOTICE

The quality of this microform is heavily dependent upon the quality of the original thesis submitted for microfilming. Every effort has been made to ensure the highest quality of reproduction possible.

If pages are missing, contact the university which granted the degree.

Some pages may have indistinct print especially if the original pages were typed with a poor typewriter ribbon or if the university sent us an inferior photocopy.

Reproduction in full or in part of this microform is governed by the Canadian Copyright Act, R.S.C. 1970, c. C-30, and subsequent amendments.

## AVIS

La qualité de cette microforme dépend grandement de la qualité de la thèse soumise au microfilmage. Nous avons tout fait pour assurer une qualité supérieure de reproduction.

S'il manque des pages, veuillez communiquer avec l'université qui a conféré le grade.

La qualité d'impression de certaines pages peut laisser à désirer, surtout si les pages originales ont été dactylographiées à l'aide d'un ruban usé ou si l'université nous a fait parvenir une photocopie de qualité inférieure.

La reproduction, même partielle, de cette microforme est soumise à la Loi canadienne sur le droit d'auteur, SRC 1970, c. C-30, et ses amendements subséquents.

THE UNIVERSITY OF ALBERTA

THE GEOLOGY AND GEOCHEMISTRY OF GOLD MINERALIZATION AT  
ATHABASCA PASS, CENTRAL ROCKY MOUNTAINS,  
BRITISH COLUMBIA, CANADA

by

Robert Peter Shaw



A THESIS

SUBMITTED TO THE FACULTY OF GRADUATE STUDIES AND REASERCH  
IN PARTIAL FULFILMENT OF THE REQUIREMENTS FOR THE DEGREE OF  
MASTER OF SCIENCE

DEPARTMENT OF GEOLOGY

EDMONTON, ALBERTA

Spring, 1990



National Library  
of Canada

Bibliothèque nationale  
du Canada

Canadian Theses Service    Service des thèses canadiennes

Ottawa, Canada  
K1A 0N4

## NOTICE

The quality of this microform is heavily dependent upon the quality of the original thesis submitted for microfilming. Every effort has been made to ensure the highest quality of reproduction possible.

If pages are missing, contact the university which granted the degree.

Some pages may have indistinct print especially if the original pages were typed with a poor typewriter ribbon or if the university sent us an inferior photocopy.

Reproduction in full or in part of this microform is governed by the Canadian Copyright Act, R.S.C. 1970, c. C-30, and subsequent amendments.

## AVIS

La qualité de cette microforme dépend grandement de la qualité de la thèse soumise au microfilmage. Nous avons tout fait pour assurer une qualité supérieure de reproduction.

S'il manque des pages, veuillez communiquer avec l'université qui a conféré le grade.

La qualité d'impression de certaines pages peut laisser à désirer, surtout si les pages originales ont été dactylographiées à l'aide d'un ruban usé ou si l'université nous a fait parvenir une photocopie de qualité inférieure.

La reproduction, même partielle, de cette microforme est soumise à la Loi canadienne sur le droit d'auteur, SRC 1970, c. C-30, et ses amendements subséquents.

ISBN 0-315-60304-6

THE UNIVERSITY OF ALBERTA

RELEASE FORM

NAME OF AUTHOR: Robert Peter Shaw

TITLE OF THESIS: THE GEOLOGY AND GEOCHEMISTRY OF GOLD  
MINERALIZATION AT ATHABASCA PASS,  
CENTRAL ROCKY MOUNTAINS, BRITISH  
COLUMBIA, CANADA

DEGREE: MASTER OF SCIENCE

YEAR THIS DEGREE WAS GRANTED: Spring, 1990

Permission is hereby granted to THE UNIVERSITY OF ALBERTA LIBRARY to reproduce single copies of this thesis and to lend or sell such copies for private, scholarly or scientific research purposes only.

The author reserves other publication rights, and neither the thesis nor extensive extracts from it may be printed or otherwise reproduced without the authors written permission.

*RP Shaw*  
.....  
(Student's signature)

*10011-57 Ave*  
.....  
(Permanent address)

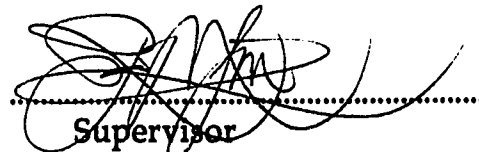
*Edmonton, Alberta*  
.....

*Canada T6E2P1*  
.....

Date: *April 12, 1990*.....

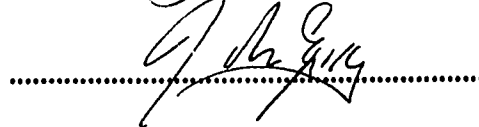
THE UNIVERSITY OF ALBERTA  
FACULTY OF GRADUATE STUDIES AND RESEARCH

The undersigned certify that they have read, and recommend to the faculty of Graduate Studies and Research for acceptance, a thesis entitled THE GEOLOGY AND GEOCHEMISTRY OF GOLD MINERALIZATION AT ATHABASCA PASS, CENTRAL ROCKY MOUNTAINS, BRITISH COLUMBIA, CANADA submitted by ROBERT PETER SHAW in partial fulfilment of the requirements for the degree of MASTER OF SCIENCE.

  
.....  
Supervisor

R. St. Lambert  
.....

RS Johnston  
.....

  
.....

Date: April 17, 1990

**Dedicated to the memory of my Father,**

**Jacob Peter Shaw**

**January 27, 1929 - July 31, 1989**

**to everything there is a season**

## ABSTRACT

Gold-bearing quartz veins were recently discovered within anchimetamorphic quartzite-rudite and pelite sequences of the Lower Cambrian McNaughton Formation at Athabasca Pass, in the Main Ranges of the central Canadian Rocky Mountains, British Columbia. Two vein types occur, namely: an early syn-tectonic, late syn- to post-metamorphic, auriferous, bedding-parallel type, generated during repeated northeast-directed compressive tectonism, and a late, post-penetrative deformational discordant type which contain only minor gold values (<500 ppb Au). Gold emplacement and discordant veining were confined to the onset of late compression leading to thrust faulting. The spatial distribution and dimensions of the veins attest to mechanically-founded lithologic anisotropy. Bedding-parallel veins are confined to pelitic rock types. Discordant veins are confined to competent quartzitic units.

Bedding-parallel vein-filling took place in two paragenetic stages, namely: a protracted, pre-gold stage (quartz  $\pm$  minor white mica and pyrite) depositing over 90 % of vein material, and a late gold-bearing - post-gold stage (quartz-pyrite-gold-galena  $\pm$  white mica and Fe-carbonate). Gold is associated with brecciated pelites and coeval sulfides. Discordant veins (quartz  $\pm$  minor pyrite) record a single stage of vein-filling coeval with gold deposition. Minor hydrothermal alteration (pyrite  $\pm$  white mica  $\pm$  carbonate) of adjacent wallrocks accompanied gold emplacement.

Trace element analysis reveals distinct enrichment of Pb, As, Ba, and Fe, and marginal enrichment of Ag, Zn, and Cu in veins with respect to host rocks. Pb, As, Ba, and Fe show distinct, although non-proportional positive correlation with gold concentration in the lodes, whilst Ag, Zn, and Cu do not. When compared with other lode-gold deposits in similar

domains, the Athabasca Pass lodes are unenriched in all trace elements except gold.

Microthermometric analyses of fluid inclusions indicates gold-stage fluids were aqueous brines containing 2 to 10 wt. % NaCl eq. and up to 12 mole % CO<sub>2</sub> ± CH<sub>4</sub>. Variations in fluid compositional-and total homogenization-data suggest that gradual fluid evolution accompanied gold mineralization. Gold deposition took place at between 275° and 350°C and 900 to ≥ 1200 bars.

Vein pyrite δ<sup>34</sup>S(CDT) values cluster between +14.2 and +16.3 ‰. Coeval galenas exhibit δ<sup>34</sup>S values between +11.4 and +13.3‰. Pyrite-galena geothermometry reveals a mean temperature of mineralization of 300 ± 43°C. Comparison of the δ<sup>34</sup>S values of vein pyrites, with values for pyrite porphyroblasts in the country rocks reveals that vein sulfur was derived from the McNaughton Formation.

δ<sup>18</sup>O(SMOW) values of McNaughton Formation quartzites and pelites cluster between +12.0 and +13.5‰, and +9.5 and +10.5‰, respectively. All quartz veins exhibit δ<sup>18</sup>O values between +13.0 and +15.0‰. Vein inclusion fluids exhibit δD values between -105 and -124‰(SMOW). Combined O-H-isotope data are most compatible with a source fluid involving chemically- and isotopically-evolved meteoric waters. A model involving vein deposition from fluids undergoing post-peak metamorphic cooling is proposed.

The geology and geochemistry of the Athabasca Pass gold-lodes indicates they are siliciclastic-hosted analogues of the Turbidite-Hosted class of gold deposits. Consideration of the processes involved in lode formation at Athabasca Pass suggests that gold-lodes may be more common in the Canadian Rocky Mountains than presently recognized. Some implications for their genesis are discussed.



## ACKNOWLEDGMENTS

Foremost, the advice and friendship of Dr. Roger Morton are gratefully acknowledged. His *renaissance* approach and undaunted optimism have helped make production of this thesis a solid and enjoyable learning experience.

Others of the academic staff, notably Drs. R.St.J. Lambert, D.G.W. Smith, H.A.K. Charlesworth, A. Changkakoti, and B.E. Nesbitt, and my thesis committee, Drs. R.E. Folinsbee, J. Gray, and R.St.J. Lambert have provided much in the way of fundamentals, discussion, and inspiration throughout my undergraduate and graduate terms.

H.A.K. Charlesworth, A. LaRiviere, and P. Erdmer are thanked for discussions and insight into computer-based structural analytical techniques. As well, Drs. J. Gray (Department. of Physics), R. Krouse (University of Calgary), and K.Muehlenbachshave provided lab access and expertise in the field of stable isotope geochemistry.

All of my fellow students have provided much in the way of companionship. Thanks for being so patient. Technical input from Felipe Ortigoza-Cruz, Pierre Maheux, Dr. J.V. Gregory Lynch, Al LaRiviere, Heather Plint, Ralph Rushton, and Jim Steer is further acknowledged.

Services rendered by technicians Dragan Kristic, Olga Levner, Len Tober (Physics isotopes), Peter Black (Thin section lab), and Frank Dimitrov (Geology graphics) have greatly facilitated research and enhanced this thesis.

Finally, special thanks are extended to Henry Mah and Gamsan Resources Ltd. (Edmonton) for financial support, field-season funding, and unlimited access to their computer and printing facilities. Edith Hutchinson typed much of the original manuscript. Field assistance from, casual conversations with, and burdens borne in the company of, Kevin Aronyk, Peter Kleespies, Tim Paquin, and the Gamsan Crew will not be forgotten.

## TABLE OF CONTENTS

CHAPTER	PAGE
<b>1 General Introduction.....</b>	<b>1</b>
<b>2 Gold Mineralization in Lower Cambrian McNaughton Formation, Athabasca Pass, Central Canadian Rocky Mountains: Structural, Mineralogical, and Temporal Relationships.....</b>	<b>3</b>
Introduction.....	3
Previous Work.....	3
Regional Geology.....	5
Local Geology.....	6
Host Rock Petrography.....	8
Structural Geology.....	9
The Quartz Veins of McGillivray Ridge.....	12
Vein Petrography and Host Rock Alteration.....	17
Deposit Classification.....	27
Concluding Statement.....	28
References.....	44
<b>3 Siliciclastic-Hosted Lode Gold Mineralization, Athabasca Pass, Central Canadian Rocky Mountains: A Trace Element and Fluid Inclusion Study.....</b>	<b>51</b>
Introduction.....	51
Regional Setting.....	51
Local Geology.....	53
Trace Element Lithogeochemistry.....	55
Fluid Inclusion Study.....	61
Discussion.....	78

Concluding Statement.....	80
References.....	91
<b>4 Origins of Metamorphogenic Lode Gold Deposits: Implications of Stable Isotope Data from the Central Rocky Mountains, Canada.....</b>	<b>99</b>
Introduction.....	99
Gold-Bearing Veins of the Athabasca Pass.....	100
Stable Isotope (S-O-H) Study.....	102
<i>Sulfur isotope study</i> .....	103
<i>Oxygen isotope study</i> .....	106
<i>Hydrogen isotope study</i> .....	109
<i>Evolution of the hydrothermal fluids</i> .....	112
Implications for Metamorphogenic Lode Gold Deposits.....	113
Concluding Statement.....	115
References.....	120
<b>5. Concluding Statement.....</b>	<b>125</b>
<b>Appendix 1. ICPES Trace Element Data.....</b>	<b>128</b>
<b>Appendix 2. Instrumental Neutron Activation Analysis Data.....</b>	<b>129</b>
<b>Appendix 3. Background Gold in the McNaughton Formation Survey.</b>	<b>130</b>
<b>Appendix 4. Type A Fluid Inclusion Data.....</b>	<b>132</b>
<b>Appendix 5 Sulfur Isotope <math>\delta^{34}\text{S}</math> Analysis Data.....</b>	<b>134</b>
<b>Appendix 6. Formulae Used for Fluid Inclusion and Stable Isotope Calculations.....</b>	<b>136</b>

## LIST OF TABLES

TABLE		PAGE
2-1	Comparison Between Athabasca Pass and Typical Turbidite Hosted Lode Gold Deposits.....	30
3-1	CO <sub>2</sub> Content and Trapping Pressure Estimates for Type B2 Fluid Inclusions.....	82
3-2	Fluid Characteristics Comparison Between the Athabasca Pass vs. Turbidite Hosted Gold Deposits..	83
4-1	Oxygen and Hydrogen Isotope Data from the Athabasca Pass.....	116

## LIST OF FIGURES

FIGURE		PAGE
2-1	Location of the Athabasca Pass.....	31
2-2	Regional Geology Surrounding Athabasca Pass.....	32
2-3	Local Geology of the Athabasca Pass Area.....	33
2-4	Photograph of the Athabasca Pass.....	34
2-5	Modal Composition of the McNaughton Formation.	35
2-6	Deformational Microstructures and Alteration in McNaughton Formation Rock Types.....	36
2-7	Photograph of the South End of McGillivray Ridge...	37
2-8	Folds in the McNaughton Formation.....	37
2-9	Illustration of Vein Structural Relationships.....	38
2-10	Contoured Lower Hemisphere Stereographic Probability Diagrams.....	39
2-11	Mineralogy and Paragenetic Sequence for the Bedding-Parallel Veins of McGillivray Ridge.....	40
2-12	Textures Exhibited by Bedding-Parallel Vein from McGillivray Ridge.....	41
2-13	Microtextures exhibited by quartz in the Bedding-Parallel of Veins McGillivray Ridge.....	42
2-14	Textural relationships among the Minerals from Bedding-Parallel Veins of McGillivray Ridge.....	43
3-1	Location and General Geology of the Athabasca Pass...	84
3-2	Selected Trace Element Data for the Athabasca Pass and Comparable Rock Types.....	85
3-3	Trace Element Variations in Bedding-Parallel Veins...	86

3-4	Scatter Plot Illustrating Gold-Silver Correlation.....	87
3-5	Photographs of Type B Fluid Inclusions in Quartz...	88
3-6	Microthermometric Data for Type B1 H <sub>2</sub> O-NaCl- Bearing Fluid Inclusions.....	89
3-7	Microthermometric Data for Type B1 H <sub>2</sub> O-NaCl- CO <sub>2</sub> ± CH <sub>4</sub> -Bearing Fluid Inclusions.....	90
4-1	Location and Geology of the Athabasca Pass.....	117
4-2	Distribution of δ <sup>34</sup> S Values at Athabasca Pass.....	118
4-3	δH Versus δ <sup>18</sup> O of the Hydrothermal Fluids at Athabasca Pass.....	119

# CHAPTER 1

## General Introduction

Gold occurrences in the Rocky Mountains of Alberta and British Columbia, either lode or placer, are rare. The few documentations, (dominantly of placer occurrences) are buried within pre-1960 discussions of regional history, or broad overviews of regional geology, and provide little detail as to the nature and origin of the gold occurrences. Much of this nonchalance regarding the gold of this region likely stems from the concepts and priorities of nineteenth century prospectors who traditionally sought rich, easily-extractable placers (such as the interiors of British Columbia and Yukon Territory offered), or igneous - lode associations, a geologic improbability in the vast sequences of sedimentary rock types dominating the Canadian Rocky Mountains. Prospecting was likely further deterred by the rugged terrain, poor accessibility, abundant glacial overburden, short working season, and lack of placer indicators characteristic of the Rocky Mountains. The lack of detailed geological mapping throughout much of the western ranges has only served to prolong these erroneous beliefs. In August of 1986 however, a series of auriferous quartz lodes hosted by low-grade meta-sedimentary rocks of Early Cambrian age, were discovered at Athabasca Pass, in the Main Ranges of the Canadian Rocky Mountains, British Columbia. The principle objective of this thesis is to provide detailed documentation of aspects of the geology and geochemistry of these gold occurrences.

This thesis is presented in "paper format," formally represented herein by Chapters 2, 3, and 4. Chapter 2 documents the physical

relationships of the gold occurrences utilizing traditional field-mapping and petrographic techniques and establishes the structural, mineralogical and temporal relationships of the gold-bearing lodes to their geological surroundings. Chapters 3 and 4 explore the geochemistry of the auriferous veins and their host strata, utilizing trace element, fluid inclusion (Chapter 3), and stable isotope (Chapter 4) analyses. As well, Chapter 4 considers some broader implications for the genesis of mesothermal gold-quartz veins in lithosedimentary domains. Some general implications regarding gold in the Rocky Mountains comprise the concluding statement (Chapter 5).

The Athabasca Pass gold occurrences are not, at present, economically viable mining entities. Their study however is warranted, from both an academic perspective, in terms of their applicability to the understanding of lode-gold genesis in low-grade meta-sedimentary domains, and from an economic perspective in view of exploration modelling for geologically similar, economically extractable deposits in the Canadian Rocky Mountains.



## **CHAPTER 2**

# **Gold Mineralization in Lower Cambrian McNaughton Formation, Athabasca Pass, Canadian Rocky Mountains: Structural, Mineralogical, and Temporal Relationships.**

### **Introduction**

The Athabasca Pass is located on the continental divide, 60 km south-southwest of Jasper, Alberta, in the northern Park Ranges of the central Canadian Rocky Mountains (Figs. 2-1 and 2-2). The pass was pioneered in the early 1800's by David Thompson, as an alternate route through the Main Ranges to the Columbia River. A trading post was established near the Committee Punch Bowl, but the route fell into disuse by the middle of the nineteenth century. The area has no recorded history of exploration or mining. This paper describes gold-bearing quartz veins which occur in quartzose clastic rocks of the Lower Cambrian Gog Group of the Athabasca Pass.

Little information regarding the geology of the Athabasca Pass has been published. Thus preliminary documentation of the general stratigraphy, lithology, and structure in the area exhibiting gold-quartz mineralization is provided. The map presented here utilizes information gathered through personal communications with E.W. Mountjoy and co-workers, unpublished Operation Bow-Athabasca data (Price and Mountjoy, 1966; Mountjoy and Price, in preparation), and field-mapping carried out by the author during 1987 and 1988.

### **Previous Work**

Geologic studies pertaining to the Athabasca Pass are few and of

regional scope. Recent studies include reconnaissance mapping at 1:250,000 scale by Campbell (1968) and at 1:50,000 scale by Price and Mountjoy (1970). The latter, a product of Operation Bow-Athabasca, includes a 1:50,000 scale map sheet corresponding to the NTS 83D/8 (Athabasca Pass) map sheet, which has yet to be published (Mountjoy and Price in preparation). More detailed documentation of the surrounding region include studies of structure, stratigraphy and metamorphism to the west and southwest of the Athabasca Pass by Craw (1978) and Klein and Mountjoy (1988), and to the north and northwest of the Athabasca Pass by Mountjoy and Price (1985; 1989), Mountjoy and Forest (1986), Leonard (1985), Oke (1982), and McDonough and Simony (1988).

Information on lode gold deposits within the Main Ranges and indeed, over the entire central Canadian Rocky Mountains is sparse. Sorensen (1955) notes the occurrence of auriferous quartz veins in Precambrian Miette "formation" near Tete Jaune Cache, however provides no details. All other recorded lode gold occurrences in this region are located west of the Rocky Mountain Trench. Reviews of mineral occurrences in the Main Ranges of the Rocky Mountains were given by Hedley (1954) and Little *et al.* (1976). Summaries of the nature and distribution of lode gold deposits in southeastern British Columbia in the vicinity of the Rocky Mountain Trench were published by Mathews (1944), Holland (1944), Sinclair *et al.* (1978), and Schroeter and Panteleyev (1986).

The occurrence of gold placers in the valleys of the central Rockies and contiguous foothills of Alberta has received only cursory attention in the literature. Brief mention of placer gold near the headwaters of the Fraser River was made by Sorensen (1955) and Boyle (1979), and in the Fort Steel

and Ptarmigan Creek regions by Mathews (1944). The distribution of placer gold in Alberta rivers draining the Rocky Mountains was reviewed by Giusti (1983).

### Regional Geology

The Athabasca Pass lies at the boundary between the eastern Main Ranges and western Main Ranges of the central Rocky Mountains (Price and Mountjoy, 1970). The boundary at this latitude is marked by a southwest-dipping thrust fault, the Chatter Creek fault (Figs. 2-2 and 2-3; Wheeler, 1963; Wheeler *et al.*, 1972), which extends from north of the headwaters of the Fraser River (Price and Mountjoy, 1966; Mountjoy and Price, 1989), southeasterly through the study area, to the northwest of Golden. Southwest of the Athabasca Pass, the hanging wall of the Chatter Creek fault is composed of grits, pelites, psammites and carbonates of the Hadrynian Miette Group, overlain by Lower Cambrian clastic rocks of the Gog Group and, near the Rocky Mountain Trench, by un-named pelites and carbonates of Middle Cambrian age (Price and Mountjoy, 1970). This region is dominated by broad open folds comprising the Baker Glacier Syncline and Porcupine Creek Anticlinorium (Price and Mountjoy, 1970; Balkwill, 1968; Klein and Mountjoy, 1988). Northwest of the Athabasca Pass, across the head of Hugh Allan Creek, the Chatter Creek thrust sheet contains another major antiformal structure, the Fraser River Antiform (Mountjoy and Forest, 1986). Within the Chatter Creek thrust sheet, metamorphic grade increases westward from greenschist grade to kyanite-staurolite-bearing assemblages of amphibolite grade (Craw, 1978; Leonard, 1985; Klein and Mountjoy, 1988). The Purcell thrust and associated structures (Price and Mountjoy, 1970) form

the western boundary of the Chatter Creek thrust sheet.

The footwall of the Chatter Creek fault, to the north and east of the Athabasca Pass is composed of Lower Cambrian Gog Group, overlain by a series of thickly-bedded, dominantly carbonate rocks, of Middle Cambrian age. The structure of this eastern sector of the Main Ranges consists of thick, relatively flat, thrust sheets with characteristically broad, open folds (Price and Mountjoy, 1970; Mountjoy and Price, 1989). Local structural complications occur along the transition between the eastern and western Main Ranges (Wheeler, 1963; Cook, 1975). Rocks of the eastern Main Ranges have been regionally metamorphosed to pumpellyite and lower greenschist grades (Read, 1988).

### Local Geology

The geology of the Athabasca Pass area is illustrated in Figures 2-3 and 2-4. To date, gold-bearing quartz veins have been found only in the lowermost formation of the Gog Group, the McNaughton.

#### *The McNaughton Formation*

The McNaughton Formation comprises a variety of mature, quartz-dominated clastic rocks of sub-greenschist metamorphic grade. The predominant rock type is a medium- to coarse-grained, moderately- to poorly-sorted, pale weathering, grey quartzite. This quartzite contains a variable amount of pelitic material, 5-10 % on average, although units grading to quartzitic pelite and pelite are not uncommon. Generally well-stratified, quartzites form sequences of 0.1 to 3 m thick beds randomly parted with pelite horizons. Most of the quartzite beds are tabular although gently undulatory and wedge-shaped beds are also present. Feldspar content is low,

generally less than 3 %. Both phyllosilicate and feldspar content are highest in the lower exposed portions of the section.

Minor conglomerate occurs as the basal portion of graded beds or as lenticular beds up to 0.3 m in thickness. Conglomerates are generally matrix supported. Subequal amounts of well rounded quartzite and vein quartz clasts, ranging up to 25 mm in greatest dimension, are contained within a poorly sorted matrix of medium to fine quartz sand and phyllosilicates, cemented by silica. Phyllosilicates average 25 % of the matrix.

Pelites comprise approximately 2-3 % of the McNaughton Formation occurring primarily as discrete, discontinuous, 5 cm to 1 m interbeds in the quartzites, or commonly, at the top of normally graded sequences. They consist almost entirely of fine-grained white micas with variable quantities of granule- to sand-sized detrital quartz grains and are generally pale green in colour. The pelites commonly contain up to 3 % very finely disseminated pyrite.

Paleoenvironmental interpretations of the McNaughton Formation include a tidally-dominated association of shallow marine shelf environments in the eastern Main Ranges (Palonen, 1976; Hein, 1984; Woberg, 1986), and fluvial braidplain to tidal complex transitions in more westerly outcrops (Young, 1979). Paleocurrent studies by Mountjoy and Aitken (1963) indicate a predominantly westward and southwestward transport of sediments, the inferred source area being the high-grade metamorphic and igneous rocks of the North American craton, with a possible minor contribution reworked from earlier-deposited sandstones (Young, 1979).

### Host-Rock Petrography

Petrographic investigation of various McNaughton rock types has been undertaken by Akehurst (1964), Palonen (1976), and Young (1979).

#### *Mineralogy*

The mineralogy of the McNaughton rock types consists of three components; quartz, white mica and, potash feldspar. The modal abundance of these components in over 90 hand specimens from the Athabasca Pass is plotted in the form of a ternary diagram (Fig. 2-5). Modal composition ranges from quartzitic pelite to feldspathic quartzite. Pelitic quartzite containing 5-10 % white mica is the most common rock type. The occurrence of white mica is variable but ubiquitous. K-feldspar content is erratic with 15-20 % feldspar recorded in some horizons, but less than 3 % being more typical. Varietal minerals are rare. Those observed in thin section include epidote, rutile, zircon, augite, and muscovite. Anhedral to euhedral porphyroblasts of pyrite are common in the more pelitic McNaughton rock types, where they may comprise up to 3 % of individual horizons. Minor (<2%) recrystallized carbonate is widespread, as is the incipient replacement of K-feldspar by white mica  $\pm$  carbonate (Fig. 2-6C).

#### *Deformation - metamorphism*

Microstructures observed in quartz grains are dominantly pressure solution features including grain-to-grain contact suturing, marked grain serration and embayment, and stylolite development (Figs. 2-6A, 2-6B). Undulatory extinction is variably developed, being pervasive in grain

supported quartzites but less distinct in matrix supported pelitic quartzites. The apparent lack of microscale sinks for pressure solution-derived quartz, such as quartz overgrowths and pressure shadows, is noteworthy.

White mica in the McNaughton rock types probably represents recrystallization, during low-grade regional metamorphism or deformation, of an originally allogenic clay component. Foliation defined by these micas becomes discernable as phyllosilicate contents reach 20 to 30 %. Individual phyllosilicate crystals average 0.05 mm in length, becoming coarser along solution contacts between quartz grains, within quartz grain embayments, and along stylolitic partings. The pyrite porphyroblasts and recrystallized carbonate noted earlier are also considered the products of regional metamorphism. Read (1988) infers McNaughton strata in the Athabasca Pass have been subjected to pumpellyite to lower-most greenschist facies regional metamorphism. An anchimetamorphic (*ca.* pumpellyite facies) regime is implied by the assemblage quartz-white mica  $\pm$  pyrite  $\pm$  carbonate (Frey and Kisch, 1987; Frey, 1987), and by the deformational microstructures (Kerrich, 1977; Beach, 1979) outlined above.

### Structural Geology

The Chatter Creek fault and northeast-verging folds dominate the geologic structure of the Athabasca Pass. The trace of the Chatter Creek fault is not exposed in the study area. The nature and geometry of this fault is not fully understood (Mountjoy and Forest, 1986; Dechesne and Mountjoy, 1988). Recent interpretations (Dechesne and Mountjoy, 1988; Mountjoy pers. comm. 1989) indicate it might be a steeply dipping, late (out-of-sequence) thrust. This conclusion was implied by earlier mapping to the south, in the

area northeast of Golden (Cook 1975). Displacement on the fault is considered to be about 3 to 4 km, and was possibly related to late movement on the Hugh Allen (Purcell) thrust (Mountjoy, 1988).

Mountjoy (1989, personal communication) indicates that at least four discrete phases of regional deformation are recorded in the Main Ranges. Extensive, premetamorphic thrust sheets which underlie the western and eastern Main Ranges formed first (Mountjoy and Dechesne, unpublished data). These structures were later folded in regional-scale antiformal culminations such as the synmetamorphic Porcupine Creek Anticlinorium and the post-metamorphic Fraser River Antiform. Out-of-sequence thrusts, including the Chatter Creek fault, post-date these structures.

#### *The structure of McGillivray Ridge*

The eastern wall of the Athabasca Pass, known as McGillivray Ridge (NTS 83 D/8; Figs. 2-3, 2-4 and 2-7 in this study) consists of about 800 m of folded and faulted McNaughton Formation. Two sets of structures, imbricate thrust faults and mesoscopic folds, are clearly exposed on the southern-most precipice of this ridge (Figs. 2-7, 2-8). Northeast-verging imbricates of McNaughton quartzite are thrust over upper Gog Group and Middle Cambrian strata along a lower-most, northeast-verging footwall splay off the Chatter Creek fault. This detachment has been mapped to the north through the Fraser Pass by Mountjoy and Price (1989) where it duplicates McNaughton strata, and is herein termed the McGillivray Fault (Figs. 2-2, 2-3, 2-4, and 2-7). A quartz-rich mylonite up to 2 m thick is associated with this sole thrust at the base of McGillivray Ridge. The thrust dips approximately 20° southwest, striking about 145° east of north. The imbricate thrusts are of similar strike, but dip more steeply (25° to 30°) and are listric in nature,



converging asymptotically with the McGillivray Fault. The structural geometry of McGillivray Ridge is that of a leading imbricate fan (Boyer and Elliott, 1982).

Tight to isoclinal, overturned mesoscopic folds (informally referred to herein as f1) occur within the imbricate quartzite slices (Fig. 2-8). These folds are northeast-verging with axial planes that dip moderately to steeply to the southwest and fold axes which trend  $140^{\circ}$  to  $150^{\circ}$ , plunging gently to the southeast. In some instances overturned fold limbs are markedly thinned and incipient planes of detachment occur parallel to the local imbricate thrust faults (Fig. 2-8). Penetrative planar fabric is weakly developed in the more pelitic quartzites, but occurrences of intact pelite contain a southwest dipping, locally crenulated, axial planar cleavage (informally referred to herein as s1). The sparsity of crenulation development suggests s1 does not overprint a previous tectonic fabric. Crenulation is considered to be the result of the folding of a variably developed, burial-enhanced, bedding-parallel schistosity. f1 folds are truncated by the imbricate faults, and are cut by late sets of conjugate shear and AC joints (Hobbs *et al.*, 1976) which are probably related to thrust faulting. f1-style folding is not seen elsewhere in the Athabasca Pass.

Correlation of fold and thrust structures on McGillivray Ridge with the deformational phases of Mountjoy (1989, personal communication) is inhibited by a lack of detailed mapping in the region surrounding the Athabasca Pass. Imbricate faulting truncates, and therefore post-dates, folding on McGillivray Ridge. These faults are not deformed nor do they appear to reactivate earlier structures. Thus they probably formed during development of the Chatter Creek fault. Folding in the McNaughton is of uncertain age

and may be related to any of the four regional events. However, elsewhere in the Main Ranges folds associated with early, premetamorphic thrusting are confined to the vicinity of early thrusts ( Mountjoy and Forest, 1986; Klein and Mountjoy, 1988; Dechesne and Mountjoy, 1988), none of which outcrop in the Athabasca Pass (Mountjoy and Price in preparation). As well, folds associated with regional syn- and post-metamorphic antiformal culminations are described as generally macroscopic, upright, and open to gentle, with associated axial planar crenulation cleavages ( Mountjoy and Forest, 1986; Klein and Mountjoy, 1988), and are thus distinctly different from those on McGillivray Ridge. Folding during development of the Chatter Creek thrust and its associated footwall imbricates is suggested by the colinear nature of the McGillivray folds and thrusts, the incipient detachment of fold limbs parallel to thrust faults, the lack of similar fold styles elsewhere in the Athabasca Pass, and the apparent lack of penetrative fabric development prior to s1. The McGillivray folds may however record later tightening and overturning of earlier phase folds. Thus, although the initiation of these folds during earlier regional thrust or antiformal development cannot be precluded entirely, much of their development, and present geometry, is probably attributable to deformation leading to development of the Chatter Creek thrust.

### **Quartz Veins of McGillivray Ridge**

Gold-quartz mineralization outcropping on the southwest slope of McGillivray Ridge is contained in a series of discrete vein structures confined to quartzites ± pelites of the McNaughton Formation. The quartzites appear unaltered on the mesoscopic scale and apparently contain

no disseminated epigenetic gold mineralization. To date over 20 veins have produced anomalous gold values. Distribution of gold within individual veins is highly erratic, grading locally from nil to over 500 g Au/tonne with visible gold observed in many cases. Channel sampling across some veins has yielded grades of between 10 and 15 g Au/tonne.

#### *Vein type, morphology and distribution*

Two categories of quartz veins are recognized on McGillivray Ridge; veins which parallel bedding planes within the McNaughton Formation, and veins which are discordant to sedimentary layering (Fig. 2-9). Only bedding-parallel veins contain high-grade gold mineralization; the discordant variety have yielded values up to *ca.* 500 ppb gold.

#### *Bedding-parallel veins*

Bedding-parallel veins vary from about 1 m in length and a few centimeters in thickness up to 50 m in length, varying between 0.7 and 1 m in thickness. They weather recessively, and locally exhibit surficial gossan due to the oxidation of pyrite. Their lateral extent is presently unknown. Inspection of bedding-parallel veins indicates that, in all cases, these structures invade bedded pelites, the remnants of which are generally seen as angular, brecciated fragments within the veins. In most cases the pelites have been entirely disrupted by veining, creating a vein-quartz supported, pelite breccia. Thus these veins essentially parallel the pelite horizons they have invaded. Vein size and distribution was fundamentally controlled by the geometry and distribution of the original pelite layers in the McNaughton Formation.

Lateral lithologic variation within pelites also appears to have exerted control on the localization and extent of bedding-parallel veining. This is suggested where individual quartz veins die out along strike, coincident with an increase in detrital quartz in the associated pelite horizon. Veining may reappear further along strike as the horizon again becomes more pelitic. Veining is not developed in horizons containing greater than approximately 30 % detrital quartz. Pelite fragments in veins generally contain less than 10 % quartz grains.

#### *Discordant veins*

Discordant veins are confined to the competent quartzitic rock types of the McNaughton Formation. Their occurrence is widespread, either as individual isolated veins, *en echelon* vein arrays, or as clustered vein stockworks which extend discontinuously for tens of meters. Individual veins are generally planar to sigmoidal in shape and range in size from centimeter-scale fracture fills to veins 3 m in length and 10 cm in thickness.

The relationships between bedding-parallel and discordant veins are illustrated in Fig. 2-9. Where the two vein systems are in contact, discordant veins usually appear as planar to sigmoidal *en echelon* vein arrays, obliquely intersecting bedding-parallel structures. They cut into, but do not offset or truncate bedding-parallel structures, nor are they truncated by them. Zones of abundant bedding-parallel veining are usually coincident with zones containing greater numbers of discordant veins.

#### *Structural geometry and evolution of the veins*

Contoured lower hemisphere stereographic probability diagrams (Fig. 2-10) project poles to both bedding-parallel and discordant vein structures, in

relation to fold axial planes and associated thrust faults on McGillivray Ridge. Orientation data were processed using the FORTRAN 77 program ORIENT (Charlesworth *et al.*, 1989). The probability method of contour estimation has been discussed by Ramsden and Cruden (1979). Regarding these cumulative data, the following deficiencies are noted: The dominant population of northeasterly dip measurements for bedding-parallel veins is considered to be biased because the complimentary southwest-dipping limbs of mesoscopic folds on McGillivray Ridge have mostly been removed by erosion. As well, although numerous mesoscopic folds are seen in outcrop (Fig. 2-8), they are generally inaccessible to physical measurement, thus the quantity of data is limited and the overall uncertainty may be high. Despite these limitations, the geometric relationships between folding, thrusting and veining (Fig. 2-10) are considered to be representative.

#### *Bedding-parallel veins*

The distribution of poles to bedding-parallel veins (Fig. 2-10A) is essentially that of a "half" girdle reflecting the paucity of southwest-dipping fold limb data. Nevertheless, the folded geometry of the bedding-parallel veins is clearly demonstrated (Ragan, 1973) implying that bedding-parallel veining was initiated prior to, or early in, the progression of folding and thrusting on McGillivray Ridge.

Hydraulic-enhanced fracturing may be advocated to explain bedding-parallel vein formation during regional tectonic compression (Secor, 1965; Hobbs *et al.*, 1976; Fyfe *et al.*, 1978; Etheridge *et al.*, 1984). In general, under passive conditions, the greatest effective principle stress ( $\sigma_1$ ) is compressive, being approximately normal to the earth's surface. As tectonic compression

progresses  $\sigma_1$  becomes essentially horizontal and thus approximately parallel to yet-undeformed bedding. The least effective principle stress ( $\sigma_3$ , also compressive) becomes approximately vertical (*i.e.* normal to the earth's surface), and varies as a function of the bulk density of the overlying fluid-saturated lithology, the acceleration due to gravity, the depth of overburden, and the ratio of pore fluid pressure to lithostatic pressure (Hubbert and Rubey, 1959; Secor, 1965). Should pore fluid pressures become sufficiently high,  $\sigma_3$  will become tensile, and horizontal, bedding-parallel, extensional fracturing and vein filling can occur. Comparable hydraulic fracture mechanisms have often been advocated in the genesis of vein-type gold deposits, particularly of the syntectonic-metamorphic (Cox *et al.*, 1986), and turbidite-hosted (Keppie *et al.*, 1986) varieties (*e.g.* Henley *et al.*, 1976; Kerrich and Allison, 1978; Graves and Zentilli, 1982; Goldfarb *et al.*, 1986; Mawer, 1986). Hydraulic fracturing within the pelite horizons of the McNaughton Formation would be favoured because these rock types form the least competent constituents in the thick, quartzite-dominated sequence. Pelite competency would be reduced by the bedding-parallel fissility and relatively higher pore-fluid pressures characteristic of pelitic rock types under low-grade metamorphic conditions (Fyfe *et al.*, 1978; Murrell, 1985).

It is not possible to fully constrain the timing of bedding-parallel veining in the Athabasca Pass. The veins are folded, and must therefore pre-date or coincide with local folding (f1). As shown, much of this folding is Chatter Creek thrust-associated. However, vein initiation during earlier, regional premetamorphic thrusting, or the development of regional antiformal culminations cannot be precluded, and rather is suggested by vein textures and mineralogy (reviewed below) indicating multiple episodes

of vein reopening and deformation, and syn- to post-peak metamorphic vein infilling.

#### *Discordant veins*

The clustered nature of discordant vein poles (Fig. 2-10B) suggests that these veins are relatively undeformed planar structures (Ragan, 1973). Sigmoidal geometries are also observed. The mean strike of discordant veins is *ca.* east-west, with dips averaging 40°-60° north. Assuming the greatest principle stress was directed at right angles to fold and thrust structures striking N140°-150°E (*i.e.* compression directed *ca.* N50°-60°E), discordant vein orientation is not compatible with fold- or thrust-associated AC or conjugate shear fracturing (Hobbs *et al.*, 1976; Ramsay and Huber, 1986). The consistent orientation, *en echelon* arrangement, and sigmoidal geometry of the veins is suggestive of lateral shear-induced (in this case sinistral) extensional fracturing, and may record a small component of shear associated with Chatter Creek deformation. Discordant veins clearly post-date f1 (Fig. 2-10). Veins are cut by unveined joints associated with late thrusting. Thrust faults contain no associated veining or alteration, suggesting veining pre-dates imbricate thrusting. Thus discordant veining is temporally constrained between late folding (f1) and early development of the Chatter Creek fault system.

#### **Vein Petrography and Host-rock Alteration**

Petrographic study of over 250 hand specimens and 80 thin- and polished-thin- sections of vein and host-rock material was undertaken in order to document vein-textural, mineralogical, and paragenetic relationships, to evaluate the degree of host-rock alteration, and to place

constraints upon the timing of vein- and gold- emplacement in relation to the local structural evolution of McGillivray Ridge. Semi-quantitative elemental analyses of specific mineral phases were obtained utilizing a Cambridge Stereoscan 250 scanning electron microscope equipped with a Kevex energy dispersive spectrometer.

### *Bedding-parallel veins*

Figure 2-11 summarizes the mineralogy, and paragenetic and structural evolution of the bedding-parallel veins. Quartz is the dominant vein-filling phase, typically comprising over 95 % of the total vein volume. Variable, unevenly distributed amounts of sulfide, carbonate, and white mica comprise the remaining modal fraction. Brecciated fragments of host pelite may comprise a significant volume within individual veins, depending on overall vein size, and the degree of fracturing and disaggregation of the pelite horizon. The distribution of hydrothermal vein constituents generally follows that of the pelite fragments, with the quantity of sulfides, carbonate, white mica, and gold being markedly higher in zones of intense pelite brecciation.

### *Internal vein structures and textures*

In general, the margins of bedding-parallel veins are marked by an abundance of brecciated pelite. These represent the remnants of pelite horizons which have been entirely disaggregated by quartz veining. Where pelite occurs at the top of normally graded beds, brecciation and veining occurs where pelite predominates.

Many of the macroscopic structures and textures exhibited by bedding-parallel veins are illustrated in Figure 2-12. The majority of quartz was



deposited as open-space fillings during one or more episodes of vein-opening. Well terminated quartz crystals indicate unimpeded crystal growth during vein filling. These crystals are usually truncated, dislocated, and overgrown by similar quartz deposited during subsequent reopening and filling events, creating a generally massive vein texture. Vein reopening took place within previously deposited vein fillings, along the wallrock-vein contact, or preferentially, along the margins of larger pelite fragments. Pelite fragments are commonly cut by more than one generation of quartz veining. Successive fracture fillings are spatially confined to the vein/pelite horizon and do not cut the quartzite wall rocks. No open spaces are observed in the veins.

Laminated textures indicative of incremental vein growth ("crack-seal filling", Ramsay, 1980; Cox and Etheridge, 1983) are locally developed (Fig. 2-13A) further suggesting multiple episodes of vein reopening.

### *Mineralogy*

Bedding-parallel vein minerals are discussed according to their paragenesis (Fig. 2-11). Pelite fragments are considered vein constituents because the original bedded character of these pelites has been destroyed by the veining process.

*Pelite fragments:* Angular fragments of pelite (Figs. 2-12 and 2-13) range in size from microscopic inclusions to several centimeters in greatest dimension. These fragments are generally most abundant near the vein margins where they may constitute greater than 50 % of the vein volume. Contacts between pelite fragments and the surrounding vein-quartz matrix are sharp, with the pelite exhibiting little visible evidence of hydrothermal alteration. A weak, pervasive foliation is present in the pelite fragments,

with a distinct crenulation cleavage being noted in some cases. Neither the pelite fragments nor their foliation exhibit a preferred orientation or common alignment within the veins.

Pelite fragments in thin section occasionally reveal a thin (<ca. 0.1 mm) selvage of relatively coarse, hydrothermally recrystallized mica with individual crystals up to 0.3 mm in length. This unfoliated selvage surrounds a finer grained core of weakly foliated white mica, the product of anchimetamorphism.

Semi-quantitative energy dispersive microanalysis of phyllosilicates from 15 pelite occurrences, including both mineralized and unmineralized horizons were performed. Cations present include the essential K, Al, and Si and, consistently, between about 3 and 6 weight % Fe ( $\pm$ Ti). This latter component is likely responsible for the greenish tint of the micas, with Fe<sup>+2</sup> substituting for Al in octahedral sites (Deer *et al.*, 1962).

Many pelite fragments contain the oxidized remnants of a finely disseminated, iron-rich phase, likely pyrite, which may be seen unaltered in the center of the inclusions. Hydrous iron oxides (limonite-goethite) now occupy the fine ( $\leq$ 0.2 mm) anhedral to subhedral casts. Based upon its petrographic character, this pyrite is considered to be metamorphic in origin.

*Quartz:* This mineral accounts for greater than 90 % of the hydrothermal vein-filling constituents. On the basis of textural and optical characteristics in hand specimen and thin section, three distinct varieties of quartz, Types I, II and, III are discernible.

Type I quartz (Figs. 2-12 and 2-13) constitutes 90-95 % of the vein-filling quartz. It is commonly comprised of massive aggregates of well terminated, millimeter- to centimeter-sized crystals. Well developed,

submillimeter-scale growth zonation in euhedral crystals is discernible in hand specimen. Fine-grained ( $\leq 0.05$  mm) white mica enhances these growth zones in thin section (Fig. 2-13C).

Type I quartz is readily identifiable in plane-polarized light by multiple generations of healed fractures, presently demarcated by trails of fluid inclusions. In cross polarized light undulatory extinction and sub-grain development are ubiquitous. Deformation lamellae are locally well developed. Pressure solution causing grain boundary suturing is widespread, and where abundant is accompanied by incipient recrystallization along neighbouring grain boundaries. Fine-grained, recrystallized quartz exhibits distinct undulatory extinction.

Type II quartz is locally developed granular, fine-grained (1-2 mm) quartz which occupies thin (0.5-2 cm), discrete veinlets contained within earlier deposited Type I quartz (Fig. 2-12). Petrographically, Type II quartz is polygonal in form and exhibits healed fractures, undulatory extinction and subgrain development. Type I quartz grains bounding these veinlets are generally highly strained and sutured (Fig. 2-13D) thus, Type II quartz is interpreted as local, pressure solution-derived vein quartz, deposited in discrete dilational fractures created during the progressive deformation of earlier deposited Type I vein-fillings.

Type III quartz (Figs. 2-12 and 2-14D) is distinguished in hand specimen by its milky white colour and fine- to medium-grained (1-5 mm) granular texture. This variety of quartz is not confined to discrete structures, but is seen filling irregular fractures and voids of variable size and shape, most commonly originating near vein margins and extending into Type I and II vein structures. Microscopically, Type III quartz exhibits a lesser degree

of deformation than Type I. Undulatory extinction is ubiquitous but of lesser intensity. Subgrains, sutured grain boundaries and healed fracture patterns are also locally developed but to a much lesser degree.

Type III quartz is also distinctive for the greater quantities of associated white mica, pyrite and native gold relative to quartz Types I and II.

*White mica:* This minor vein constituent (<1%) is fine-grained (0.01-0.1 mm), occurring as disseminations and aggregates along late, partially healed fractures in all quartz types.

The origin of much of the fine disseminated and fracture dispersed white mica is considered to be in part hydrothermal, but a significant quantity (perhaps 50%) of all the white mica is considered to have been derived through brecciation and dispersal  $\pm$  recrystallization of original pelitic host-rock (Figs. 2-12 and 2-13A). It is generally not possible to petrographically distinguish these mica types.

*Pyrite:* Two generations of pyrite are recorded. The first, diagenetic or metamorphic pyrite in pelite has been described. The second (< 1% of total vein volume) consists of 0.05 to 5 mm subhedral to euhedral cubes which commonly exhibit finely striated crystal faces, and is hydrothermal in origin. The majority of hydrothermal pyrite occurs as disseminations, clusters and fine stringers in Type III quartz, or in the immediate vicinity of (ca. 5 mm radius), nucleated upon, or replacing pelite fragments in Types I and III quartz. Pelite-unaccompanied pyrite in Type I quartz is rare.

Post-depositional deformation of hydrothermal pyrite is uncommon. Minor fracturing is filled with quartz, and occasionally, native gold (Fig. 2-14A). Sporadic inclusions of white mica, quartz, and native gold also occur in pyrite.

*Gold:* Although most of the bedding-parallel veins contain gold, its

distribution within individual veins is erratic, its presence being enhanced in zones containing abundant pelite fragments, hydrothermal pyrite and Type III quartz, concentrated near vein margins.

Gold is present exclusively as native metal. Sub-equant inclusions range from 0.04 to about 2 mm in size, occurring close to, or abutting against, brecciated pelite fragments or hydrothermal pyrite crystals (Figs. 2-14B and 2-14C). Less commonly, inclusions in pyrite are seen.

Native gold also occurs as fracture fillings in Types I and III quartz (Figs. 2-14A, 2-14B, and 2-14D). In Type I quartz, gold occurs as fine dendritic fillings up to 5 mm in greatest dimension. Gold filled fractures are generally traceable to nearby (up to 1 cm distant) zones of Type III quartz mineralization. Fractures confined to Type III quartz also contain gold and usually propagate from zones rich in hydrothermal pyrite, white mica and pelite breccia. Very rarely, gold with pyrite fills fractures in Type II quartz.

Energy dispersive microanalysis of the native gold indicates it is of exceptionally high fineness. Over 100 spot analyses failed to detect the presence of any element other than gold.

*Galena:* Occurrences of galena are limited to sporadic, irregular, undeformed fracture fillings in Types I and III quartz, where it is commonly accompanied by native gold (Fig. 2-14D). Minor replacement by hydrous iron-oxides has taken place at the perimeter of galena fills. Although the presence of galena is a good indicator of enhanced gold concentrations, galena is actually less common than visible native gold.

*Carbonate:* Occurrences of small (<3 mm), anhedral to euhedral inclusions of rust-brown weathering carbonate are rare. When present, this mineral is seen abutting pelite fragments in Type I quartz, or accompanying

pyrite  $\pm$  native gold in Types II and III quartz. Based upon its brownish color the carbonate is likely ankeritic in composition.

#### *Discordant veins*

Discordant veins are filled with quartz, and rarely minor pyrite (<0.5-1%). Quartz is medium-grained, massive to granular, anhedral, and exhibits fracturing, undulatory extinction, and minor pressure solution. Pyrite is fine-grained (<3 mm) and subhedral to euhedral. Discordant veins exhibit essentially one stage of vein filling. Gold values range from less than 5ppb to 500 ppb and appear to correlate with pyrite content. Visible gold has not been observed.

#### *Hydrothermal alteration*

Wall-rock alteration is notably absent adjacent to most bedding-parallel veins. Where veining was initiated at the top of graded beds minor pyritization is occasionally developed in the adjacent, unveined pelitic quartzite. Similar sulfidation is also noted where discordant vein structures cut pelitic quartzites which lack bedding-parallel vein development. Zones of sulfidation immediately adjacent to veins may carry up to 1 ppm gold.

More widespread is the incipient replacement of detrital potash feldspar by white mica  $\pm$  minor iron-rich carbonate (Fig. 2-6C). The origin of these constituents is ambiguous as their occurrence is not restricted to the strata adjacent to veins. They may represent a hydrothermal assemblage associated with vein filling, but are more likely the products of regional anchimetamorphism.

### *Paragenesis*

Two broad generations of vein filling are recorded in the bedding-parallel veins of McGillivray Ridge (Fig. 2-11). The first of these (pre-gold stage), represented by pelite fragments, Types I and II quartz and hydrothermal white mica  $\pm$  minor pyrite and carbonate, records a protracted history of repeated vein opening and filling during which over 90 % of the hydrothermal vein constituents were precipitated, predominantly as open space  $\pm$  laminated fillings. The second generation (gold and post-gold stages) of vein filling represents a late, volumetrically minor incursion of hydrothermal fluids during which most of the gold was deposited. Within this stage, deposition of most of the Type III quartz and pyrite  $\pm$  white mica and carbonate was followed by late co-precipitation of quartz, pyrite, gold and galena. Discordant veins exhibit a single stage of vein-filling during which quartz and occasional pyrite were co-precipitated.

The sparse occurrence of  $s_1$  cleavage  $\pm$  crenulation in pelite fragments indicates that pre-gold bedding-parallel vein filling was initiated prior to cleavage development, and hence before  $f_1$ . The absence of earlier phase microstructures precludes specific correlation of vein initiation with the regional deformations of Mountjoy (personal communication). However, vein textures indicative of multiple vein fillings, and the highly variable strain states observed in vein quartz suggest vein filling took place during prolonged or repeated deformation and continued during  $f_1$ . The weakly deformed state of the paragenetically-late gold-bearing assemblage (quartz-pyrite-gold-galena) suggests gold deposition occurred late during or post-dating penetrative deformation (*i.e.*  $f_1$ ). The lack of veining or alteration along imbricate thrust planes suggests the Chatter Creek fault post-dates vein

filling and gold deposition.

As outlined earlier, discordant veins also post-date  $f_1$  and pre-date the Chatter Creek thrust. Thus a broad temporal relationship between discordant veins and gold emplacement is implied. The discordant veins however contain only minor gold. These observations, and the fact that the gold-bearing assemblage is generally associated with pelite fragments in bedding-parallel veins, suggests that fluid interaction with pelite may have triggered gold deposition. Studies by Seward (1984) indicate gold may travel as sulfur complexes in hydrothermal solutions. Disseminated, diagenetic sulfide in the McNaughton rock types may have provided sulfur for the complexing of gold by mineralizing fluids. Iron released from the pelites may have stimulated sulfidation reactions (Phillips *et al.*, 1984; Tomkinson, 1988) which destabilized gold-sulfur complexes, resulting in the deposition of pyrite and native gold in the vicinity of pelite fragments. This hypothesis would account for the localization of gold in bedding-parallel structures, and for the lack of gold in discordant veins and quartzitic rock types. The discordant veins cut only quartzite and contain no pelite fragments. Quartzites would be intrinsically non-reactive and would not have triggered gold deposition. Thus, as well as providing dilatant zones for focussing fluid flow, pelites may have acted as chemical traps for the localization of gold mineralization on McGillivray Ridge.

Based upon its spatial association with bedding-parallel veins and auriferous nature, wallrock sulfidation likely accompanied gold-stage vein-filling. Sulfidation adjacent to some discordant veins also suggests a penecontemporaneous gold-stage-d discordant vein-sulfidation relationship. The more widespread assemblage white mica  $\pm$  carbonate  $\pm$  disseminated pyrite is not uniquely associated with vein structures, and is considered the



product of regional anchimetamorphism. Notable is the mineralogical congruency between the vein (quartz-white mica  $\pm$  pyrite  $\pm$  carbonate), alteration (pyrite  $\pm$  white mica  $\pm$  carbonate), and anchimetamorphic (quartz-white mica  $\pm$  pyrite  $\pm$  carbonate) assemblages. This suggests subcontemporaneous vein-filling-alteration-metamorphism, and thus broad chemical and thermal equilibrium between the vein-filling fluids and the surrounding host rocks (Rose and Burt, 1979). As well, the relatively local derivation of the major vein-filling constituents is implied (Norris and Henley, 1976; Etheridge *et al.*, 1984; Kerrich *et al.*, 1978). With respect to regional metamorphism this mineralogical congruency, and the preservation of primary vein-filling textures and highly variable strain states in vein quartz, suggests late syn- to post-peak metamorphic vein filling. Thus vein filling may have been initiated during development of the synmetamorphic Porcupine Creek Anticlinorium (Mountjoy and Dechesne, 1989, personal communication).

### Deposit Classification

Within the Main Ranges, the gold lodes of the Athabasca Pass are unique. As well, geochemical data (trace elements, fluid inclusions, stable isotopes) are lacking. Hence, detailed comparison and quantitative process model classification would be premature. However, in terms of their setting and morphology, the Athabasca Pass lodes are considered to represent a siliciclastic-hosted analogue of the Turbidite-Hosted (Boyle, 1979 and Keppie *et al.*, 1986; Hutchinson, 1987) class of gold deposits. Lithotectonic, metamorphic, structural, temporal, and vein textural-mineralogical analogies to turbidite-hosted deposits are clearly evident (Table 2-1).

However they are distinct in terms of host-rock composition, *i.e.* predominantly mature siliciclastics in the Athabasca Pass versus immature greywacke-argillite in turbidite-hosted deposits. Geochemical differences from the turbidite-hosted deposit model, such as the paucity of wallrock alteration and the mineralogical simplicity of the Athabasca Pass lodes, may be attributable to the non-reactive nature and the limited elemental spectrum of mature quartzite-dominated sequences compared with less mature turbidite-hosted rock types. Further comparison and classification must await geochemical data and/or the discovery of comparable siliciclastic-hosted lode systems.

#### Concluding Statement

The thick, clastic-dominated, Lower Paleozoic sedimentary sequences comprising the Main Ranges of the Canadian Rocky Mountains have previously been viewed as unfavourable environments for the search for gold-lodes (Matthews, 1944; Holland, 1944; Sinclair, *et al.*, 1978). In light of the present study the Main Ranges may be considered as a distinct metallogenic domain containing sediment-hosted lode gold associations. Although presently unique, the Athabasca Pass lodes provide some first-order observations for lode exploration. With respect to regional deformation, gold mineralization appears to be late-stage, hence structures and veining associated with late-stage out of sequence thrust faulting (Mountjoy, 1989, personal communication) may prove significant. Locally, the important role of pelitic rock types in siliciclastic sequences such as the McNaughton Formation is emphasized. Such pelites provide ideal structural and geochemical contrasts for the localization of hydrothermal fluids and

**gold in siliciclastic-dominated domains.**

Table 2-1. Characteristics of the Athabasca Pass vs. typical turbidite-hosted \* lode-gold deposits

	Athabasca Pass	Turbidite-Hosted
Geologic-tectonic setting:	Thick platformal clastic sequences in Rocky Mountain Thrust and Fold Belt	Thick flyschoid clastic sequences in fold-and thrust-belts ± transcurrent domains
Associated rock types:	Predominantly mature sedimentary rocks (pelitic quartzite, quartzite, pelite, conglomerate)	Predominantly immature sedimentary rocks (graywacke, argillite-slate, quartzite)
Metamorphic grade:	Pumpellyite-lower greenschist	Dominantly prehnite-pumpellyite to middle greenschist
Host-rock age:	Lower Cambrian	Upper Proterozoic to Lower Paleozoic
Relative timing of veins:	Early-syn-tectonic, syn- to post peak-metamorphic	Early-syn to post-tectonic, syn- to post peak-metamorphic
Ore-hosting structures:	Discrete bedding-parallel ± discordant veins	Discrete bedding-parallel and discordant veins saddle reefs, fault structures
Alteration:	Absent to minor; silicification, sulfidation carbonitization, sericitization	Absent to distinct; silicification, sulfidation carbonitization, sericitization, chloritization
Vein textures:	Open-space filling, host-rock fragments minor laminations	Open-space filling, host-rock fragments and laminations
Vein mineralogy:	Quartz, pyrite, white mica, galena, carbonate	Quartz, pyrite, arsenopyrite, carbonate±galena, sphalerite stibnite, scheelite, pyrrhotite, white mica, chlorite
Nature and distribution of gold:	Coarse-grained native gold, confined to veins, erratic grades	Coarse-grained native gold ± sulfide associations, confined to veins ± wallrock enrichment, erratic grades
Gold fineness(Au/Ag):	Very high (> 20:1)	High (average 9:1, range 3:1 to 20:1)
* Principle references: Keppie <i>et al.</i> (1986), Graves and Zentilli (1982), Hutchinson (1987).		

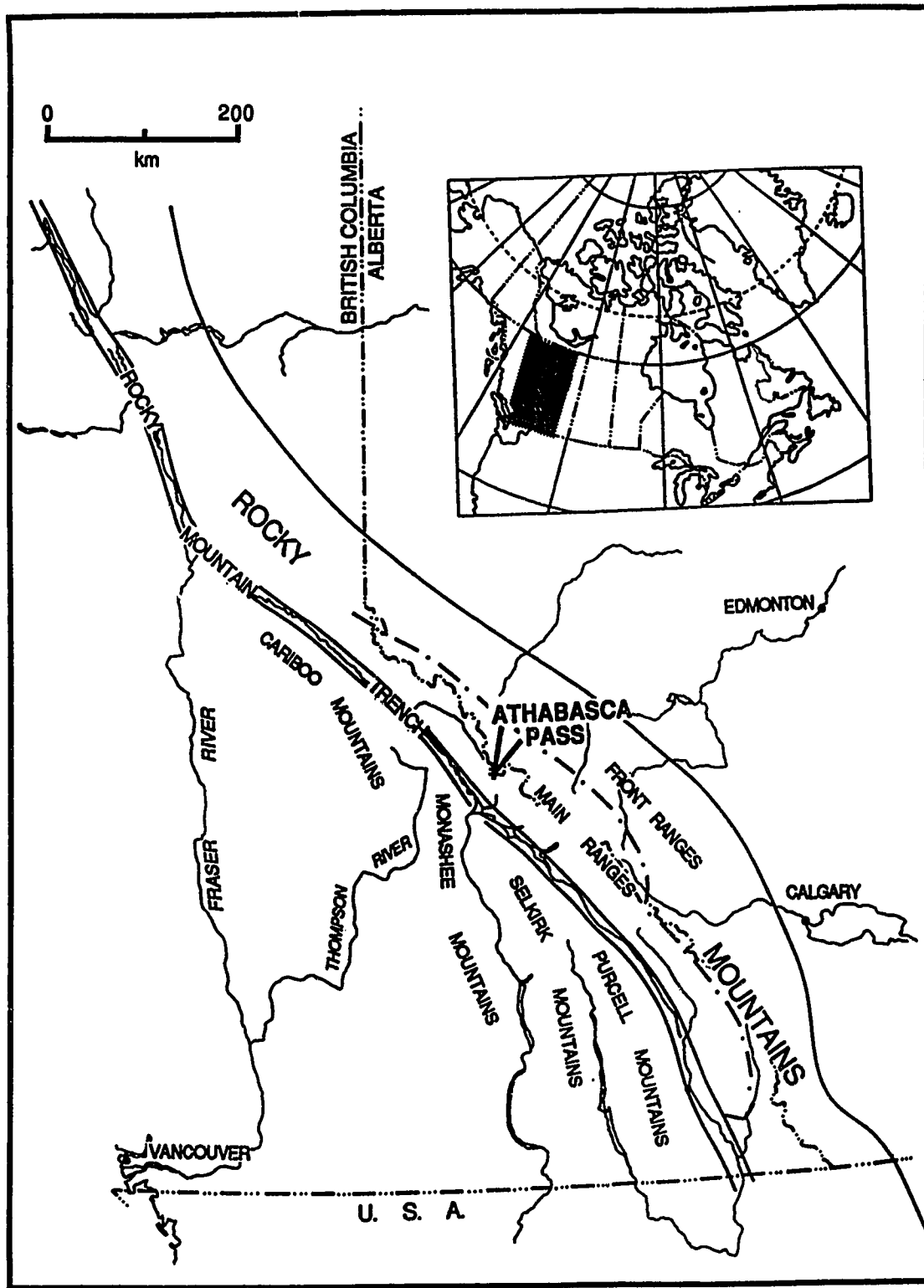


Figure 2-1. Location of the Athabasca Pass.



Figure 2-2. Regional geology surrounding Athabasca Pass. Modified after Wheeler *et. al* (1972).

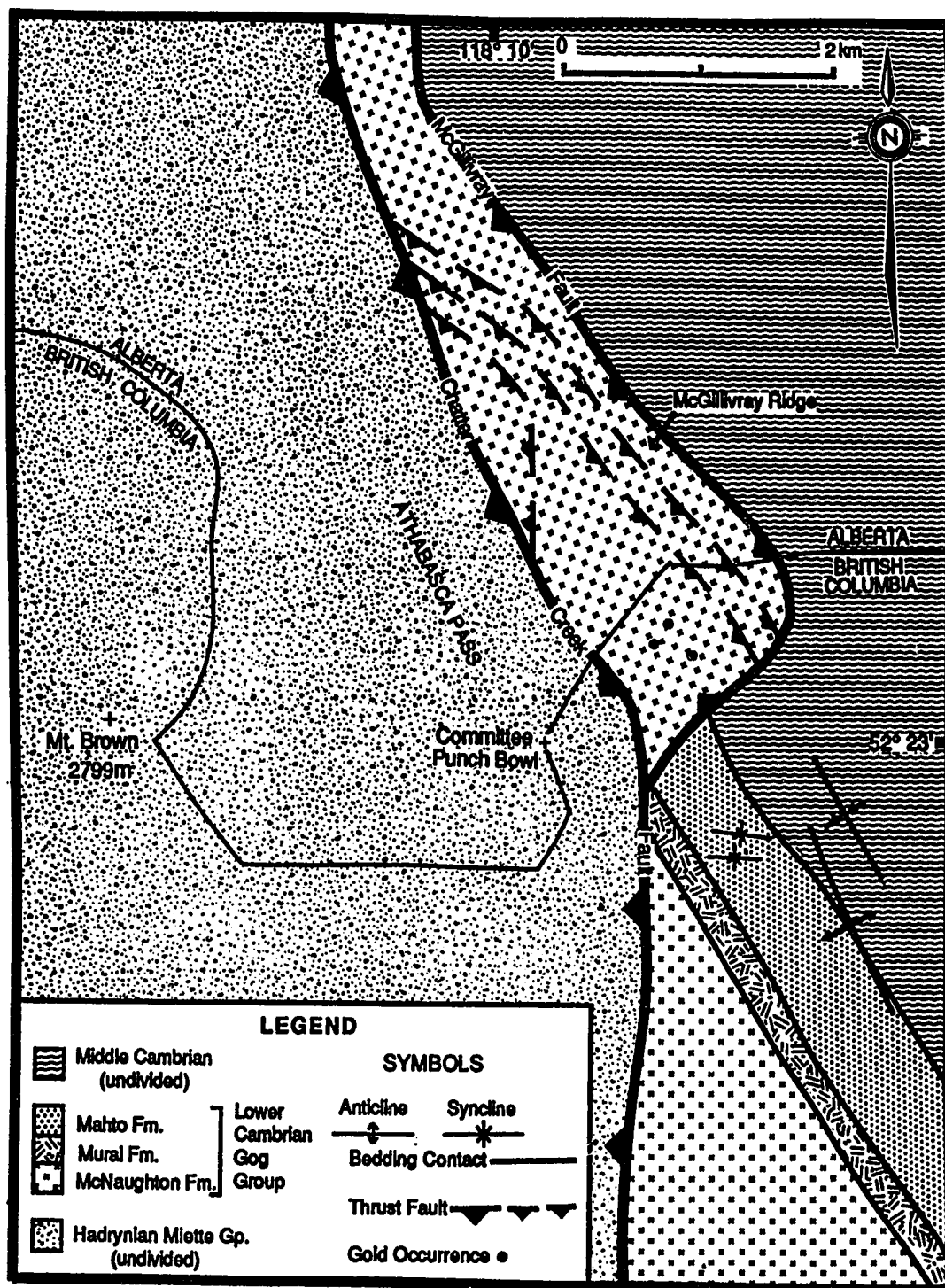
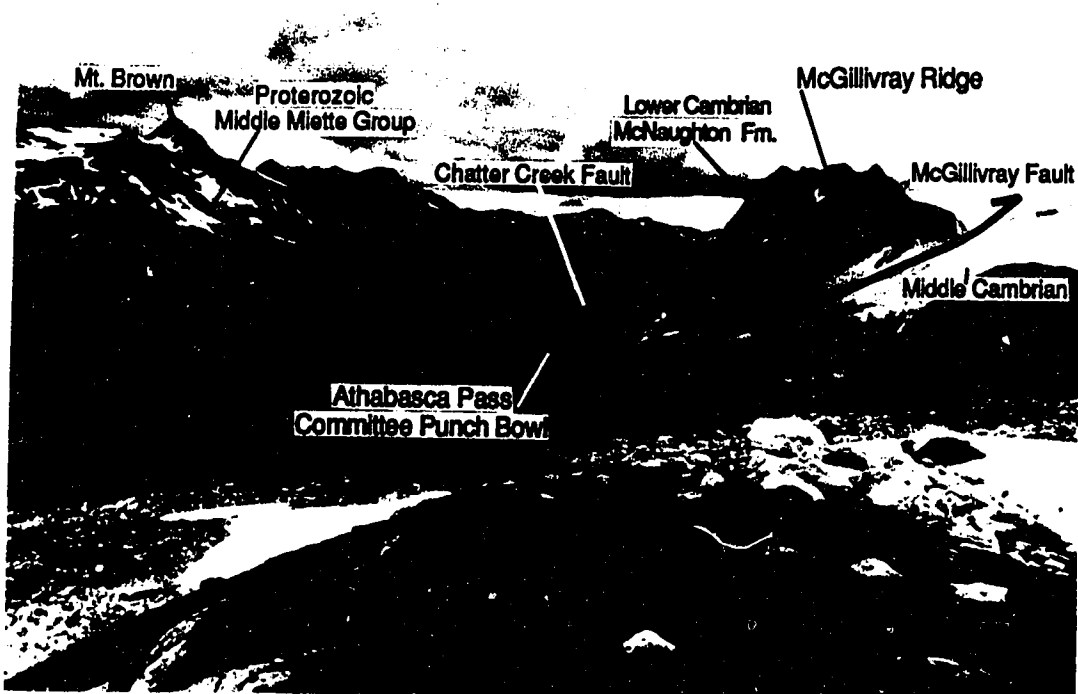
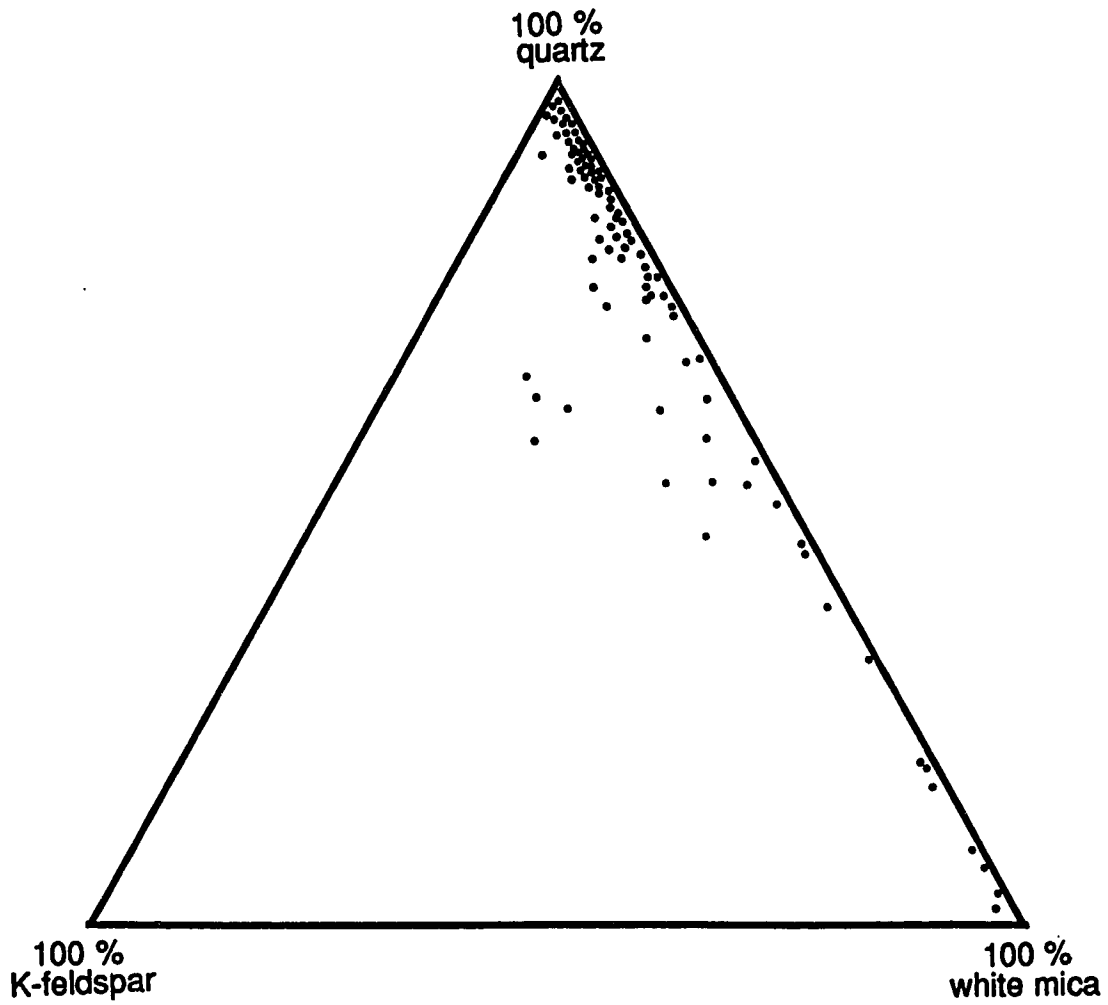


Figure 2-3. Local geology of the Athabasca Pass area (modified after Mountjoy and Price (in preparation.). Gold occurrences represent clusters of mineralized veins.



**Figure 2-4.** Photograph of the Athabasca Pass viewed from the south. The Chatter Creek thrust does not outcrop in the Athabasca Pass. Its position is inferred from outcrops of Middle Miette grit to the west. Distance to McGillivray Ridge is approximately 3 km.





**Figure 2-5.** Modal composition of the McNaughton Formation rock types of McGillivray Ridge.

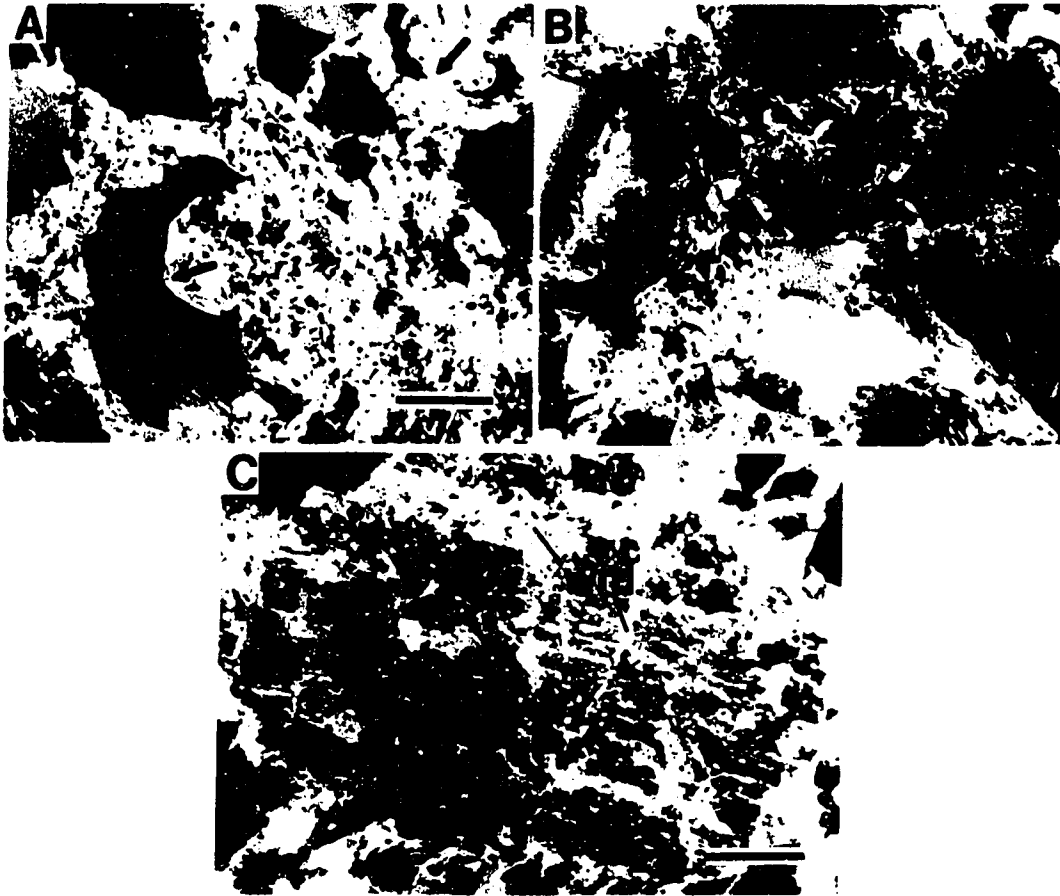


**Figure 2-6.** Typical deformational microstructures and alteration exhibited by the McNaughton rock types of McGillivray Ridge; transmitted light, crossed-polarized. A-B. Solution embayment of quartz grains ( $\leftrightarrow$ ) in typical pelitic quartzite. Scale bar=0.3 mm. C. Incipient replacement of a detrital potash feldspar grain by white mica (wm) and carbonate (ca); transmitted light, crossed-polars. Scale bar=0.3 mm.

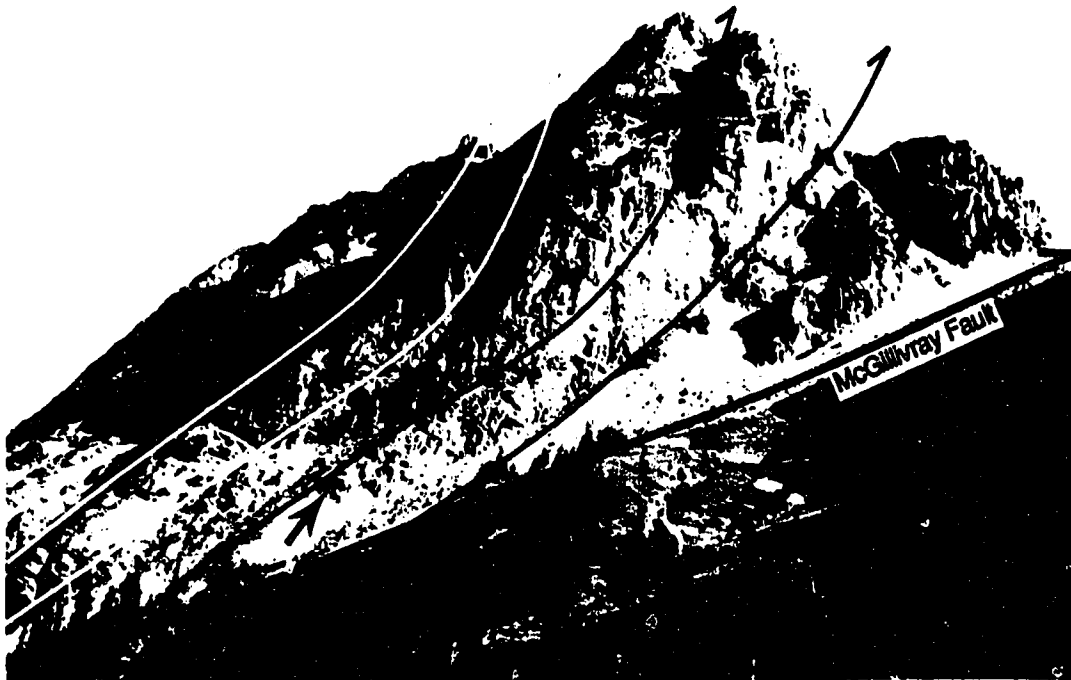


**Figure 2-7.** View of the south end of McGillivray Ridge showing imbricate thrust geometry in the McNaughton Formation. The major thrusts are line-enhanced. Distance along McGillivray Fault is approximately 1.2 km. Location of Fig. 8 indicated by arrow.

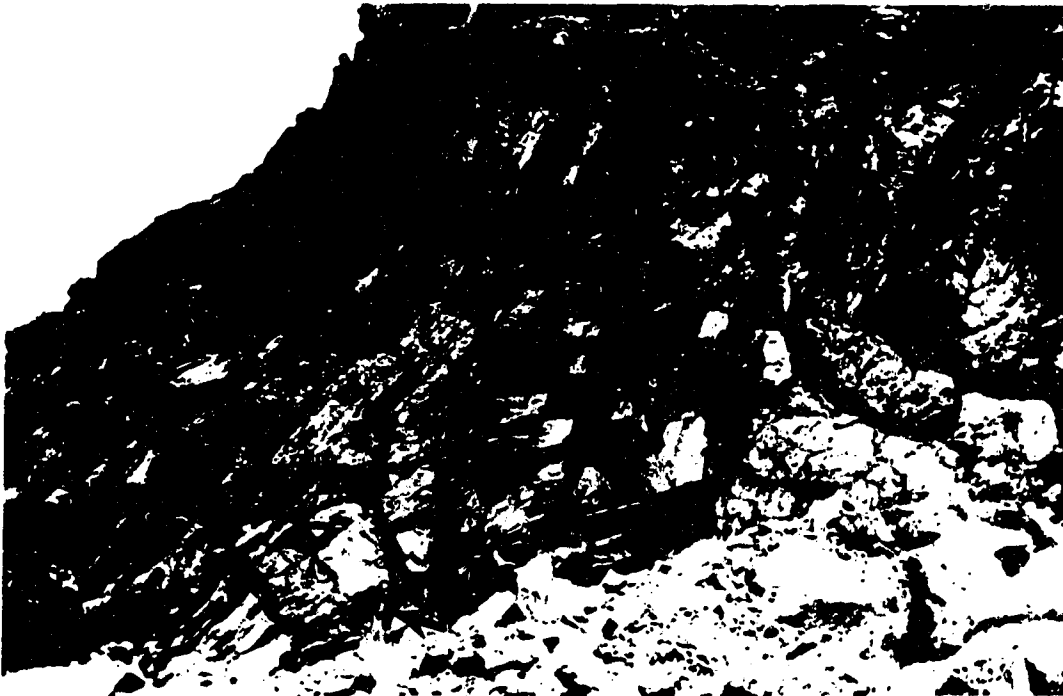


**Figure 2-8.** Folds in the McNaughton Formation of McGillivray Ridge at location shown in Fig. 7. View facing approximately north. Man in foreground is 1.4 m tall.

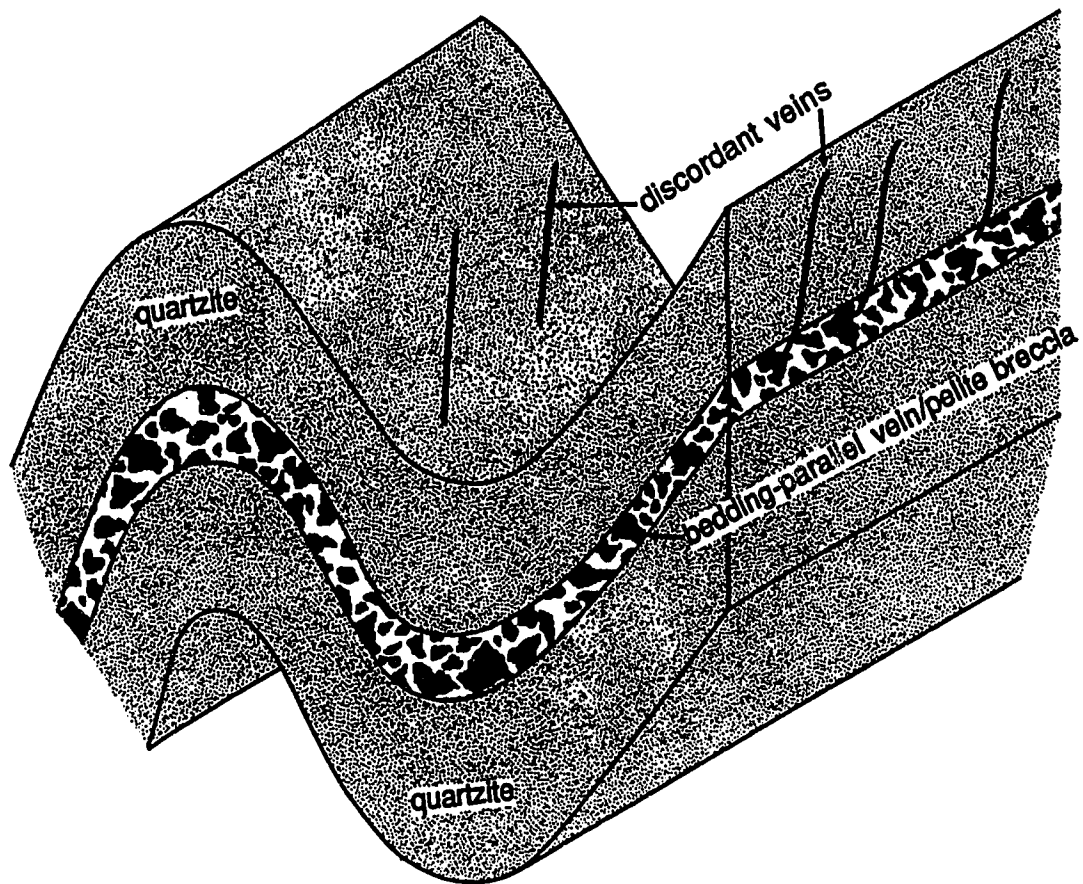


**Figure 2-9.** Schematic illustration of the general field relationships between bedding, folding, bedding-parallel veining, and discordant veining on McGillivray Ridge.

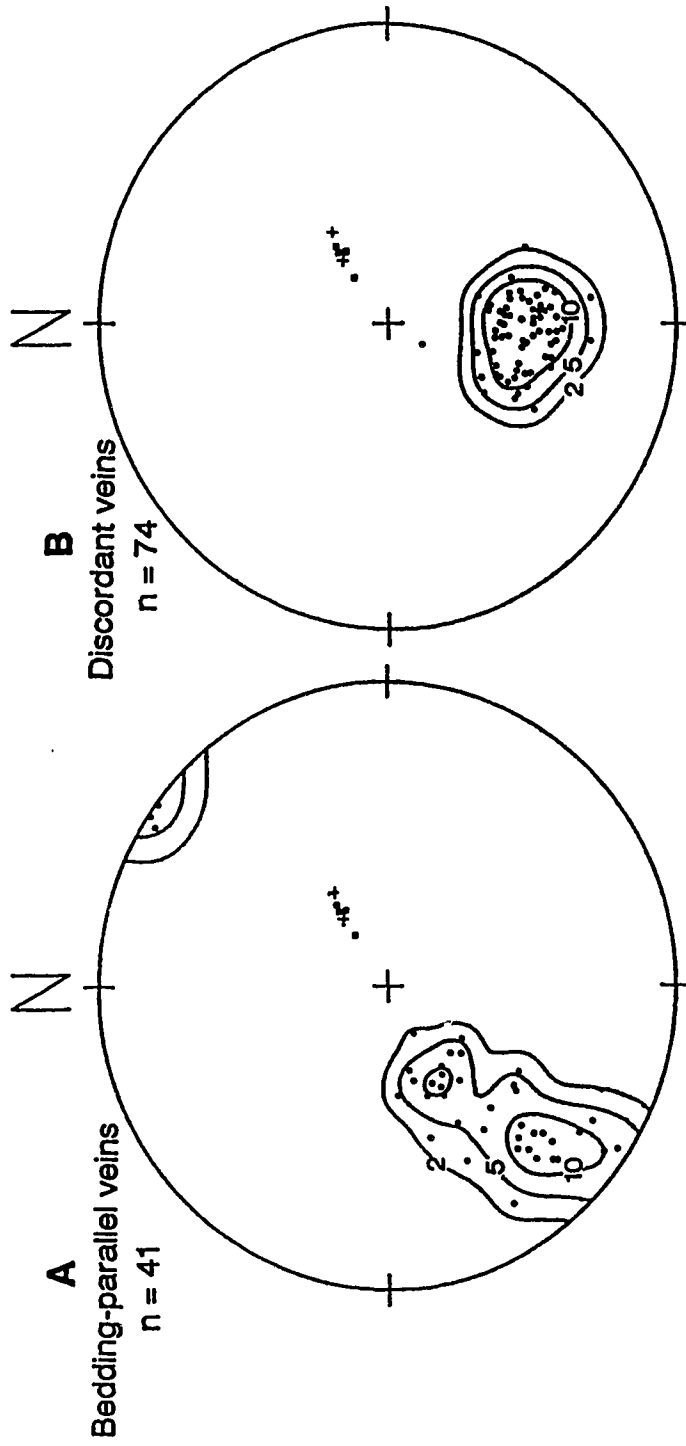


**Figure 2-10.** Contoured lower hemisphere stereographic probability diagrams projecting poles to bedding-parallel (A) and discordant (B) vein structures, in relation to fold axial planes (·) and thrust faults (+) on McGillivray Ridge. Contours at densities 2, 5, and 10.

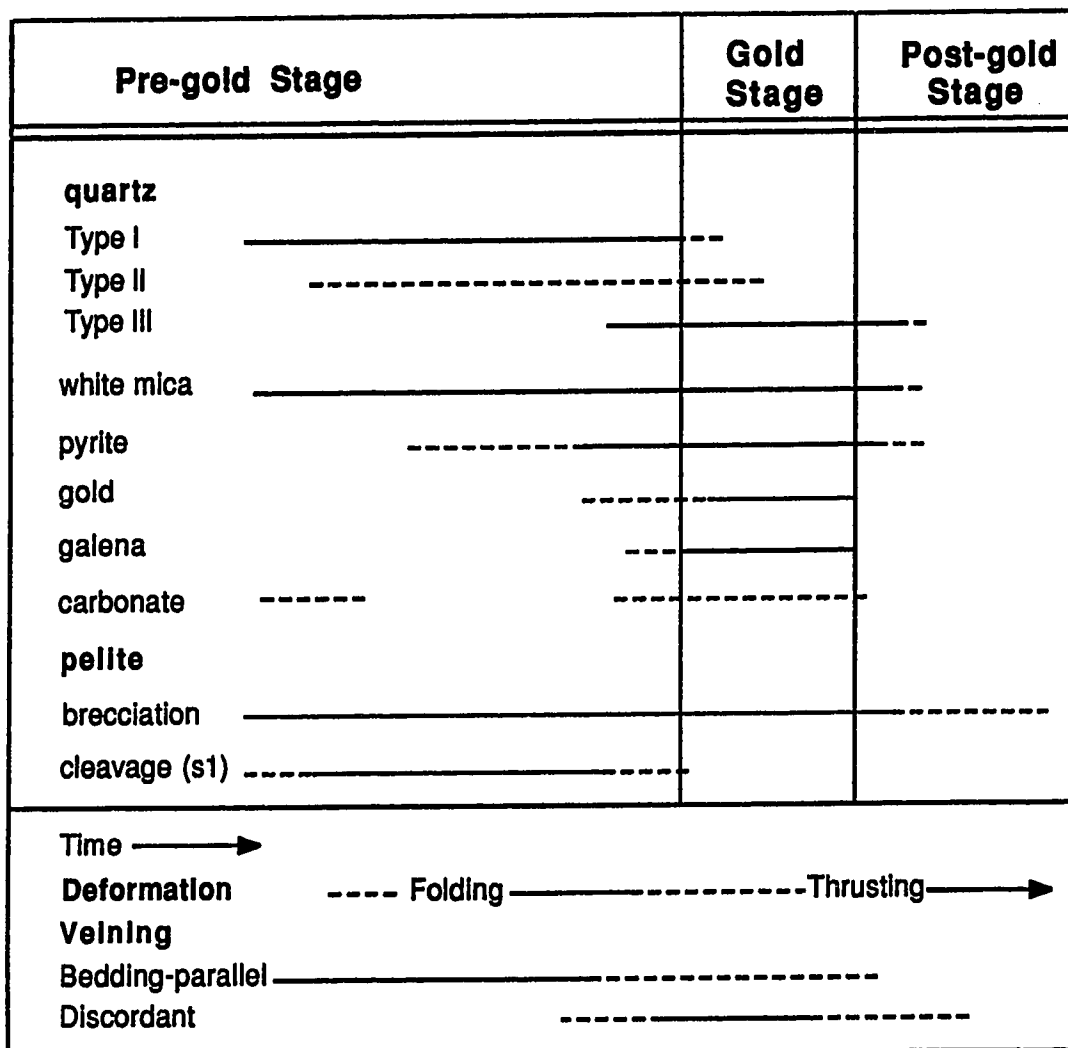
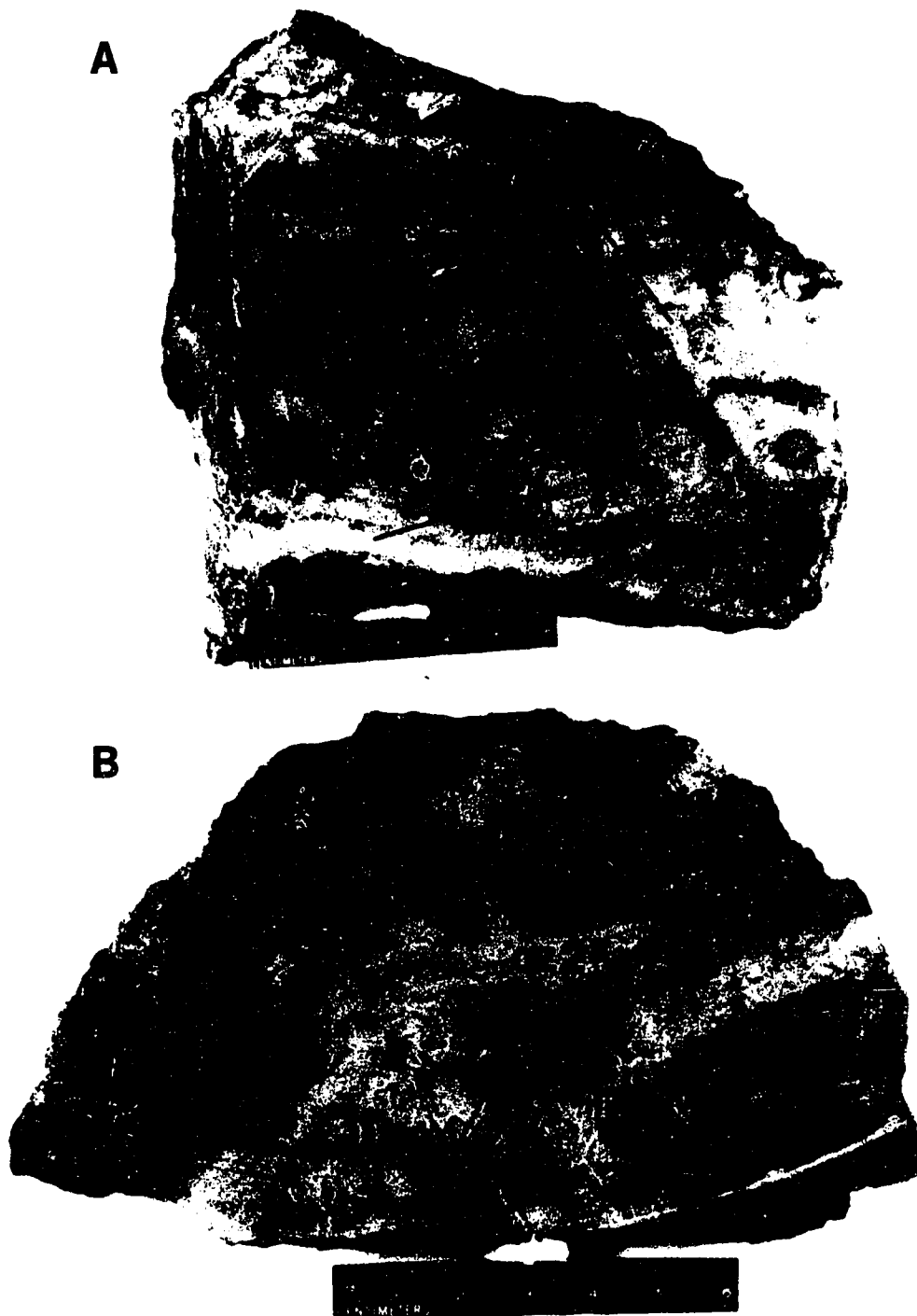
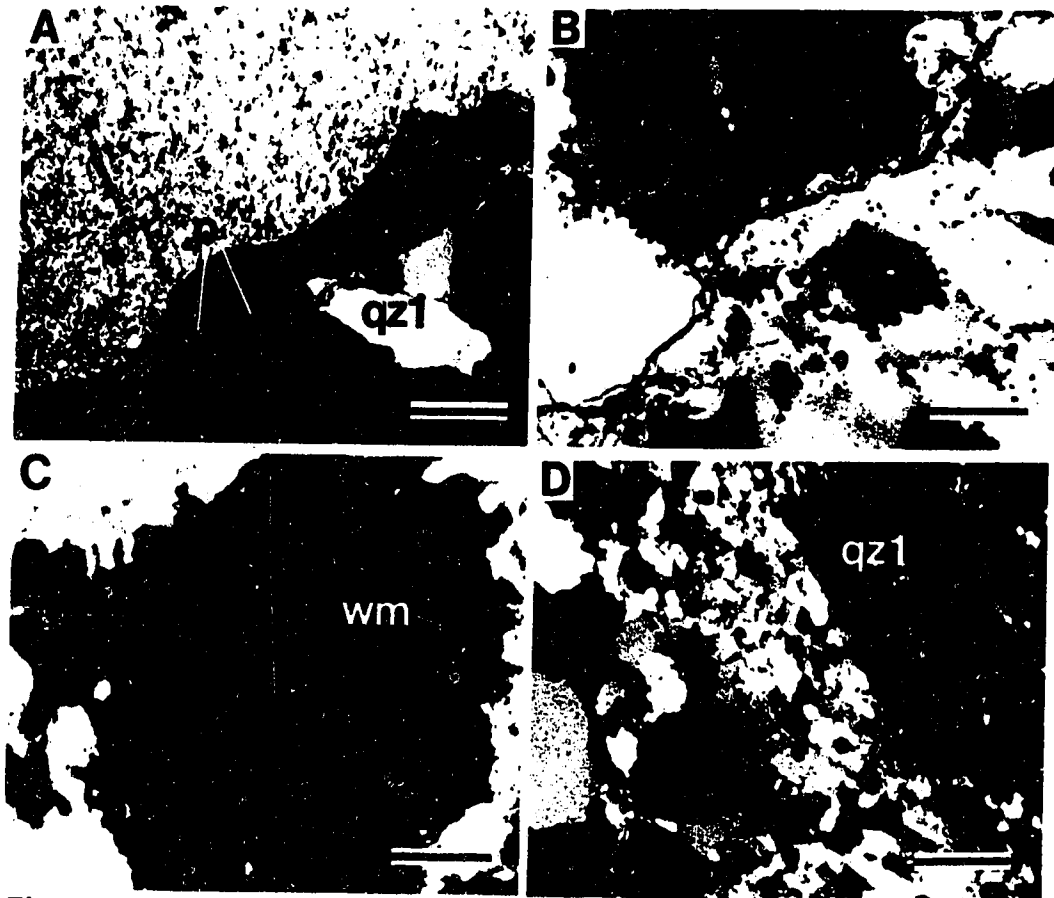


Figure 2-11. Mineralogy and paragenetic sequence for the auriferous bedding-parallel veins of McGillivray Ridge. Dashed lines represent possible minor quantities. Relative timing of vein formation and mineralization with respect to the deformations of Mountjoy (pers. comm.) is discussed in the text.



**Figure 2-12.** Typical textures exhibited by bedding-parallel veins from McGillivray Ridge. A. Massive Type I quartz (qz1) with pelite fragments (p) cut by milky Type III quartz (qz3) and a late discordant vein (d). B. Massive Type I quartz (qz1) containing pelite fragments (p), and a Type II quartz vein derived during progressive deformation of previously deposited Type I quartz.



**Figure 2-13.** Microtextures exhibited by quartz in the bedding-parallel veins of McGillivray Ridge; transmitted light, crossed-polarized. Scale bar=0.3 mm in all photographs. A. Laminations of pelite (p) incorporated into Type 1 quartz (qz1) during incremental vein growth. B. Undulatory extinction, sub-grain development, and incipient recrystallization in Type I quartz. Diagonal black fracture (lower left to upper right) was introduced during polishing. C. Co-precipitated inclusions of white mica (wm) lining a growth zone in Type I quartz. D. Relatively unstrained Type II quartz (qz2) adjacent to earlier, deformed Type I quartz (qz1).



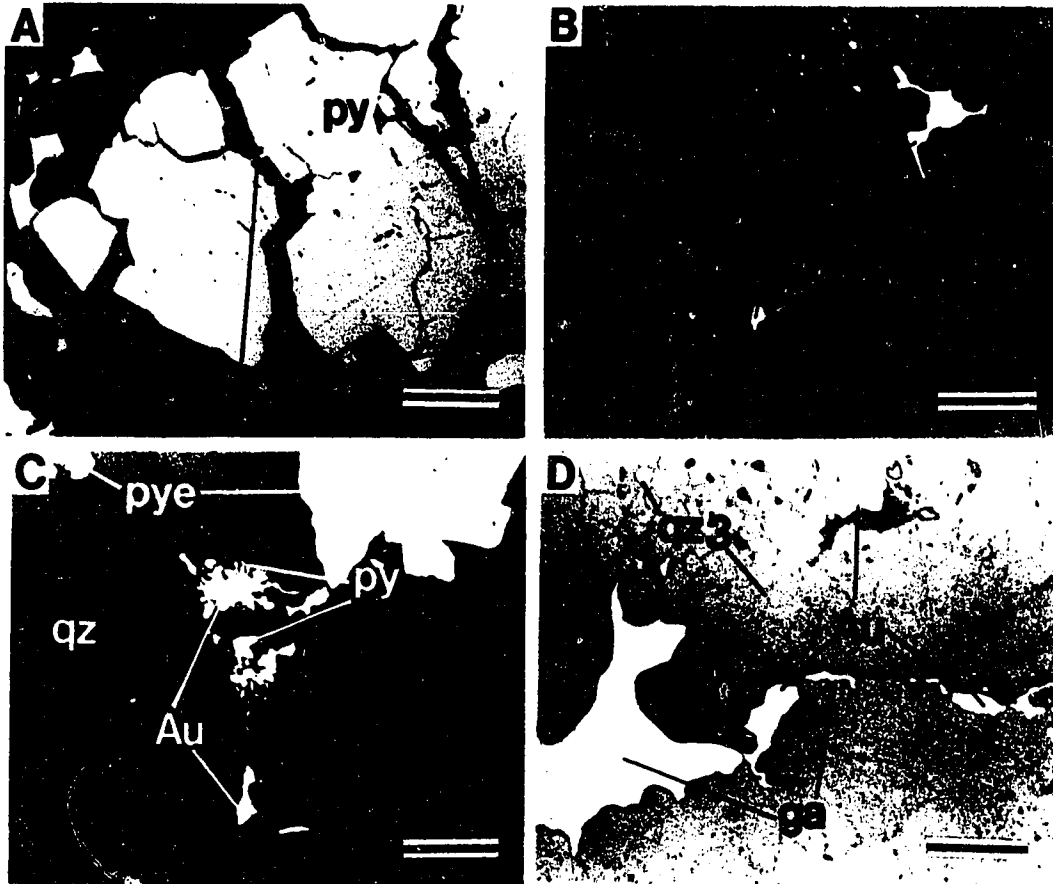


**Figure 2-14.** Textural relationships among the minerals from bedding-parallel veins of McGillivray Ridge; reflected plane-polarized light. Scale bar=0.5 mm in all photographs. A. Quartz (qz) and native gold (Au) filling fractures in and around pyrite (py). B. Native gold (Au) abutting pyritized pelite (p) fragments in Type III quartz. C. Subcontemporaneous native gold (Au) and pyrite (py) filling fractures in quartz (qz) with paragenetically earlier pyrite (pye). D. Native gold (Au), galena (ga) and Type III quartz (qz3) filling late fractures in Type I quartz.

### References

- Akehurst, J.L. 1964. The Jasper Formation, Jasper, Alberta. M. Sc. thesis, University of Alberta, Edmonton, Alberta.
- Balkwill, H.R. 1968. Structural analysis of the Western Ranges, Rocky Mountains, Golden, British Columbia. *In* Report of activities, part A. Geological Survey of Canada, Paper 68-1, pp. 193-196.
- Beach, A. 1979. Pressure solution as a metamorphic process in deformed terrigenous sedimentary rocks. *Lithos*, 12: 51-58.
- Boyer, S.E., and Elliott, D. 1982. Thrust systems. *American Association of Petroleum Geologists Bulletin*, 66: 1196-1230.
- Boyle, R. W. 1979. The geochemistry of gold and its deposits. Geological Survey of Canada, Bulletin 280.
- Campbell, R. B. 1968. Canoe River (83D), British Columbia. Geological Survey of Canada, Map 15-1967, Scale 1:250,000.
- Charlesworth, H.A.K., Cruden, D. M., Ramsden, J., and Huang, Q 1989. ORIENT, an interactive FORTRAN 77 program for processing orientations on a microcomputer. *Computers and Geoscience*, 15: 275-293.
- Cook, D.G. 1975. Structural style influenced by lithofacies, Rocky Mountain Main Ranges, Alberta-British Columbia. Geological Survey of Canada, Bulletin 233.
- Cox, S.F., and Etheridge, M.A. 1983. Crack-seal fibre growth mechanisms and their significance in the development of oriented layer silicate microstructure. *Tectonophysics*, 92: 147-170.
- Cox, S.F., Etheridge, M.A., and Wall, V.J. 1986. The role of syn-tectonic mass transport and localization of metamorphic vein-type ore deposits. *Ore Geology Reviews*, 2: 65-86.
- Craw, D. 1978. Metamorphism, structure and stratigraphy of the Southern

- Park Ranges, British Columbia. *Canadian Journal of Earth Sciences*, 15: 86-98.
- Deschene, R.D., and Mountjoy, E.W. 1988. Structural geology of part of the Main Ranges near Jasper, Alberta. *In Current research, part E. Geological Survey of Canada, Paper 88-1E*, pp. 171-176.
- Deer, W. A., Howie, R.A., and Zussman, J. 1962. Rock-forming minerals, volume 3 sheet silicates. Longmans Group Ltd., London.
- Etheridge, M.A., Wall, V.J., Cox, S.F., and Vernon, H.R. 1984. High fluid pressures during regional metamorphism and deformation: Implications for mass transport and deformation mechanisms. *Journal of Geophysical Research*, 89, (B6): 4344-4358.
- Frey, M. 1987. Very low-grade metamorphism of clastic sedimentary rocks. *In Low temperature metamorphism. M. Frey, Ed. Blackie, Glasgow*, pp. 9-58.
- Frey, M. and Kisch, H.J. 1987. Scope of Subject. *In Low temperature metamorphism. M. Frey, Ed. Blackie, Glasgow*, pp. 1-8.
- Fyfe, W.S., Price, N.J. and Thompson, A.B. 1978. Fluids in the earth's crust. Elsevier, Amsterdam.
- Giusti, L. 1983. The distribution, grades, and mineralogical composition of gold-bearing placers in Alberta. M. Sc. thesis, University of Alberta, Edmonton, Alberta.
- Goldfarb, R.J., Leach, D.L., Miller, M.L., and Pickthorn, W.J. 1986. Geology, metamorphic setting and genetic constraints of epigenetic lode gold mineralization within the Cretaceous Valdez Group, south-central Alaska. *In Turbidite-hosted deposits. J.D. Keppie, R.W. Boyle and S.J. Haynes, Eds. Geological Association of Canada, Special Paper 32*, pp. 87-105.
- Graves, M.C., and Zentilli, M. 1982. A review of the geology of gold in Nova Scotia. *In Geology of Canadian gold deposits. F W. Hodder and W.*

- Petrak, *Eds.* Canadian Institute of Mining and Metallurgy, Special Volume 24, pp. 233-242.
- Hedley, M.S. 1954. Mineral deposits in the southern Canadian Rocky Mountains of Canada. Alberta Society of Petroleum Geologists, Fourth Annual Field Conference Guide Book, pp. 110-118.
- Hein, F.J. 1987. Tidal littoral offshore shelf deposits - Lower Cambrian Gog Group, Southern Canadian Rocky Mountains. *Sedimentary Geology*, 52: 155-182.
- Henley, R.W., Norris, R.J., and Paterson, C.J. 1976. Multistage ore genesis in the New Zealand Geosyncline, a history of post-metamorphic lode emplacement. *Mineralium Deposita*, 11: 180-196.
- Hobbs, B.E., Means, W.D., and Williams, P.F. 1976. An outline of structural geology, John Wiley and Sons, New York.
- Holland, S.S. 1944. Lode Gold Deposits: Northeastern British Columbia and Cariboo and Hobson Creek areas. British Columbia Department of Mines, Bulletin No. 20, Part 6.
- Hubbert, M.K., and Rubey, W.W. 1959. Mechanics of fluid-filled porous solids and its application to overthrust faulting. *Geological Society of America Bulletin*, 70: 115-166.
- Hutchinson, R.W. 1987. Metallogeny of Precambrian gold deposits: space and time relationships. *Economic Geology*, 82: 1993-2007.
- Keppie, D.J., Boyle, R.W., and Haynes, S.J., *editors*. 1986. Turbidite-hosted gold deposits. Geological Association of Canada, Special Paper 32.
- Kerrich, R. 1977. A historical review and synthesis of research on pressure solution. *Zentralblatt für Geologie und Paläontologie I*: 512-550.
- Kerrich, R., and Allison, I. 1978. Vein geometry and hydrostatics during Yellowknife mineralization. *Canadian Journal of Earth Sciences*, 15 : 1653-1660.

- Kerrick, R., Beckinsale, R.D., and Shackleton, N.J. 1978. The physical and hydrothermal regime of tectonic vein systems: evidence from stable isotopes and fluid inclusion studies. *Neues Jahrbuch Mineralogie, Abhandlung*, 131: 225-239.
- Kisch, H.J. 1987. Correlation between indicators of very low-grade metamorphism. *In* Low temperature metamorphism. M. Frey, *Ed.* Blackie, Glasgow, pp. 227-300.
- Klein, G.A., and Mountjoy, E.W. 1988. Northern Porcupine Creek Anticlinorium and footwall of the Purcell Thrust, Northern Park Range, B.C. *In* Current research, part E. Geological Survey of Canada, Paper 88-1E, pp. 163-170.
- Leonard, R. 1985. Variable structural style, stratigraphy, total-strain and metamorphism adjacent to the Purcell thrust near Blackman Creek, B.C. M. Sc. thesis, McGill University, Montreal, Quebec.
- Little, H.W., Belyea, R., Stott, D. F., Latour, B. A., and Douglas, R. J. W. 1976. Economic minerals of western Canada, *In* Geology and economic minerals of Canada. by R. J. W. Douglas, *Ed.* Geological Survey of Canada, Economic Geology Report No. 1, pp. 489-546.
- Mathews, W.H. 1944. Lode Gold Deposits: Southeastern British Columbia. British Columbia Department of Mines, Bulletin No. 20, Part 2.
- Mawer, C.K. 1986. The bedding-concordant gold-quartz veins of the Meguma Group, Nova Scotia. *In* Turbidite-hosted gold deposits. J.D. Keppie, R.W. Boyle and S.J. Haynes, *Eds.* Geological Association of Canada, Special Paper 32, pp. 135-148.
- McDonough, M. R., and Simony, P. S. 1988. Structural evolution of basement gneisses and cover, Bulldog Creek area, Rocky Mountains, British Columbia. *Canadian Journal of Earth Sciences*, 25: 1686-1702.
- Mountjoy, E.W. 1988. The Hugh Allan (Purcell) fault at Hugh Allan Creek: a low angle west-dipping thrust fault. *In* Current research, Part E.

- Geological Survey of Canada, Paper 88-1E, pp. 97-104.
- Mountjoy, E.W., and Aitken, J.D. 1963. Early Cambrian and late Precambrian paleocurrents, Banff and Jasper National Parks. *Bulletin of Canadian Petroleum Geology*, 11: 161-168.
- Mountjoy, E.W., and Price, R.A. 1985. Jasper (83D/16) geological map and cross-sections. Geological Survey of Canada, Map 1611A, scale 1:50,000.
- Mountjoy, E.W., and Price, R.A. 1989. Amethyst Lakes (83D/9) geological map and cross-sections. Geological Survey of Canada, Map 1657A, scale 1:50,000.
- Mountjoy, E.W., and Price, R.A. (in preparation). Athabasca Pass (83D/8) geological map and cross-sections. Geological Survey of Canada.
- Mountjoy, E.W., and Forest, R. 1986. Revised structural interpretation, Selwyn Range between Ptarmigan and Hugh Allan Creeks, British Columbia. *In Current research, Part A. Geological Survey of Canada, Paper 86-1A, pp. 177-183.*
- Murrel, S.A.F. 1985. Aspects of relationships between deformation and prograde metamorphism that causes evolution of water. *In Metamorphic reactions: Kinetics, textures and deformation.* A.B. Thompson and D.C. Rubie, *Eds.* Springer-Verlag, New York, pp. 211-241.
- Norris, R.J., and Henley, R.W. 1976. Dewatering a metamorphic pile. *Geology*, 4: 333-336.
- Oke, C. 1982. Structure and metamorphism of Precambrian basement and its cover in the Mt. Blackman area, British Columbia. M. Sc. thesis, University of Calgary, Calgary.
- Palonen, P. 1976. Sedimentology and stratigraphy of the Gog Group sandstones in southern Canadian Rockies. Ph.D. thesis, University of Calgary, Calgary.
- Phillips, G. N., Groves, D. I., and Martyn, J. E. 1984. An epigenetic origin for

- Archean banded iron-formation-hosted gold deposits. *Economic Geology*, 79: 162-171.
- Price, R.A., and Mountjoy, E.W. 1966. Operation Bow-Athabasca, Alberta-British Columbia. *In* Report of activities, Part A. Geological Survey of Canada, Paper 66-1A, pp. 106-112.
- Price, R.A., and Mountjoy, E.W. 1970. Geological structure of the Canadian Rocky Mountains between Bow and Athabasca Rivers - a progress report. *In* Structure of the southern Canadian Cordillera. J.O. Wheeler, *Ed.* Geological Association of Canada, Special Paper 6, pp. 7-25.
- Ragan, D.M. 1973. Structural geology. John Wiley and Sons, New York.
- Ramsay, J.G. 1980. The crack-seal mechanism of rock deformation. *Nature*, 284: 135-139.
- Ramsay, J.G. and Huber, M. 1986. The techniques of modern structural geology: Volume 2, folds and fractures. Academic Press, London.
- Ramsden, J., and Cruden, D.M. 1979. Estimating densities in contoured orientation diagrams: Summary. *Geological Society of America Bulletin*, 90: 229-230.
- Read, P.B. 1988. Metamorphic map of the Canadian Cordillera. Geological Survey of Canada, Open File 1893.
- Rose, A.W. and Burt, D.M. 1979. Hydrothermal Alteration. *In* Geochemistry of hydrothermal ore deposits. H.L. Barnes, *Ed* John Wiley and Sons, New York, pp. 173-235.
- Schroeter, T.G., and Panteleyev, A. 1986. Gold in British Columbia. British Columbia Ministry of Energy, Mines and Petroleum Resources, Preliminary Map 64.
- Secor, D.T. Jr. 1965. Role of fluid pressure in jointing. *American Journal of Science*, 263: 633-646.

- Seward, T.M. 1984 The transport and deposition of gold in hydrothermal systems. *In* Gold '82: The geology, geochemistry, and genesis of gold deposits. R. P. Foster, *Ed.* Balkema, Rotterdam, pp.165-181.
- Sinclair, A.J., Wynne-Edwards, H.R., and Sutherland-Brown, A. 1978. An analysis of distribution of mineral occurrences in British Columbia. British Columbia Ministry of Mines and Petroleum Resources, Bulletin 68.
- Sorensen, M. K. 1955. Some observations on the geology of the Rocky Mountain Trench between latitudes 53° and 53° 30'. Alberta Society of Petroleum Geologists, Fifth Annual Field Conference Guide Book, pp. 53-68.
- Tomkinson, M. J. 1988 Gold mineralization in phyllonites at the Haile Mine, South Carolina. *Economic Geology*, 83:1392-140.
- Turner, F.J. 1981. *Metamorphic petrology: Mineralogical, field and tectonic aspects*. 2nd edition. McGraw-Hill, New York.
- Wheeler, J.O. 1963. Rogers Pass map area, British Columbia and Alberta. Geological Survey of Canada, Paper 62-32.
- Wheeler, J. O., Campbell, R. B., Reesor, J. E., and Mountjoy, E. W. 1972. Structural style in the southern Canadian Cordillera. 24th International Geological Congress, Montreal, Excursion A-01 - X-01.
- Woberg, A.C. 1986. Sedimentology of the Lower Cambrian Gog Group, British Columbia: An early Cambrian tidal deposit. M. Sc. thesis, University of Alberta, Edmonton, Alberta.
- Young, F.G., 1979. The lowermost Paleozoic McNaughton Formation and equivalent Cariboo Group of eastern British Columbia: Piedmont and tidal complex. Geological Survey of Canada, Bulletin 288.



## **CHAPTER 3**

### **Siliciclastic-Hosted Lode-Gold Mineralization, Athabasca Pass, Central Canadian Rocky Mountains: A Trace Element and Fluid Inclusion Study.**

#### **Introduction**

The recent discovery of gold-bearing quartz veins in Lower Cambrian siliciclastic strata, which comprise much of the Main Ranges of the central Canadian Rocky Mountains, attests to the metallogenic potential of this vast, yet sparsely prospected, lithotectonic domain. Information on lode-gold deposits within this domain is lacking, the apparent first comprehensive documentation of gold-lodes in this region being that given in Chapter 1. In that paper the structural, mineralogical and paragenetic relationships of gold-quartz veins contained within the McNaughton Formation of the Athabasca Pass were established, and the hypothesis was forwarded that the Athabasca Pass lodes represented a siliciclastic-hosted analogue of the Turbidite-Hosted (Keppie *et al.*, 1986; Hutchinson, 1987) class of gold deposits.

In order to geochemically characterize the gold-lodes of the Athabasca Pass, and to place constraints upon the physico-chemical environments of vein formation, a trace-element geochemical and fluid inclusion study was undertaken.

#### **Regional Setting**

The Athabasca Pass is situated on the Continental Divide 60 km south of Jasper, Alberta, at the boundary between the eastern Main Ranges

and the western Main Ranges (Price and Mountjoy, 1970) of the central Canadian Rocky Mountain belt (Fig.3-1). The boundary in this region is marked by a southwest-dipping thrust fault, the Chatter Creek fault (Wheeler, 1963), which extends from the headwaters of the Fraser River, southeasterly through the Athabasca Pass, into the region northeast of Golden, British Columbia (Price and Price, 1989; Mountjoy and Price, in prep.). In the Athabasca area, this fault has transported a thick sequence of grits, greywackes, pelites, and carbonates of the Upper Proterozoic Miette Group over quartzites, quartz-pebble conglomerates, pelites, and carbonates of the Lower Cambrian Gog Group. Within the hanging wall of the Chatter Creek thrust sheet, regional metamorphic grade increases southwestward from greenschist grade to kyanite-staurolite-bearing assemblages of amphibolite grade (Craw, 1978; Klien and Mountjoy, 1988). Rocks of the immediate footwall have been regionally metamorphosed to sub-greenschist and lower greenschist grades, decreasing to burial metamorphic facies southeastwards (Read, 1988). The occurrence of igneous rocks is rare throughout the Main Ranges.

Deformation in the Main Ranges evolved through the accretion of allochthonous terranes to the western margin of North America beginning in the Late Jurassic, which resulted in the northeastward translation and thrust-stacking of thick sequences of parautochthonous miogeoclinal sedimentary rocks derived from the North American craton to the east, onto the flank of the craton (Price and Mountjoy, 1970; Price *et al.*, 1985). The geologic structure of the region is dominated by complex folding patterns and by widely spaced thrust faults. Penetrative deformation is pronounced in the western Main Ranges, and less pervasive to absent in the east (Price

and Mountjoy, 1970).

Information on lode-gold deposits in the Main Ranges, and in the Canadian Rocky Mountains in general, is lacking. The mineral occurrences and metallogeny of this region have been reviewed by Hedley (1954), Little *et al.* (1976), and Sinclair *et al.* (1978). Principal deposit-types occur to the south of the Athabasca Pass area, and include stratiform lead-zinc ( $\pm$ silver) replacement bodies in Middle Cambrian carbonates, and generally small, quartz-carbonate vein systems containing a variety of base-metal sulfide assemblages (dominantly galena-sphalerite-pyrite-chalcopyrite). Gold production has not been reported from these occurrences. Brief mention of placer gold occurrences in the Main Ranges was made by Boyle (1979), and by Mathews (1944).

### Local Geology

The general geology of the Athabasca Pass area is shown in Figure 3-1. To date, gold mineralization has been found only in the lowermost formation of the Gog Group, the McNaughton. The McNaughton Formation is composed of a series of well-stratified, mature, quartz-dominated clastic rock types (pelitic quartzite, quartzite, matrix-supported quartz-pebble conglomerate) randomly parted by discrete, discontinuous interbeds of quartz-sericite pelite. The sequence has been subjected to archimetamorphic (*ca.* pumpellyite facies) conditions during regional metamorphism. Penetrative planar fabric is evident in the quartz-dominated rock types as phyllosilicate contents reach approximately 30 percent. The pelites contain a variably developed, locally crenulated cleavage (s1). Evidence of igneous activity is entirely lacking.

The McNaughton Formation in the Athabasca Pass is confined to an 800 m-thick folded and faulted section known as McGillivray Ridge. Structurally, McGillivray Ridge consists of a series of northeast-verging thrust faults which truncate northeast-verging, upright to overturned, mesoscopic folds (f1) in individual imbricated slices of McNaughton quartzite. The structural geometry of McGillivray Ridge is that of a leading imbricate fan and is attributed to late-stage northeast-directed compressional tectonism.

#### *Mineralized veins of the Athabasca Pass*

Two vein-types, outcropping on McGillivray Ridge, have been identified: a folded, early syn-tectonic, syn-to post-metamorphic bedding-parallel variety recording prolonged or multiple stages of northeast-directed compression, and a post-folding discordant variety generated during minor sinistral shear associated with incipient, late-stage regional thrusting. Vein localization and geometry exhibit lithostructural control with bedding-parallel veins being confined to the less-competent pelitic rocks, and discordant veins being confined to the competent quartzitic units. High concentrations of gold are confined to bedding-parallel veins, with only a few discordant veins being slightly enriched in gold (up to *ca.* 500 ppb).

The mineralogy of bedding-parallel veins consists of quartz and brecciated host-pelite with minor quantities of white mica, pyrite, Fe-carbonate, galena and native gold. Two broad paragenetic stages have been identified, namely: an early protracted pre-gold stage depositing quartz and white mica  $\pm$  minor Fe-carbonate and pyrite, and a late, volumetrically minor gold-bearing and post-gold stage during which quartz, pyrite, native gold and galena  $\pm$  minor white mica and Fe-carbonate were deposited. Gold

is largely associated with pelite fragments and paragenetically sub-contemporaneous sulfides. Discordant veining was approximately coeval with gold emplacement, however these veins contain only quartz and occasional pyrite. It was postulated that pelites played an important chemical role in triggering gold deposition uniquely within bedding-parallel veins.

### Trace Element Lithochemistry

In order to characterize the trace-element geochemistry of the McNaughton Formation in the Athabasca Pass, 26 samples, including (a) unveined pelitic quartzite and conglomerate, (b) unveined pelite, (c) highly anomalous (arbitrarily  $> ca. 15$  ppm Au) gold-bearing vein, (d) slightly anomalous (arbitrarily  $< ca. 1$  ppm Au) gold-bearing vein, (e) brecciated pelite  $\pm$  minor vein material, and (f) unmineralized discordant quartz vein were analyzed by inductively coupled plasma emission spectrometry (ICPES), for 31 elements. Gold and silver contents were determined by atomic absorption spectrometry (AAS) and fire assay. All analyses were performed by a commercial laboratory (Eco-Tech Laboratories, Kamloops, B.C.). From the multi-element analyses, the element suite: arsenic-lead-zinc-copper-barium-iron was selected for presentation here, as this suite contains elements commonly found in anomalous concentrations in association with lode-gold mineralization (Boyle, 1979; Nesbitt, 1988). Other elements commonly concentrated in lode gold deposits, including antimony, tungsten, boron, tellurium and thallium were found to be below their limit of detection (DL) in both vein and unmineralized host-rock material in the present study (*i.e.* 5 ppm, 10 ppm, 2 ppm, 10 ppm, 10 ppm

respectively), and thus are not included here. Major element analyses were not carried out.

### ***Results***

Figure 3-2 portrays data from ICPES and AAS analyses (also see Appendices 1 and 2). For comparative purposes, histograms of average concentrations of the same element-suite for similar unmineralized rock types (quartzite, argillite/slate, conglomerate, greywacke) drawn utilizing data compiled from the literature are also included. Comparing the trace-element concentrations of the unmineralized McNaughton rock types of Athabasca Pass (Figs. 3-2A, 3-2B) with estimates of average element contents in comparable rock types (Figs. 3-2G, 3-2H) it is evident that although consistently somewhat lower than average in trace element contents, the Athabasca Pass rock types are not significantly different from the average comparable rock-types from other localities. This apparent depletion is perhaps attributable to the fact that the McNaughton Formation in the Athabasca Pass is a very mature clastic sequence composed dominantly (*ca.* 97 %) of quartz-rich (averaging >90 % quartz) rock types which only rarely contain significant quantities of varietal minerals or of feldspar. The remaining few percent of strata comprising the McNaughton Formation at this locality are pelites composed of fine-grained greenish-white mica with variable proportions of detrital quartz. Thus, in view of this mature, almost monomineralic (hence limited elemental) spectrum relatively low abundances of trace elements are understandable. Also, the McNaughton rock types have been subjected to anchimetamorphic conditions, during which a variable degree of recrystallization of allogenic quartz and clay

constituents has taken place. Although unmineralized samples were collected over 200 m from the nearest gold-bearing veins and the samples appeared visibly unaltered, some trace element mobilization/depletion during recrystallization cannot be precluded. Finally, some discrepancy may have been introduced by the inclusion of data from the literature for samples which vary in mineralogical maturity and hence exhibit different trace-element chemistry from the McNaughton rock types. The effect of such variation is evidenced by the higher trace element contents exhibited by less mature sedimentary rocks such as greywacke, as shown in Figure 3-2I.

#### *Athabasca Pass rock types*

Focussing upon the Athabasca Pass data, the following observations are noteworthy. In general, vein and vein-associated rock types (Figs. 3-2C, 3-2D, 3-2E, 3-2F) show a variable, yet distinct, enrichment of most trace elements in the suite with respect to the unmineralized host rocks (Figs. 3-2A, 3-2B). Gold shows the greatest enrichment in all vein samples. Silver, zinc and copper show negligible to minor (near level-of-detection, therefore possibly only apparent) enrichments, while lead, arsenic and barium show enrichment between approximately two and ten times their concentrations in the host rocks. The behaviour of iron is somewhat more complex with the mineralized rock types showing enrichment over the quartzose host rocks (Fig. 3-2A) and depletion with respect to the unmineralized pelitic rocks (Fig. 3-2B). The vein samples were selected to contain as few pelite fragments as possible, thus the iron in these samples is contained dominantly in the form of pyrite (and secondary Fe-oxides) whilst that in

the pelitic rocks would be structurally contained within the phyllosilicate minerals of the rock.

In order to identify and portray sympathetic variations in trace-element concentrations with respect to gold, data from the vein samples used to generate the averages shown in histograms 3-2C (highly anomalous bedding-parallel veins) and 3-2D (moderately anomalous bedding-parallel veins) were plotted in the form of a concentration versus element line graph (Fig. 3-3). Eight samples representing four orders of magnitude of gold concentration (*i.e.* 0.4 ppm to 573 ppm Au) were selected for comparison. From these data it is evident that silver, zinc and copper are of essentially constant concentration in the vein structures, regardless of gold content. Lead, arsenic and barium show relatively good (albeit non-proportional) positive correlation with gold content. Positive lead correlation is in accord with the observation that galena is paragenetically sub-contemporaneous with native gold, its presence often being indicative of higher gold grades. Arsenic is likely contained in isomorphous solution within pyrite which is also broadly coeval with gold (instrumental neutron activation analyses of vein pyrite separates contained up to 1800 ppm arsenic (Appendix 2)). No discrete arsenide phases have been identified in the veins. Barium is likely present substituting for potassium in the white micas ( $\pm$  pelite fragments) contained within the vein structures. Hydrothermal white mica deposition is again demonstrably coeval with gold emplacement.

Points A and B, shown on Figure 3-3, denote the silver content (8.8 ppm) of sample 524 and the zinc content (147 ppm) of sample 599 respectively. These points represent isolated, anomalously high (1 to 2 orders of magnitude) concentrations of silver and zinc with no apparent correlations within the general data trend and are interpreted to suggest the



presence of minor mineral phases (Ag and Zn sulfides?) which have not been detected during hand specimen and thin section petrography.

Of interest is the overall low concentration of silver, and the apparent lack of gold-silver correlation within the mineralized veins of the Athabasca Pass. Numerous works documenting gold fineness and Au/Ag ratios across essentially the entire spectrum of hypogene gold-bearing deposit types (see Boyle, 1979 for a literature review of gold fineness and Au/Ag ratios) have shown that silver is almost ubiquitously alloyed with native gold, and that silver-bearing sulfides and/or sulfosalts are common in the ore assemblages of many gold deposits. With respect to the general turbidite-hosted class of gold deposits, both gold fineness and Au/Ag ratios are, in general, relatively high (averaging approximately 850-900 fine and 4:1 to 9:1 respectively). Energy dispersive analyses of native gold grains from the Athabasca Pass lodes failed to reveal the presence of silver (or of any other trace metal) in quantities detectable by this method (DL ca 1-2 %). In order to further investigate gold-silver relationships in the Athabasca Pass lodes, 30 samples of gold-bearing vein material were analysed for gold and silver by AAS. The results of this survey, portrayed in simple scatter-plot form in Figure 3-4 emphasize the sparse concentration of silver and the lack of gold-silver correlation. These data support the homogeneity and high fineness of the native gold implied by the energy dispersive analyses. Also, the few isolated concentrations of silver indicated by AAS further suggest the occasional presence of a minor silver-bearing phase in the Athabasca Pass lodes.

### *Discussion of trace element data*

An integrated discussion of these data, and data derived from the fluid inclusion study will be undertaken following presentation of the latter. At this point some conclusions regarding the trace element distributions will be emphasized.

Of importance is the observation that, although the mineralized rock types of the McNaughton Formation are enriched in trace-elements with respect to their host rocks, they are, when compared with Turbidite-Hosted, and lode-gold systems in general, conspicuously non-enriched with respect to all trace elements, excepting gold (*e.g.* Boyle, 1979; Foster *et al.*, 1986; Steed and Morris, 1986). This characteristic is observed directly in the relatively simple mineralogy exhibited by the mineralized Athabasca Pass structures, and may be attributable to 1) the paucity of trace elements in the source regions and channel-ways of the mineralizing fluids leading to only sparse concentrations within depositional structures, or 2) the inability of the fluids responsible for vein-filling to mobilize, transport, or deposit trace elements and hence create anomalous concentrations.

With respect to gold, the arithmetic average of 22 ppb Au for the unmineralized quartzitic rock types of the Athabasca Pass (Fig. 3-2A) falls central within the range given by Boyle (1979) and Crocket (1974) for average quartz sandstone/conglomerate (31 ppb) (Fig. 3-2G) and greywacke (3 to 13 ppb, Fig. 3-2H). A more extensive survey of unmineralized rock types in the Athabasca Pass involving 60 analyses of McNaughton quartzite indicates gold values range between limit of detection (5ppb) and 115 ppb, with 8 samples containing over 30 ppb Au (Appendix 3). Thus, although the McNaughton rock types contain, in general, "average" quantities of gold, it

is evident that they may locally contain anomalously high gold concentrations. The nature of this gold is open to speculation (Boyle, 1979). Samples containing sulfide in any form were avoided during this survey, precluding potential epigenetic gold concentrations in this form. If one considers the McNaughton Formation to represent a thick, mature, quartzitic sequence deposited under prolonged fluvial braidplain to shallow marine conditions (Young, 1979; Palonen, 1976; Woberg, 1986), the gold contained within these rocks would potentially be of a detrital nature. Greater concentrations within the host rocks may represent low-grade, syngenetic placer accumulations, derived during the erosion of Precambrian North American basement rocks to the east (Burwash, 1951; Mountjoy and Aiken, 1963). In comparison with studies investigating local rock types as the potential source for lode-contained gold in sedimentary domains (*e.g.* Glasson and Keays, 1976; Graves and Zentilli, 1982; Henley *et al.*, 1976; Crocket *et al.*, 1982), the unmineralized McNaughton rock types of the Athabasca Pass apparently contain ample gold which could have been concentrated by mobilization into lode-type structures. The mobilization of detrital gold, likely of enhanced fineness due to the preferential leaching of silver and other metals in the placer regime (Desborough, 1970; Boyle, 1979), could account for the very high fineness of gold now contained within the Athabasca Pass lodes.

### Fluid Inclusion Study

To investigate the fluid compositional and P-T regime, and to gain insight into the processes involved in gold-quartz mineralization in the Athabasca Pass, a detailed study of fluid inclusions in mineralized vein

quartz was undertaken. A brief outline of the vein-quartz paragenetic relationships is summarized here in order to clarify the paragenetic relationships between gold-stage mineralization and the fluid inclusions examined in this study (see chapter 1 for a complete discussion of vein paragenesis).

On the basis of textural, optical and paragenetic characteristics, observed in hand specimen and in thin sections, three varieties of quartz, Types I, II and III have been defined within the gold-bearing veins of the Athabasca Pass. Type I quartz, comprising 90 to 95 percent of most veins, represents a prolonged, paragenetically early, pre-gold stage of multiple vein infillings, and has been subject to penetrative deformation during f1 folding. Deformational characteristics including undulatory extinction, deformation lamellae, and sub-grain development have been overprinted by episodes of late, variably healed, brittle fracturing. The gold-stage assemblage native gold  $\pm$  pyrite  $\pm$  galena  $\pm$  minor white mica and Fe-carbonate is commonly seen where late fractures intersect fragments of pelitic host rock contained within the veins. Type II quartz occurs as discrete dilational fracture-fillings in Type I quartz. It is a minor vein filling phase ( $\leq 2\%$ ) considered to have been derived through pressure solution of local, Type I quartz during progressive deformation. Type III quartz is seen filling diffusely bound fractures and voids of irregular size and shape in Types I and II quartz. It is paragenetically late and is petrographically distinguishable by its relatively unstrained appearance (minor undulatory extinction and brittle fracturing). Emplacement of the gold-stage assemblage is sub-contemporaneous with this latter quartz type.

### ***Methodology***

Analyses were made on fluid inclusions in 12 samples containing Types I and III quartz from high-grade gold-bearing veins outcropping on McGillivray Ridge. Thirty doubly-polished quartz-plates were prepared from these samples. Microthermometric measurements were performed using a U.S. Geological Survey gas-flow heating-freezing stage which was calibrated using liquid nitrogen, the triple points of pure CO<sub>2</sub> and H<sub>2</sub>O, and the Merck standard 9800 (melting point 200°C). Analytical reproducibilities were  $\pm 0.2^\circ\text{C}$  for freezing and  $\pm 4^\circ\text{C}$  for heating to temperatures of approximately 300°C.

### ***Classification of fluid inclusions***

Due to the pervasively deformed nature of much of the quartz vein material, and to the multiple generations of fracturing, vein filling, and fracture healing (precluding establishment of fluid inclusion paragenesis), fluid inclusions were classified primarily on their mode of occurrence in relation to the gold  $\pm$  galena  $\pm$  pyrite assemblage, and subsequently on their appearance upon cooling to 0-10°C. Thus, two general types of fluid inclusions, Type A and Type B have been defined. Type A inclusions were studied in most inclusion plates but bore no physically traceable link to gold mineralization. A full range of physical and microthermometric data were recorded for Type A inclusions, but these data were utilized only as a general survey of the various fluid inclusion types *sensu lato* observed in the Athabasca Pass gold-quartz lodes. Little interpretive weight is placed on Type A data, due to their uncertain, likely varied origin. Type A inclusions are considered secondary or pseudosecondary (Roedder, 1984) with respect to

gold stage mineralization.

Fortunately, abundant coarse-grained visible gold is observed in the Athabasca Pass lodes. Thus, 15 inclusion plates representing 9 different samples of vein material containing the assemblage native gold  $\pm$  galena  $\pm$  pyrite, hosted by Types I and III quartz were prepared. Clearly visible groups of inclusions were located in relatively undeformed quartz surrounding and filling embayments in native gold and galena. Type B inclusions are defined by this occurrence (Fig. 3-5). Most Type B inclusions analysed were less than 100  $\mu\text{m}$  distant from native gold. Those fluid inclusions exhibiting any evidence of necking, leakage or (rarely) erratic liquid to vapor-phase ratios were not used. Type B inclusions may be classified as secondary and/or pseudosecondary with respect to Type I quartz, but relative to Type III quartz and the gold  $\pm$  galena  $\pm$  pyrite assemblage, they were considered to be primary and hence representative of the fluids responsible for gold mineralization in the Athabasca Pass.

#### *Description of Fluid Inclusions*

**Type A:** This fluid inclusion type occurs in both Types I and III quartz, distributed as isolated inclusions, random inclusion clusters, and along late and partially healed fractures. Type A inclusions generally contain two phases at room temperature, H<sub>2</sub>O-rich liquid and vapor, although 3 phases (H<sub>2</sub>O-rich liquid, carbonaceous fluid and vapor) are occasionally observed. Disregarding inclusions which have obviously undergone post-entrapment modification (necking, leakage *etc.*), Type A inclusions are generally subequant to ellipsoidal in shape (although irregular and negative crystal shapes were also recorded), and range in

greatest dimension from 4 to 45  $\mu\text{m}$ , averaging 10.5  $\mu\text{m}$ . Phase ratios for Type A inclusions vary between approximately 5 and 30, with most containing between 10 and 20 volume percent vapor. Vapor-rich Type A inclusions are rare. Those observed exhibit no phase changes between  $-140^\circ$  and  $300^\circ\text{C}$  and are likely "empty", the result of natural decrepitation or leakage (Roedder, 1984). Daughter phases were not observed in any Type A fluid inclusions.

*Type B:* This fluid inclusion type is also found in both Types I and III quartz, but based upon petrographically established relationships is considered primary with respect to the gold assemblage. Two varieties of Type B fluid inclusions were defined based upon the number of phases observed upon cooling to  $0-10^\circ\text{C}$ .

*Type B1. Two phase  $\text{H}_2\text{O}$ -rich liquid + vapor  $\pm$  (not visible)  $\text{CO}_2$ -bearing fluid inclusions.* This inclusion type ranges in size from 4 to 24  $\mu\text{m}$ , averaging approximately 10  $\mu\text{m}$  in greatest dimension. Generally, sub-angular to sub-rounded and sub-equant to prismatic in shape, Type B1 inclusions occur as isolated individual fluid inclusions or randomly arranged inclusion clusters. Freezing experiments indicated Type B1 inclusions contain  $\text{H}_2\text{O}$ -rich brine. Clathrate formation (melting at less than  $10^\circ\text{C}$ ) indicated the presence of small quantities of  $\text{CO}_2$  in about one half of all Type B1 inclusions, but a discrete liquid  $\text{CO}_2$  phase was not observed. Such inclusions may contain up to 3 mole percent  $\text{CO}_2$  at pressures between *ca.* 10.4 and 45 bars (Hedenquist and Henley, 1985).

*Type B2. Three phase  $\text{H}_2\text{O}$ -rich liquid + carbonaceous liquid + vapor-bearing fluid inclusions.* Based upon habit and mode of occurrence, at room temperature Type B2 fluid inclusions are indistinguishable from

Type B1. Slow cooling, usually below about 15°C nucleated a third, CO<sub>2</sub>-rich vapor phase, defining Type B2 inclusions. Phase changes recorded during freezing experiments (including heating up to the homogenization temperature of CO<sub>2</sub>) indicated the presence of variable (generally small) but ubiquitous quantities of additional volatiles and dissolved salts. CO<sub>2</sub> in all Type B2 inclusions homogenized exclusively to the liquid state.

As noted, based upon appearance at room temperature, Type B1 and B2 fluid inclusions are indistinguishable. Both types may occur in a single inclusion cluster, but generally one type is dominant over the other (ratios generally  $\geq 10:1$ ). Phase ratios of liquid to vapor in Type B1 inclusions and H<sub>2</sub>O-rich liquid to CO<sub>2</sub>-rich liquid in Type B2 inclusions are similar, varying only slightly between different samples and being uniform within individual samples and inclusion clusters. Visual estimates of phase volumes obtained using a graduated ocular lens, and diagrams illustrating degree-of-fill and volume percentages (Roedder, 1984; Shepherd *et al.*, 1985) for various fluid inclusion shapes, range from 9 to 20 and average 12 to 18 volume percent vapor (Type B1) or liquid CO<sub>2</sub> (Type B2). Such visual estimates are subject to potentially large errors due to the uncertainties and assumptions made in estimating the depth dimension of fluid inclusions (Bodner, 1983; Roedder, 1984; Shepherd *et al.*, 1985). Neither daughter crystals nor vapor-rich inclusions were observed during Type B inclusion study.

#### ***Microthermometric analysis of fluid inclusions***

In order to minimize the effects of phase metastability during freezing-heating runs, all phase changes were observed during the heating cycle. Data recorded through phase changes included; 1) the temperature of



final CO<sub>2</sub> melting ( $T_{mCO_2}$ , observed in Type B2 inclusions), 2) the temperature of final ice melting ( $T_{mice}$ , observed in Types A, B1 and B2 inclusions), 3) the temperature of final clathrate melting ( $T_{mclath.}$ , observed in Types A, B1 and B2 inclusions), 4) the temperature of CO<sub>2</sub> homogenization ( $T_{hCO_2}$ , observed in three phase Type A inclusions, and Type B2 inclusions), 5) the temperature of decrepitation ( $T_{decrep.}$ , observed dominantly in Type B2 and occasionally Type B1 and Type A inclusions) and, 6) the temperature of total phase homogenization ( $T_{htotal}$ , observed where possible in all inclusion types).

Estimates of aqueous fluid salinities (expressed as weight % NaCl equivalent) were derived from  $T_{mice}$  and  $T_{mclath.}$  data utilizing phase relations and techniques described by Potter *et al.* (1978; H<sub>2</sub>O-NaCl equivalent system), and by Bozzo *et al.* (1975) and Collins (1979; H<sub>2</sub>O-CO<sub>2</sub>-NaCl system). Additional constraints were placed upon bulk fluid composition and phase densities utilizing  $T_{mCO_2}$ ,  $T_{hCO_2}$  and  $T_{htotal}$  data in conjunction with phase relations in the H<sub>2</sub>O-NaCl system (summarized by Crawford, 1981 and Roedder, 1984), and in the H<sub>2</sub>O + CO<sub>2</sub> ± NaCl ± CH<sub>4</sub> systems (summarized by Hollister and Burruss, 1976; Eurruss, 1981; Pichavant *et al.*, 1982; Roedder, 1984; and Seitz *et al.*, 1987). Microthermometrically-derived analytical results for all Type A fluid inclusions studied are listed in Appendix 4. Data for all Type B inclusions are graphically portrayed in Figures 6 and 7.

*Type A.* Due to the unconstrained origin of Type A inclusions, data from these types will not be reviewed in detail here other than to note the overall similarity between inclusion Types A and B (see Appendix 4 for comparison with Type B inclusions). The more varied phase ratios,

salinities and temperatures of total homogenization observed in Type A inclusions likely reflect a potentially more varied origin or some post-trapping modification, but the general congruence between many Type A and Type B1 inclusion data suggests many Type A inclusions may share an origin similar to that of the Type B inclusions.

**Type B1.** This inclusion type is essentially defined by the system  $\text{H}_2\text{O} + \text{NaCl} \pm \text{CO}_2$ . NaCl-equivalent salinities calculated from aqueous fluid freezing-point depression ( $T_{m_{\text{ice}}}$ ) data for those inclusions showing no evidence of the presence of  $\text{CO}_2$  (*i.e.* clathrate formation) range from 7 to 10, averaging 8.5 wt. percent NaCl equivalent (Fig. 3-6A). Hedenquist and Henley (1985) note that the presence of small quantities of dissolved  $\text{CO}_2$  (< *ca.* 1 mole %) in aqueous solutions may go undetected, enhancing freezing point depression, hence the above salinity estimates are considered as maxima. Where clathrate formation was detected, coexisting aqueous solution, liquid  $\text{CO}_2$  and vapor phase were not present upon clathrate melting, thus accurate salinity estimates based upon clathrate melting are precluded. Such estimates are erroneously high (Collins, 1979). Nevertheless, salinities were calculated from Type B1  $T_{m_{\text{clath.}}}$  data, providing approximate maxima, and hence constraining the salinity of clathrate-forming Type B1 inclusions to values somewhat less than those calculated (*i.e. ca.* 4 to 10, averaging 5 wt. % NaCl equivalent). This implies that Type B1 inclusions containing enough  $\text{CO}_2$  to form clathrate (between *ca.* 1 and 3 mole %; Hedenquist and Henley, 1985) are distinctly less saline than those which do not form clathrate (Fig. 3-6A).

$T_{h_{\text{total}}}$  data for Type B1 inclusions vary from approximately 190° to 290°C with most data clustering in the 210 to 225°C range (Fig. 3-6B). Based

upon an average salinity of 8.5 wt. percent NaCl equivalent and negligible CO<sub>2</sub> content, this translates to fluid densities of approximately 0.9 to 0.92 g cm<sup>-3</sup> (Haas, 1976). Significant differences in Th<sub>total</sub> between clathrate-forming and non-clathrate forming Type B1 inclusions were not observed.

**Type B2.** This fluid inclusion type is compositionally approximated by the system H<sub>2</sub>O + carbonaceous fluid + NaCl. Consistent depression of the CO<sub>2</sub> freezing point (T<sub>mCO<sub>2</sub></sub>) below the pure CO<sub>2</sub> invariant point (-56.6°C) indicates the presence of small quantities of additional volatile components in Type B2 inclusions. T<sub>mCO<sub>2</sub></sub> measurements range from approximately -60° to -57°C clustering about -58°C (Fig. 3-7A), and are interpreted to indicate T<sub>mCO<sub>2</sub></sub> depression due to the presence of minor quantities of CH<sub>4</sub> (Hollister and Burruss, 1976; Burruss, 1981; Roedder, 1984). Other gases including higher hydrocarbons, N<sub>2</sub>, SO<sub>2</sub>, and/or H<sub>2</sub>S may also be present (Roedder, 1984). Due to the preferential partitioning of CH<sub>4</sub> into the vapor phase, T<sub>mCO<sub>2</sub></sub> does not uniquely define the bulk carbonaceous phase CH<sub>4</sub> content (Burruss, 1981); such data must be used in conjunction with Th<sub>CO<sub>2</sub></sub>.

Th<sub>CO<sub>2</sub></sub> data for Type B2 inclusions are summarized in Figure 3-7B. Carbonaceous phase liquid-vapor homogenization temperatures range from approximately -7° to +25°C, clustering in the +23°C region. Carbonaceous liquid-vapor homogenization occurs exclusively to the liquid phase. Applying the graphical methods of Heyen *et. al.* (1982) for estimation of CH<sub>4</sub> content from combined T<sub>mCO<sub>2</sub></sub> and Th<sub>CO<sub>2</sub></sub> data, the carbonaceous phase CH<sub>4</sub> content of Type B2 inclusions ranges from 2 to 16 mole percent, averaging *ca.* 8 mole percent CH<sub>4</sub>. Combined with typical values for T<sub>mCO<sub>2</sub></sub> and Th<sub>CO<sub>2</sub></sub> of -58°C and +18°C respectively, this translates to a

typical bulk carbonaceous fluid phase density of approximately  $0.7 \text{ g cm}^{-3}$ . It is noted, however, that  $T_{m\text{CO}_2}$  vs.  $T_{h\text{CO}_2}$  measurements in Type B2 fluid inclusions do not vary in a linear fashion, and samples exhibiting similar  $T_{m\text{CO}_2}$  do not necessarily homogenize at the same  $T_{h\text{CO}_2}$ . Such inconsistencies might be attributed to variations in fluid density and/or variations in fluid composition (Seitz *et. al.*, 1987).

Aqueous phase salinity estimates for Type B2 inclusions (Fig. 3-7C) were derived using the relationship between final clathrate melting ( $T_{m\text{clath.}}$ ) and salinity given by Bozzo *et. al.* (1975). As discussed by Hollister and Burruss (1976), and Collins (1979) the presence of additional volatile compounds such as  $\text{CH}_4$  shifts  $T_{m\text{clath.}}$  to higher temperatures, due to the formation of mixed  $\text{CO}_2\text{-CH}_4$  hydrates, hence counteracting the effect of  $T_{m\text{clath.}}$  depression by NaCl. However, the effect of  $\text{CH}_4$  on clathrate decomposition temperatures is considered to be minimal in this study. Clathrate decomposition in Type B2 inclusions is tightly clustered between  $7.5^\circ$  and  $8^\circ\text{C}$ , rarely extending above  $8.5^\circ\text{C}$ , and shows no sympathetic increase with increasing  $\text{CH}_4$ . As well, recent study of  $\text{CO}_2\text{-CH}_4$  hydrates by Seitz *et. al.*, (1987) implies negligible partitioning of  $\text{CH}_4$  into clathrate at low  $\text{CH}_4$  abundances. Furthermore,  $T_{m\text{ice}}$  data for Type B2 inclusions imply residual fluid (hence maximum) salinities of between 6 and 10 wt. percent NaCl equivalent, thus salinities averaging between 3.5 and 6 wt. percent NaCl equivalent derived from Type B2  $T_{m\text{clath.}}$  data appear reasonable.

Figure 3-7D portrays  $T_{\text{decrep.}}$  and  $T_{h\text{total}}$  (exclusively to liquid) data derived from Type B2 fluid inclusions.  $T_{h\text{total}}$  data were obtained for less than *ca.* one third of Type B2 homogenizations attempted, with temperatures acquired ranging from  $210^\circ$  to  $315^\circ\text{C}$ , and most data falling

between 225° and 245°C. More commonly, decrepitations were witnessed for Type B2 inclusions, generally in the temperature range 150° to 220°C. It was observed that prior to decrepitation, most of these inclusions exhibited only minor bubble contraction hence the average homogenization temperature observed (*ca.* 230°C) may represent a relatively low value with respect to the entire Type B2 inclusion population.

The lack of published empirical data pertaining to the compositional and volumetric properties of the H<sub>2</sub>O-NaCl-CO<sub>2</sub>-CH<sub>4</sub> system at high temperatures precludes quantitative assessment of bulk fluid density in Type B2 fluid inclusions via the non-destructive analytical techniques used in this study. The predictive capabilities of theoretical equations of state developed in recent years are restricted in general to three component systems (*e.g.* H<sub>2</sub>O-CO<sub>2</sub>-CH<sub>4</sub>; Jacobs and Kerrick, 1981; H<sub>2</sub>O-CO<sub>2</sub>-NaCl; Bowers and Helgeson, 1983a), and extrapolation to the fourth component is relatively unconstrained (Holloway, 1981). However, it is well established that addition of even small quantities of NaCl and/or CH<sub>4</sub> to the complimentary three component system will significantly affect the P-V-T properties of the bulk fluid by overall expansion of the two phase (liquid-vapor) field to higher temperatures and pressures (*e.g.* Bowers and Helgeson, 1983b; Hollister and Burruss, 1976).

In order to semi-quantitatively estimate bulk fluid densities and compositions of Type B2 inclusions used herein, the bulk density of the carbonaceous phase was adjusted to a "CO<sub>2</sub>-equivalent" density using the method of Swanenberg (1979). This data, in the form of an adjusted Th<sub>CO<sub>2</sub></sub> (the addition of *ca.* 1°C per mole % CH<sub>4</sub> (Arai *et al.*, 1971)), was then inserted along with Tm<sub>clath.</sub> and Th<sub>total</sub> data for individual inclusions

into an iterative computer program (Lynch, 1988) which calculates  $X_{CO_2}$ , bulk molar volume, and pressure (on the two phase boundary) of  $H_2O-CO_2-NaCl$  fluid inclusions from salinity,  $Th_{CO_2}$ , and  $Th_{total}$  data based upon the method of Parry (1986). This method applies calculations and phase relationships presented by Bodner (1983) and Bowers and Helgeson (1983a,b) to three phase  $H_2O-CO_2-NaCl$  fluid inclusions, and requires only accurate freezing and heating measurements. The method is advantageous in that the accuracy of the  $X_{CO_2}$  estimate obtained is not related to a volumetric estimate of the  $CO_2$  phase as is required for other methods (e.g. Burruss, 1981; Bodner, 1983), but only to the accuracy of the temperature data generated through heating and freezing experiments. Thus uncertainty, potentially large inaccuracies related to the visual estimation of phase volumes in fluid inclusions (Bodner, 1983; Roedder, 1984; Shepherd *et al.*, 1985) are avoided. Applying the above outlined method to appropriate Type B2 fluid inclusions (*i.e.* those for which  $T_{m,clath.}$ ,  $Th_{CO_2}$ , and  $Th_{total}$  data were obtained, see Table 3-1), compositional estimates range from 4 to 11 averaging 7 to 8 mole percent  $CO_2$  "equivalent" with bulk fluid densities averaging approximately  $0.9$  to  $0.95$   $g\ cm^{-3}$ .  $X_{CO_2}$  within individual fields of inclusions is noted to be relatively constant. Application of a graphical procedure given by Schwartz (1989) yielded comparable results.

### ***Summary of Fluid Inclusion Data***

Two general types of fluid inclusions, two phase Type B1, and three phase Type B2 have been identified as coeval with gold mineralization in the quartz lodes of the Athabasca Pass. Three broad fluid compositions are preserved in these inclusions. Type B1  $H_2O-NaCl\pm CO_2$ -bearing inclusions

may be subdivided into two varieties, namely: 1) those which form gas hydrates upon cooling and thus contain between approximately 1 and 3 mole percent CO<sub>2</sub> (Hedenquist and Henley, 1985), and 2) those which do not form gas hydrates and thus contain less than approximately 1 mole percent CO<sub>2</sub>. Based upon  $T_{m_{ice}}$  data, Type B1 inclusions exhibit salinities between 5 and 10 wt. percent NaCl equivalent with clathrate-forming inclusions being somewhat less saline.  $T_{h_{total}}$  data for Type B1 inclusions are relatively well constrained in the 215° to 225°C range.

Type B2 H<sub>2</sub>O-NaCl-CO<sub>2</sub> ±CH<sub>4</sub>-bearing inclusions exhibit aqueous phase salinities between approximately 1.5 and 6, averaging 3.8 wt. percent NaCl equivalent. Expressed on a "CO<sub>2</sub>-equivalent" basis (Swanenberg, 1979), Type B2 inclusions contain between 4 and 12 averaging approximately 8 mole percent total carbonaceous phase (dominantly CO<sub>2</sub> containing 2 to 16 mole % CH<sub>4</sub>).  $T_{h_{total}}$  data for Type B2 inclusions is limited due to frequent decrepitation prior to homogenization.  $T_{h_{total}}$  measurements obtained cluster between 225° and 245°C and are considered to represent a minimum  $T_{h_{total}}$  value. Inclusion decrepitation generally occurred between 150° and 220°C.

Type B1 and B2 fluid inclusions are petrographically indistinguishable at room temperature, being of similar size and shape, exhibiting comparable apparent phase ratios, and occupying an equivalent paragenetic position with respect to the native gold ± galena ± pyrite assemblage.

### *Interpretation*

The constant phase ratios and relatively well-constrained

compositional and  $Th_{total}$  data exhibited by Type B1 and Type B2 fluid inclusions suggests entrapment of homogeneous one phase fluids accompanied gold emplacement in the Athabasca Pass lodes. Although Types B1 and B2 inclusions appear paragenetically sub-contemporaneous, it is evident from their relative spatial distribution, contained phase ratios, and the general P-V-T-X relationships in the  $H_2O-NaCl-CO_2 (\pm CH_4)$  system that the observed fluid compositions were likely not generated through fluid immiscibility processes (effervescence, unmixing, etc; see Ramboz *et al.* 1982). One feasible alternative is the mixing of two compositionally distinct fluids, in this case a moderately saline, relatively cooler aqueous brine (Type B1), mixed with a warmer  $H_2O-CO_2 \pm CH_4$ -bearing fluid of low salinity (Type B2). This interpretation, however, is precluded by a general lack of fluid mixing trends in the overall data set. For instance fluid inclusions of intermediate bulk composition are relatively rare, and correlation between  $Th_{total}$  and salinity, and/or mole percent  $CO_2$  and salinity is lacking. Furthermore, as noted earlier, inclusion fields containing compositionally mixed fluids are not observed. Clathrate-forming Type B1 inclusions studied here may in part represent these mixtures, but the data are too sparse to be conclusive.

A second alternative process involves the evolution of the gold-mineralizing fluid from a relatively warmer,  $CO_2$ -rich aqueous fluid (Type B2) to a cooler  $CO_2$ -poor aqueous brine (Type B1). This interpretation also suffers from the general lack of progressively developed, intermediate fluid compositions. However, it better accounts for the absence of compositionally mixed fields of fluid inclusions; individual inclusion clusters tend to be isocompositional because they have trapped homogeneous fluids at unique instances during the progressive



mineralizing event. This interpretation implies that, within the gold depositional stage, Type B1 inclusions were trapped somewhat later than Type B2, an inference suggested by the lower  $T_{\text{total}}$  temperatures recorded for Type B1 inclusions. Clathrate-forming Type B1 inclusions may again represent intermediate fluid compositions.

### *P-T conditions of fluid entrapment*

The fluids trapped as inclusions in the auriferous quartz lodes of the Athabasca Pass exhibit no evidence of immiscibility, hence only minimum pressure and temperature conditions during mineralization are provided by  $T_{\text{total}}$  and fluid compositional data.  $T_{\text{total}}$  for the majority of Type B1 and Type B2 inclusions fall between 210° and 245°C with Type B2 data averaging approximately 15°C higher than Type B1 (*ca.* 230°C versus *ca.* 215°C respectively). Pressure estimates at  $T_{\text{total}}$  (*i.e.* on the 2 phase solvus) for H<sub>2</sub>O-NaCl-"CO<sub>2</sub> equivalent"-bearing Type B2 fluid inclusions, obtained utilizing the technique and phase relationships described by Parry (1986) and Bowers and Helgeson (1983 a,b) respectively are listed in Table 3-1. Because of frequent decrepitation prior to  $T_{\text{total}}$ , the quantity of data is limited. Regardless the estimates obtained for individual samples (four are represented) are consistent, with minimum (*i.e.*  $T_{\text{total}}$ ) pressure estimates ranging from approximately 1000 to 1200 bars. Such estimates are in accord with the general tendency for Type B2 inclusions to decrepitate prior to homogenization implying internal inclusion pressures in excess of approximately 1000 bars (Leroy, 1979; Roedder and Bodner, 1980). As well, moderately high ambient pressures would be required to prevent the unmixing of Type B2 H<sub>2</sub>O-NaCl-CO<sub>2</sub> ± CH<sub>4</sub> fluids (Takenouchi and

Kennedy, 1965; Bowers and Helgeson, 1983a,b). In the absence of an independent geobarometer or geothermometer, further constraint of the pressure and temperature range of trapping cannot be derived from Type B2 inclusion data alone.

Type B1 fluid inclusions, as discussed earlier, were trapped sub-contemporaneously with or (if progressive fluid evolution is considered) slightly later than Type B2 inclusions. If the apparent lack of fluid unmixing, and the generally consistent minimum fluid pressure estimates derived for Type B2 inclusions may be considered to represent relatively stable fluid pressure conditions during inclusion entrapment, then the pressure of trapping estimates for Type B2 inclusions should also apply to Type B1 inclusions. Hence, because phase separation takes place at higher pressures in carbonaceous phase-bearing brines than in brines containing no carbonaceous phase (e.g. Takenouchi and Kennedy, 1965; Haas, 1976), a semi-quantitative, pressure correction may be derived for Type B1 inclusions. Consider an average Type B1 fluid composition (aqueous liquid + ca. 8.5 wt. % NaCl eq.) which homogenizes at 215°C. A pressure of trapping in the vicinity of 900 to 1200 bars is reasonable if the fluids are assumed to have been trapped coeval with or slightly later than Type B2 (decrepitation was also observed prior to  $T_{h\text{total}}$  for a number of Type B1 inclusions, supporting trapping pressures in this range). Thus, interpolating pressure correction data for the H<sub>2</sub>O-NaCl system given by Potter (1977), addition of approximately 80° to 110°C for the pressure range and average fluid composition outlined above yields pressure-corrected  $T_{h\text{total}}$ -temperatures for Type B1 inclusions of 295° to 315°C. A similar temperature increment must also apply to Type B2 inclusions assuming

penesynchronous Type B<sup>1</sup> and B2 inclusion trapping. Thus pressure-corrected  $T_{\text{total}}$  temperatures for Type B2 inclusions fall in the 310° to 330°C range.

It must be emphasized that the corrected P-T conditions of inclusion trapping proposed above are conservative, minimum approximations as they are based upon a minimum estimate of trapping pressure, *i.e.* on the two phase boundary for Type B2 inclusions. In view of the lack of fluid immiscibility, and the frequency with which inclusion decrepitation was observed, fluid pressures at trapping were likely significantly above this solvus. As well, the expansion of the two phase field due to the presence of minor CH<sub>4</sub> (Hollister and Burruss, 1976) has not been taken into account. With respect to the proposed pressure corrections, these estimates are based upon average fluid composition and  $T_{\text{total}}$  measurements for which there are in fact ranges. Compensating for fluid compositional and  $T_{\text{total}}$  variation involves corrections of  $\pm 20^\circ\text{C}$  for the temperatures of entrapment proposed above.

It is concluded that the P-T conditions prevalent during gold mineralization in the Athabasca Pass were in the range of 295° to 330°  $\pm 20^\circ\text{C}$  at pressures in the order of 900 to  $\geq 1200$  bars. The absence of independent, quantitative geobarometric-thermometric techniques applicable to the Athabasca Pass gold-quartz lodes has been noted above. However, it is noteworthy that P-T constraints proposed above are in agreement with the broader constraints imposed by the regional anchimetamorphic-pumpellyite facies (*ca.* 200° to 350°C and 1 to 4 kb (Turner, 1981; Kisch, 1987)) conditions under which the Athabasca Pass lodes are considered to have been emplaced.

### Discussion

Based upon a wide range of geological parameters, including lithotectonic setting, metamorphic regime, and vein temporal, structural, textural and mineralogical relationships, the gold-quartz lodes of the Athabasca Pass were previously classified as a siliciclastic-hosted analogue of the Turbidite Hosted class of gold deposits (Keppie *et al.*, 1986; Hutchinson, 1987). Based upon integrated geological-geochemical parameters turbidite-hosted deposits have been termed mesothermal in character.

A comparison between fluid compositional and P-T constraints derived for the Athabasca Pass lodes and data summarized for a number of turbidite-hosted gold deposits is presented in Table 3-2. From this table, it is evident that the fluid compositional data for the Athabasca Pass lodes is typical of turbidite-hosted deposits, *i.e.* essentially low salinity brines containing generally low, but variable, quantities of CO<sub>2</sub>, with minor quantities of other volatiles, dominantly CH<sub>4</sub> ( $\pm$  N<sub>2</sub>). As shown, P-T constraints proposed for gold-stage mineralization in the Athabasca Pass in terms of both minimum Th<sub>total</sub> and pressure corrected scenarios are also in the general range for those derived from turbidite-hosted deposits, and mesothermal gold-lodes in general. With respect to fluid processes and gold depositional mechanisms, it is notable that many authors studying turbidite-hosted gold deposits consider, as is documented herein, fluid immiscibility to be absent from or unimportant with respect to the gold mineralizing event (Paterson, 1986; Steed and Morris, 1986; Goldfarb *et al.*, 1986; Kontak *et al.*, 1988).

In view of a fluid and P-T regime in the Athabasca Pass typical of mesothermal turbidite-hosted gold deposits, a comparable suite of associated trace elements accompanying gold mineralization might be expected.

However as documented earlier, in terms of both the sparse variety and overall abundance of trace elements in the Athabasca Pass lodes, this is not the case. A fundamental difference between the Athabasca Pass and turbidite-hosted gold deposits in general involves the nature of the host rocks *i.e.*, mature, quartz-dominated  $\pm$  pelitic clastic rocks in the Athabasca Pass versus a wide variety of generally immature volcano-sedimentary clastic rock types in turbidite-hosted deposits. The general paucity of trace elements in quartz-dominated clastic rocks accounts for lower concentrations of trace-elements, as well suggests the relatively local derivation and control of lode trace element concentrations by the quartzitic rock types hosting the mineralized Athabasca Pass structures. Such an inference would also suggest that the fluids responsible for mineralization in the Athabasca Pass were either dominantly interstratigraphically derived, or that their circulation was relatively restricted to the quartz-dominated rocks of the McNaughton Formation or the Gog Group (a regionally correlatable stratigraphic unit in excess of 1 km thick throughout much of the Main Ranges of the Rocky Mountains). Interestingly, Miette Group strata which underly the McNaughton Formation and outcrop immediately to the west of the Athabasca Pass (Fig. 3-1) contain quartz veins which host a variety of sulfide minerals including pyrite, chalcopyrite, galena and arsenopyrite. Host rocks include thick turbidite-lain sequences of grit, greywacke, semi-pelite and slate; immature rock types from which a variety of trace elements would be more readily available.

With respect to the interstratigraphic derivation of fluids from the host rocks of the Athabasca Pass abundant pressure solution and recrystallization of allogenic clays to white mica in the host quartzites,

pebble-conglomerates and pelites of the McNaughton Formation have been documented. Both of these processes have been attributed to regional anchimetamorphism in the Main Ranges of the Rocky Mountains, and notably provide a potential fluid source (and mode of gold-trace element mobilization) from which mineralized lodes may be derived. Similar processes have frequently been advocated in the genesis of turbidite-hosted, and mesothermal-metamorphic vein-type gold deposits. (e.g. Boyle, 1979; Cox *et al.*, 1986; Graves and Zentilli, 1982; Kerrich and Allison, 1978; Paterson, 1986; Tomkinson, 1988). As discussed previously, the general congruency between the regional metamorphic, host-rock alteration, and vein mineralogical assemblages would further imply the relatively local derivation of the vein-filling constituents in the Athabasca Pass. Stable isotopic analysis of host-rock and vein-constituents may provide a more complete evaluation of potential fluid sources for the Athabasca Pass lodes.

### *Concluding Statement*

The gold metallogenic potential of low-grade meta-sedimentary fold belts such as Victoria, Australia, and Nova Scotia, Canada has been widely recognized. These and other districts, which have founded the classical turbidite-hosted lode gold deposit-type, have in recent years, become of renewed interest in exploration programs (e.g. Kontak and Smith, 1988; Watchorn *et al.*, 1988; Wilson *et al.*, 1988). The siliciclastic-hosted lode-gold system documented herein may be viewed as an analogue of the turbidite-hosted class of gold deposits, thus the potential of siliciclastic domains should not be overlooked in the broad context of turbidite-hosted, and mesothermal lode-gold exploration programs. The Main Ranges of the

Rocky Mountains may be viewed as a viable region for the exploration for such deposits.

Table 3-1. Mole % CO<sub>2</sub> and pressure of trapping estimates for Type B2 fluid inclusions.

Sample no.	T <sub>m</sub> CO <sub>2</sub> , °C	T <sub>h</sub> CO <sub>2</sub> , °C	CH <sub>4</sub> carb. Mole % <sup>1</sup>	Salinity, wt.% Cl eq. <sup>2</sup>	T <sub>h</sub> total, °C	CO <sub>2</sub> <sup>3</sup> Mole %	Pressure, bars <sup>4</sup>
PE-A3	-57.3	22.5	5	5.6	253	10	1084
	-57.8	19.5	7	4.1	221	6	1107
	-58.0	19.4	8	3.9	226	6	1108
	-58.2	14.1	9	3.2	220	8	1101
	-58.1	17.9	8	3.4	229	8	1106
	-57.7	22.9	5	3.9	231	6	1097
	-57.0	21.6	4	4.3	243	11	1117
PB-A11	-58.3	22.4	9	3.8	232	5	1097
	-57.5	23.6	5	3.9	229	6	1103
	-57.8	23.4	5	4.5	225	5	1142
	-57.4	23.9	9	3.9	232	10	1094
	-57.4	23.0	6	3.8	219	5	1098
PB-A16	-57.2	22.4	5	3.8	231	8	1089
	-57.5	22.3	5	3.9	234	8	1090
	-57.9	16.8	8	4.3	244	11	1094
	-58.1	15.8	8	3.0	236	11	1102
	-58.1	17.5	8	2.8	244	11	1096
PB-A24	-57.7	20.6	6	3.6	242	10	1095
	-57.9	18.5	8	4.1	239	9	1102
	-57.3	24.5	5	5.1	211	4	1107

<sup>1</sup> Estimated from the graphs of Heyen *et al.*, 1982.

<sup>2</sup> Calculated from relations given by Bozzo *et al.*, 1976.

<sup>3,4</sup> Calculated using the method of Parry, 1986.



Table 3-2. Fluid inclusion characteristics of the Athabasca Pass vs. typical turbidite-hosted \* and mesothermal †:ode-gold deposits.

	Athabasca Pass	Turbidite-Hosted	Mesothermal
Th total, °C:	190-315	range ~200-400	...
Est. mole %CO <sub>2</sub> :	0-11 average ~8	range 0-20 generally <15	>4
Dominant additional volatiles:	CH <sub>4</sub> ± N <sub>2</sub>	CH <sub>4</sub> ± N <sub>2</sub>	±CH <sub>4</sub> , N <sub>2</sub>
Est. salinity, wt.% NaCl eq.:	≤10	0-7	0-4
Inferred temperature and pressure of gold deposition:	275°-350°C, ≥900 bars	290°-360°C, 500-3000 bars	250°-350°C, >700 bars

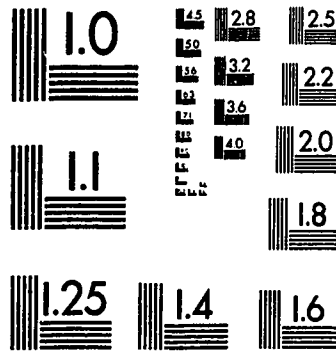
Principle references: \*Goldfarb *et al.* (1986), \*Kontak *et al.* (1988), \*Paterson (1986),

\*Steed and Morris (1986), † Nesbitt (1988).

2

of/de

2



MICROCOPY RESOLUTION TEST CHART  
NATIONAL BUREAU OF STANDARDS  
STANDARD REFERENCE MATERIAL 1010a  
(ANSI and ISO TEST CHART No. 2)

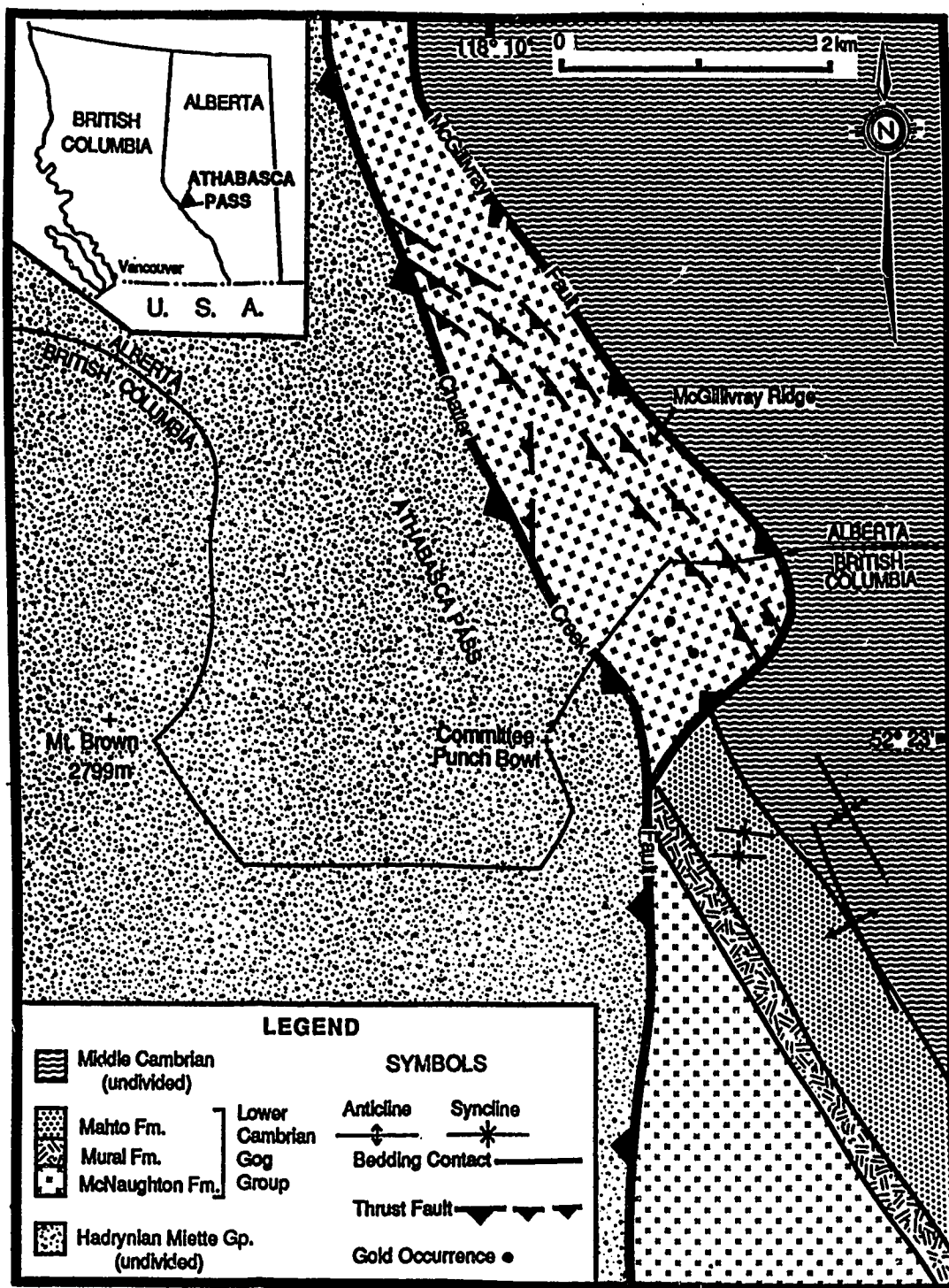
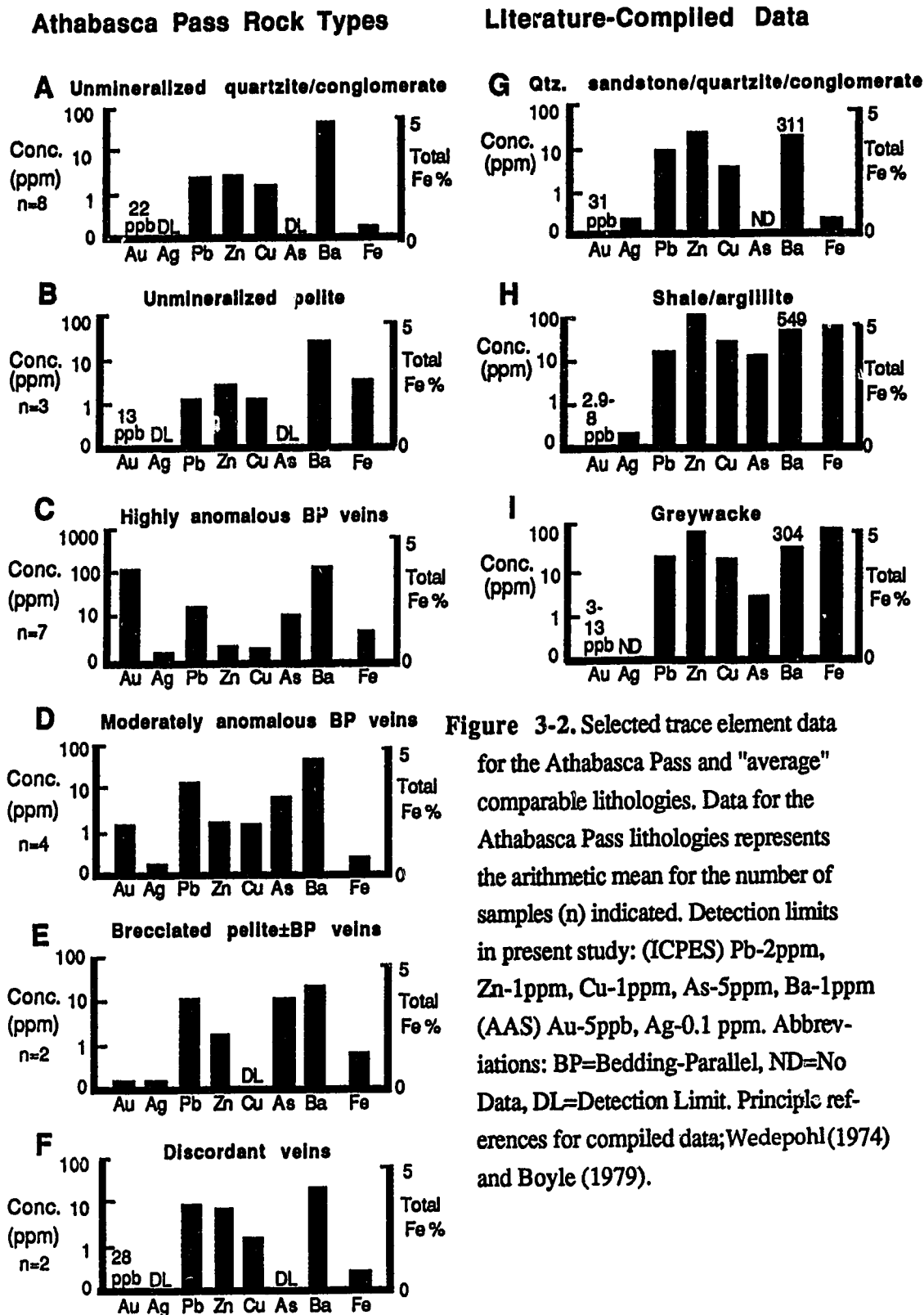


Figure 3-1. Location and general geology of the Athabasca Pass area. Data compiled from Mountjoy and Price (in prep.) and thesis data. Gold occurrences represent clusters of mineralized veins.



**Figure 3-2.** Selected trace element data for the Athabasca Pass and "average" comparable lithologies. Data for the Athabasca Pass lithologies represents the arithmetic mean for the number of samples (n) indicated. Detection limits in present study: (ICPES) Pb=2ppm, Zn=1ppm, Cu=1ppm, As=5ppm, Ba=1ppm (AAS) Au=5ppb, Ag=0.1 ppm. Abbreviations: BP=Bedding-Parallel, ND=No Data, DL=Detection Limit. Principle references for compiled data; Wedepohl(1974) and Boyle (1979).

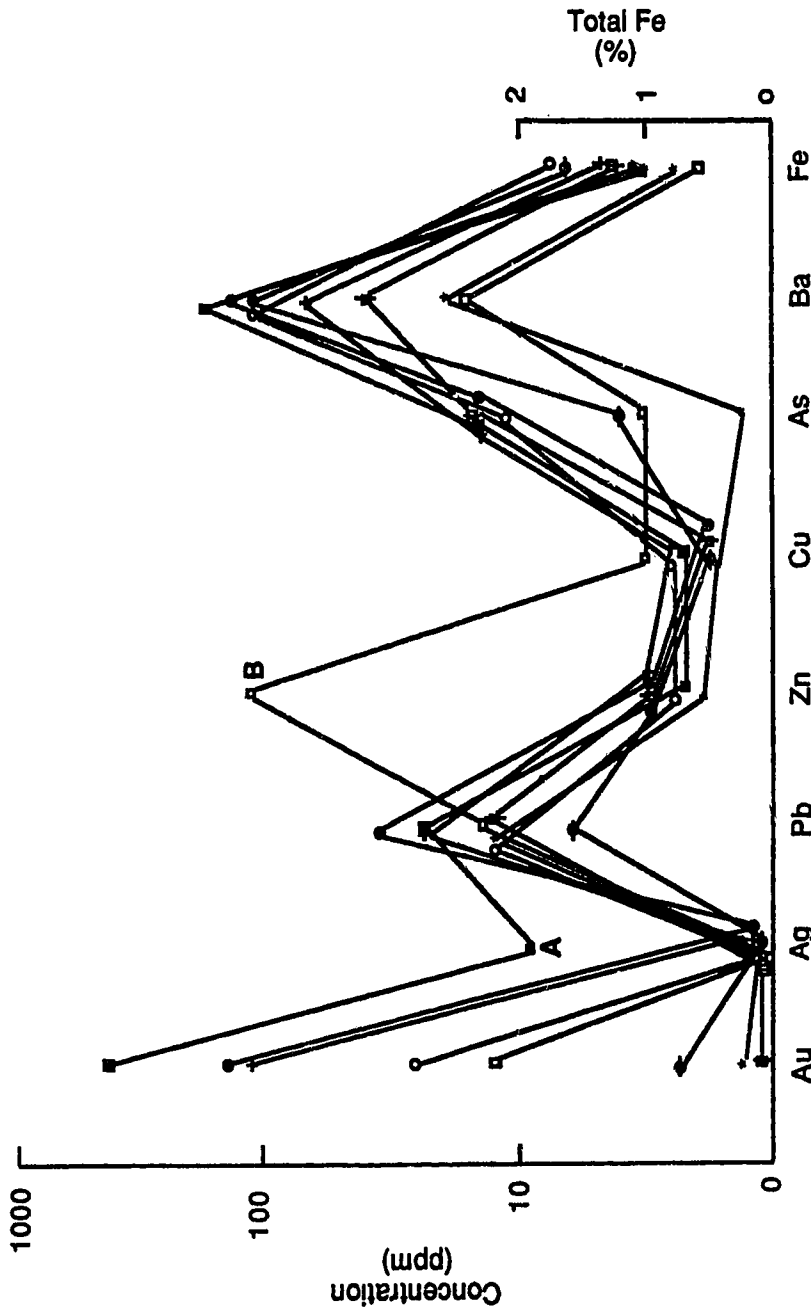
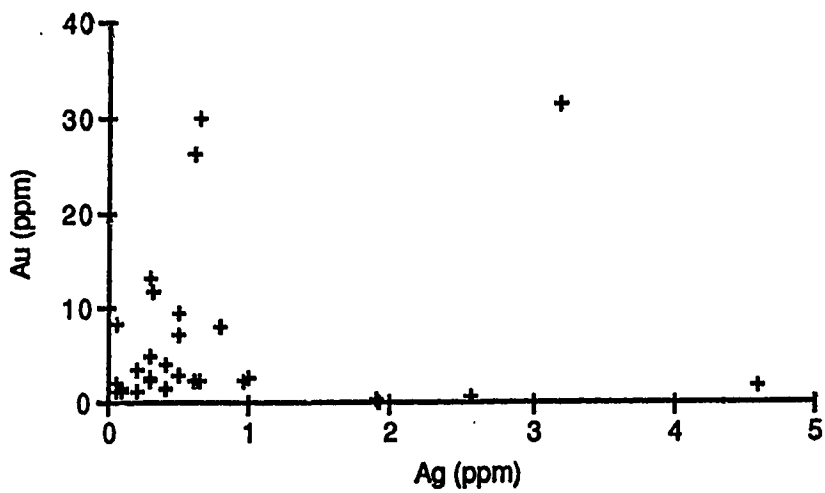
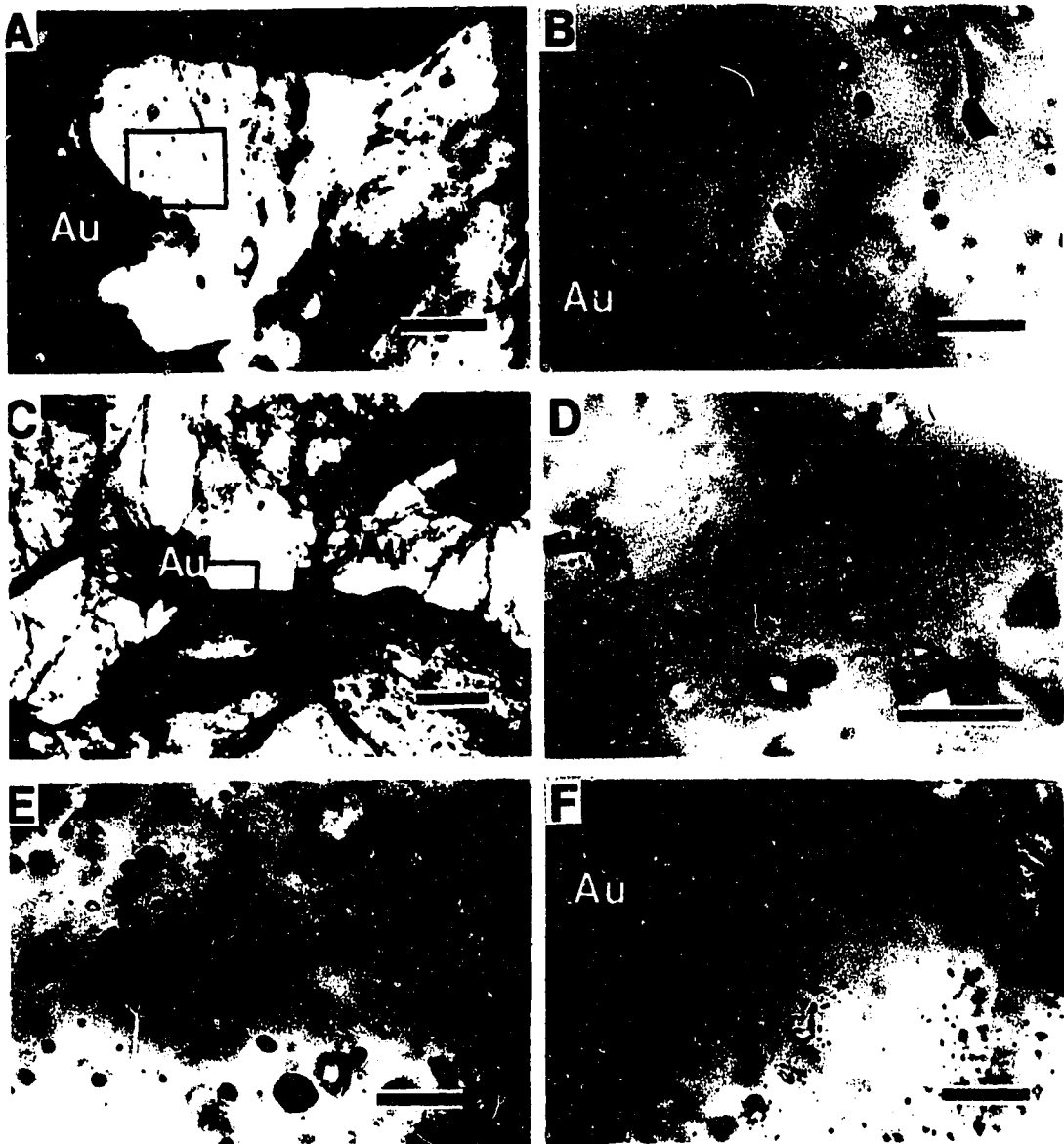


Figure 3-3. Trace element variations exhibited by 8 samples of Au-bearing bedding-parallel vein material (Figs. 3-2C and 3-2D) from the Athabasca Pass. Symbols denote individual samples. Points A and B are referred to in the text.



**Figure 3-4.** Scatter plot illustrating the poor correlation between gold and silver for 30 samples of auriferous bedding-parallel vein material from the Athabasca Pass.



**Figure 3-5. Type B fluid inclusions in quartz from some Au-bearing veins on McGillivray Ridge. All photographs taken at room temperature (ca. 22° C). A. Quartz-filled embayment in native gold (Au). Rectangle approximates area in photograph B. Scale bar = 80µm. B. Type B1 fluid inclusions adjacent to native gold (Au). Scale bar = 20µm. C. Gold-filled (Au) fractures in quartz. Rectangle approximates area in photograph D. Scale bar = 80µm. D. Type B1 fluid inclusions adjacent to native gold. Scale bar = 25µm. E. Numerous Type B2 fluid inclusions adjacent to native gold (Au). Scale bar = 25µm. F. Solitary Type B2 fluid inclusion adjacent to native gold (Au). Scale bar = 80µm.**

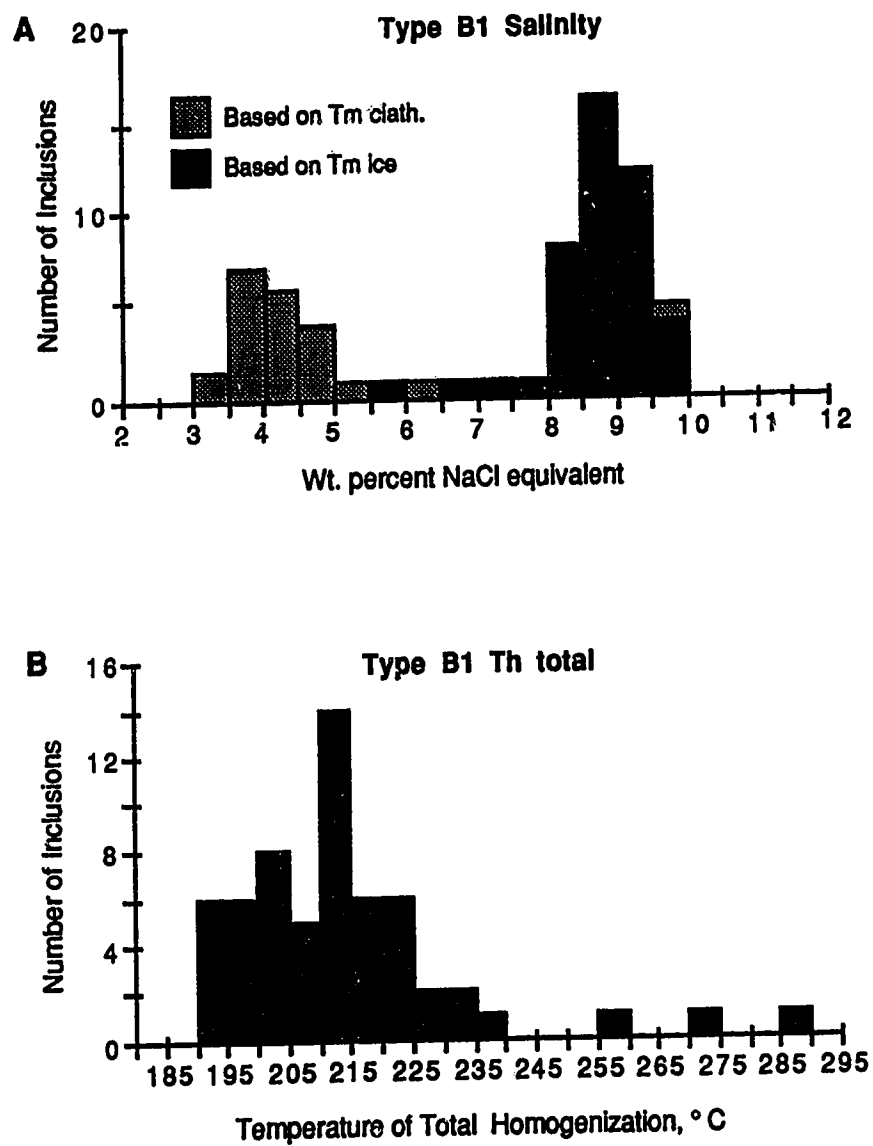


**Figure 3-6** Microthermometric data for Type B1 H<sub>2</sub>O-NaCl±CO<sub>2</sub>-bearing fluid inclusions contained within auriferous vein quartz from the Athabasca Pass. Salinity estimates based upon clathrate melting are approximate maxima.



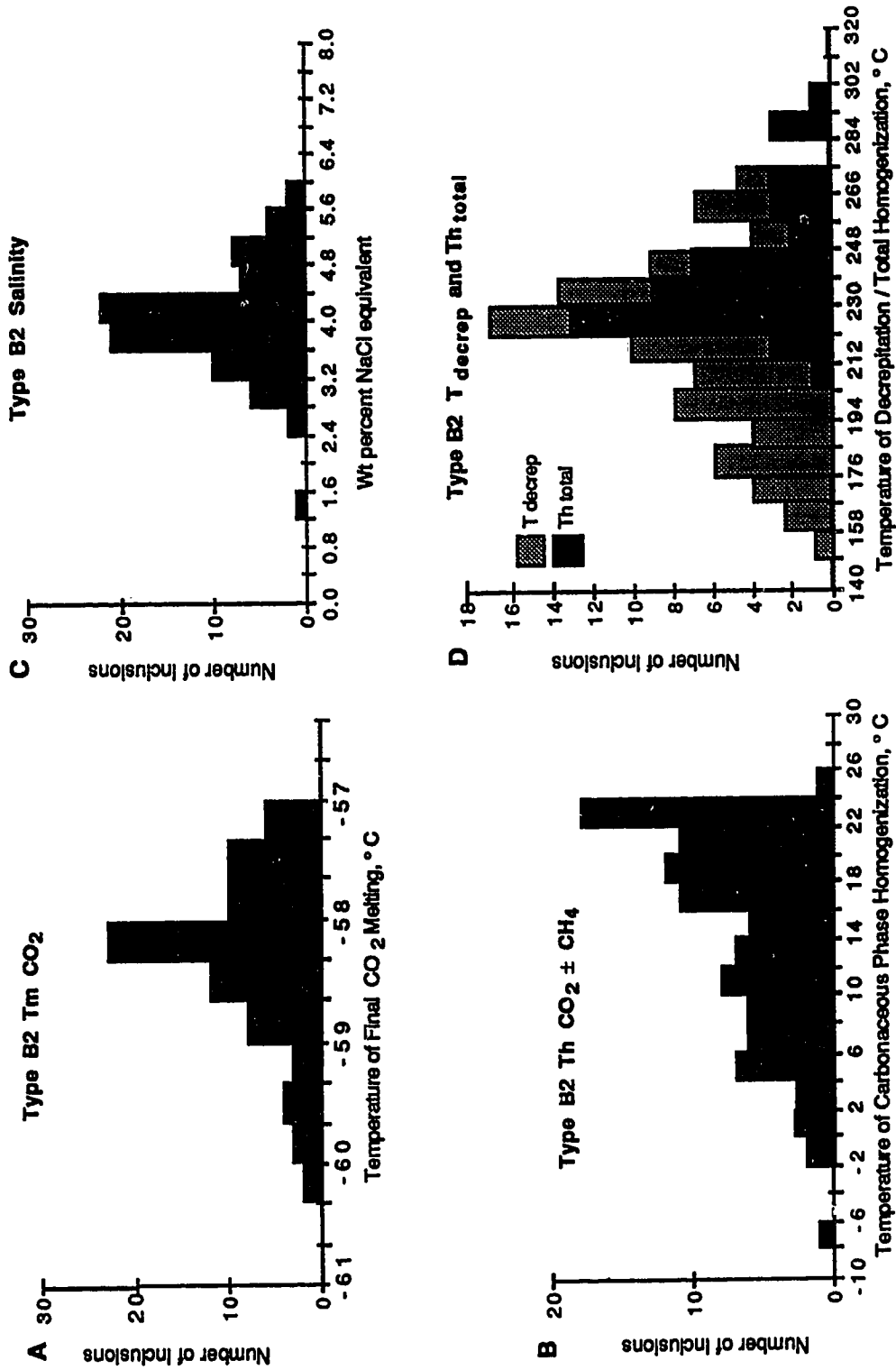


Figure 3-7. Microthermometric data for Type B2 H<sub>2</sub>O-NaCl-CO<sub>2</sub>-CH<sub>4</sub>-bearing fluid inclusions contained within auriferous vein quartz from the Athabasca Pass.

### References

- Arai, Y., Kaminishi, G., and Saito, S., 1971, The experimental determination of the P-V-T-X relations for the carbon dioxide-nitrogen and carbon dioxide-methane systems: *J. Chem. Eng. Jap.*, v. 4, p. 113-122.
- Bodner, R. J., 1983, A method of calculating fluid-inclusion volumes based on vapor bubble diameters and P-V-T-X properties of fluid inclusions: *Economic Geology*, v. 78, p. 535-542.
- Bowers, T.S., and Helgeson, H.C., 1983a, Calculations of the thermodynamic and geochemical consequences of nonideal mixing in the system H<sub>2</sub>O-CO<sub>2</sub>-NaCl on phase relations in geologic systems: Equation of state for H<sub>2</sub>O-CO<sub>2</sub>-NaCl fluids at high pressures and temperatures: *Geochimica et Cosmochimica Acta*, v. 47, p. 1247-1275.
- Bowers, T. S., and Helgeson, H. C., 1983b, Calculations of the thermodynamic consequences of nonideal mixing in the system H<sub>2</sub>O-CO<sub>2</sub>-NaCl on phase relations in geologic systems: Metamorphic equilibria at high pressures and temperatures: *American Mineralogist*, v. 68, p. 1059-1075.
- Boyle, R. W., 1979, The geochemistry of gold and its deposits: *Geological Survey of Canada, Bulletin 280*.
- Bozzo, A.T., Chen, J. R., Kass, J. R., and Barduhun, A. J., 1973, The properties of the hydrates of chlorine and carbon dioxide: *International Symposium on Fresh Water from the Sea, Amaraussion, Greece, 1973, Proc.*, v. 3, p. 437-451.
- Burruss, R. C., 1981, Analysis of phase equilibria in C-O-H-S fluid inclusions: *Mineralogical Association of Canada, Short Course Handbook*, v. 6, p. 39-74.
- Burwash, R. A., 1951, The Precambrian under the central plains of Alberta: M. Sc. thesis, University of Alberta, 40 p.
- Collins, P. L. F., 1979, Gas hydrates in CO<sub>2</sub>-bearing fluid inclusions and the

- use of freezing data for estimation of salinity: *Economic Geology*, v. 74, p. 1435-1444.
- Cox, S.F., Etheridge, M.A., and Wall, V.J., 1986, The role of syn-tectonic mass transport and localization of metamorphic vein-type ore deposits: *Ore Geology Reviews*, v. 2, p. 65-86.
- Craw, D., 1978, Metamorphism, structure and stratigraphy of the southern Park Ranges, British Columbia: *Canadian Journal of Earth Sciences*, v. 15, p. 86-98.
- Crawford, M. L., 1981, Phase equilibria in aqueous fluid inclusions: *Mineralogical Association of Canada Short Course Handbook*, v. 6, p. 75-100.
- Crocket, J. H., 1974, Gold, *In Handbook of Geochemistry*. Wedepohl, K. H., Ed. Springer-Verlag, Berlin, v. II/5, Chapter 79, sections B-O.
- Crocket, J. H., Clifford, P. M., Fueten, F., and Kabir, A., 1983, Distribution and localization of gold in Meguma Group rocks. Part 2: Implications of background geochemistry and cleavage development - A preliminary report: *Current Research, Part B, Geological Survey of Canada, Paper 83-1B*, p. 285-290.
- Desborough, G. A., 1970, Silver depletion indicated by micro-analysis of gold from placer occurrences, Western United States: *Economic Geology*, v. 65, p. 304-311.
- Foster, R. P., Furber, F. M. W., Gilligan, J. M., and Green, D., 1986, Sharnva gold mine, Zimbabwe: A product of calc-alkaline-linked exhalative, volcanoclastic, and epiclastic sedimentation in the late Archean, *In Turbidite-hosted gold deposits.*, J.D. Keppie, R.W. Boyle, and S.J. Haynes, Eds. Geological Association of Canada Special Paper 32, p. 41-66.
- Glasson, M. J., and Keays, R. R., 1977, Gold mobilization during cleavage development in sedimentary rocks from the auriferous slate belt of

- Central Victoria, Australia: Some important boundary conditions: *Economic Geology*, v. 73, p. 496-511.
- Goldfarb, R.J., Leach, D.L., Miller, M.L. and Pickthorn, W.J., 1986, Geology, metamorphic setting and genetic constraints of epigenetic lode-gold mineralization within the Cretaceous Valdez Group, south-central Alaska. *In Turbidite-hosted deposits* J.D. Keppie, R.W. Boyle, and S.J. Haynes, *Eds.* Geological Association of Canada, Special Paper 32, p. 87-105.
- Graves, M.C. and Zentilli, M., 1982, A review of the geology of gold in Nova Scotia. *In Geology of Canadian gold deposits.* R.W. Hodder and W. Petrak, *Eds.* Canadian Institute of Mining and Metallurgy, Special Volume 24, p. 233-242.
- Haas, Jr., J. L., 1976, Physical properties of the coexisting phases and the thermochemical properties of the H<sub>2</sub>O component in boiling NaCl solutions: U. S. Geological Survey Bulletin, 1421-A, 73 p.
- Hedenquist, J. W., and Henley, R. W., 1985, The importance of CO<sub>2</sub> on freezing point measurements of fluid inclusions: Evidence from active geothermal systems and implications for epithermal ore deposition: *Economic Geology*, v. 80, p. 1379-1406.
- Hedley, M.S., 1954, Mineral deposits in the Southern Canadian Rocky Mountains of Canada: Alberta Society of Petroleum Geologists, Fourth Annual Field Conference Guide Book, p. 110-118.
- Heyen, G., Ramboz, C., and Dubessy, J., 1982, Simulation des equilibres de phases dans le systeme CO<sub>2</sub>-CH<sub>4</sub> en dessous de 50° et de 100 bar. Application aux inclusions fluides: *C. R. Acad. Sci. Paris*, v. 294, série II, p. 203-206.
- Hollister, L. W., and Burruss, R. C., 1979, Phase equilibria in fluid inclusions from Khtada Lake Metamorphic complex: *Geochimica et*

- Cosmochimica Acta, v. 40, p. 163-175.
- Hutchinson, R.W., 1987, Metallogeny of Precambrian gold deposits: Space and time relationships: *Economic Geology*, v. 82, p. 1993-2007.
- Jacobs, G. K., and Kerrick, D. M., 1981, An equation of state with application to the ternary system H<sub>2</sub>O-CO<sub>2</sub>-CH<sub>4</sub>: *Geochimica et Cosmochimica Acta*, v. 45, p. 607-614.
- Keppie, D.J., Boyle, R.W., and Haynes, S.J., *Eds.*, 1982, Turbidite-hosted Gold Deposits: Geological Association of Canada, Special Paper 32, 185 p.
- Kerrick, R. and Allison, I., 1978, Vein geometry and hydrostatics during Yellowknife mineralization: *Canadian Journal of Earth Sciences*, v. 15, p. 1653-1660.
- Kisch, H.J. 1987, Correlation between indicators of very low-grade metamorphism. *In* Low Temperature Metamorphism M. Frey, *Ed.* Glasgow, Blackie and Son Limited, p. 227-300.
- Klien, G.A. and Mountjoy, E.W., 1988, Northern Porcupine Creek Anticlinorium and footwall of the Purcell Thrust, northern Park Ranges, B.C.: Current research, part E: Geological Survey of Canada, Paper 88-1E, p. 163-170.
- Kontak, D.J., MacDonald, D., and Smith, P.K., 1988, Fluid inclusion study of the Beaver Dam gold deposit, Meguma Terrane, Nova Scotia: Nova Scotia Department of Mines and Energy, Mineral Resources Division Department of Activities 1988, Part A, Report 88-3, p. 63-69.
- Kontak, D. J., and Smith, P. K., 1988, The emergence of a major, turbidite-hosted gold province in the Lower Paleozoic Meguma Group, Nova Scotia, Canada. *In* Bicentennial Gold 88, A.D.T. Goode, E.L. Smyth, W.D. Birch, and L.I. Bosma, *Eds.* Geological Society of Australia Abstracts Series, Number 23, p. 224-226.
- Leroy, J., 1979, Contribution à l'étalonnage de la pression interne des inclusions fluides lors de leur décrépitation: *Bulletin de Minéralogie*,

v. 102, p. 584-593.

- Little, H.W., Belyea, R., Stott, D. F., Latour, B. A., and Douglas, R. J. W., 1976, Economic minerals of western Canada, *In* Geology and Economic Minerals of Canada. R.J.W.Douglas, *Ed.* Geological Survey of Canada, Economic Geology Report No. 1, p. 489-546.
- Lynch, J. V. G., 1989, Hydrothermal zoning in the Keno Hill Ag-Pb-Zn veins system, Yukon: A study in structural geology, mineralogy, fluid inclusions, and stable isotope geochemistry: Unpublished Ph. D. thesis, University of Alberta, 217 p.
- Mathews, W.H., 1944, Lode-gold deposits: Southeastern British Columbia: British Columbia Department of Mines, Bulletin No. 20, Part 2.
- Mountjoy, E.W. and Aitken, J.D., 1963, Early Cambrian and late Precambrian paleocurrents, Banff and Jasper National Parks: Bulletin of Canadian Petroleum Geology, v. 11, p. 161-168.
- Mountjoy, E. W. and Price, R. A., 1985, Amethyst Lakes (83D/9) geological map and cross-sections: Geological Survey of Canada, Scale 1:50,000 (in press).
- Nesbitt, B.E., 1988, Gold deposit continuum: A genetic model for lode Au mineralization in the continental crust: *Geology*, v. 16, p. 1044-1048.
- Palonen, P., 1976, Sedimentology and stratigraphy of the Gog Group sandstones in southern Canadian Rockies: Ph.D. thesis, University of Calgary, Alberta, 187 p.
- Parry, W. T., 1986, Estimation of CO<sub>2</sub>, P, and fluid inclusion volume from fluid inclusion temperature measurements in the system NaCl-CO<sub>2</sub>-H<sub>2</sub>O: *Economic Geology*, v. 81, p. 1009-1013.
- Paterson, C. J., 1986, Controls on gold and tungsten mineralization in metamorphic-hydrothermal systems, Otago, New Zealand, *In* Turbidite-hosted gold deposits. J.D. Keppie, R.W. Boyle, and S.J.Haynes, *Eds.* Geological Association of Canada Special Paper 32, p.

25-39.

- Pichavant, M., Ramboz, C., and Weisbrod, A., 1982, Fluid immiscibility in natural processes: Use and misuse of fluid inclusion data I. Phase equilibria analysis - a theoretical and geometrical approach: *Chemical Geology*, v. 37, p. 1-27.
- Potter, II, R. W., 1977, Pressure corrections for fluid inclusion homogenization temperatures based on the volumetric properties of the system NaCl-H<sub>2</sub>O: *U. S. Geological Survey Journal of Research*, v. 5, no. 5, p. 603-607.
- Potter, II, R. W., Clynne, M. A., and Brown, D. L., 1978, Freezing point depression of aqueous sodium chloride solutions: *Economic Geology*, v. 73, p. 284-285.
- Price, R. A., Monger, J. W. H., and Roddick, J. A., 1985. *In* Field guides to geology and mineral resources in the Southern Canadian Cordillera D. Templeman-Kluit. , *Ed.* Geological Society of America Cordilleran Section, Annual Meeting, Vancouver.
- Price, R.A. and Mountjoy, E.W., 1966, Operation Bow-Athabasca, Alberta-British Columbia, *In* Report of activities, Part A. Geological Survey of Canada, Paper 66-1A, p. 106-112.
- Price, R. W., and Mountjoy, E. W., 1970, Geological structure of the Canadian Rocky Mountains between Bow and Athabasca Rivers - a progress report. *In* Structure of the southern Canadian Cordillera J.O. Wheeler, *Ed.* Geological Association of Canada, Special Paper 6, p. 7-25.
- Ramboz, C., Pichavant, M., and Weisbrod, A., 1982, Fluid immiscibility in natural processes. Use and misuse of fluid inclusion data II. Interpretation of fluid inclusion data in terms of immiscibility: *Chemical Geology*, v. 37, p. 29-48.

- Read, P.B., 1988, *Metamorphic Map of the Canadian Cordillera: Geological Survey of Canada, Open File, 1893.*
- Roedder, E., 1984, *Fluid Inclusions: Reviews in Mineralogy*, v. 12, 644 p.
- Roedder, E., and Bodner, R. J., 1980, *Geologic pressure determinations from fluid inclusion studies: Annual Review of Earth and Planetary Sciences*, v. 8, p. 263-301.
- Schwartz, M. O., 1989, *Determining phase volumes of mixed CO<sub>2</sub>-H<sub>2</sub>O inclusions using microthermometric measurements: Mineralium Deposita*, v. 24, p. 43-47.
- Seitz, J. C., Pasteris, J. D., and Wopenka, B., 1987, *Characterization of CO<sub>2</sub>-CH<sub>4</sub>-H<sub>2</sub>O fluid inclusions by microthermometry and laser raman microscope spectroscopy: Inferences for clathrate and fluid equilibria: Geochimica et Cosmochimica Acta*, v. 51, p. 1651-1664.
- Shepherd, T. J., Rankin, A. H., and Alderton, D. H. M., 1985, *A practical guide to fluid inclusion studies: Glasgow, Blackie and Son Limited*, 239 p.
- Sinclair, A.J., Wynne-Edwards, H.R. and Sutherland-Brown, A., 1978, *An analysis of distribution of mineral occurrences in British Columbia: British Columbia Ministry of Mines and Petroleum Resources, Bulletin 68.*
- Steed, G. M. and Morris, J. H., 1986, *Gold mineralization in Ordovician greywackes at Clontibret, Ireland, In Turbidite-hosted gold deposits. J.D. Keppie, R.W. Boyle, and S.J. Haynes, Eds. Geological Association of Canada Special Paper 32*, p. 67-86.
- Swanenberg, H. E. C., 1979, *Phase equilibria in carbonic systems and their applications to freezing studies of fluid inclusions: Contributions to Mineralogy and Petrology*, v. 68, p. 303-306.
- Takenouchi, S., and Kennedy, G. C., 1965, *The solubility of carbon dioxide in NaCl solutions at high temperatures and pressures: American*



- Journal of Science, v. 263, p. 445-454.
- Tomkinson, M. J., 1988, Gold mineralization in phyllonites at the Haile Mine, South Carolina: *Economic Geology*, v. 83, p. 1392-1400.
- Turner, F.J., 1981, *Metamorphic Petrology: Mineralogical Field and Tectonic Aspects*. 2nd edition: New York, McGraw-Hill.
- Watchorn, R.B., Wilson, C.J.L., Will, T. M., Quick, D., and Cathcart, J.C., 1988, Structural control on gold mineralization at Stawell. Victoria, *In Bicentennial Gold 88*. A.D.T. Goode, E.L. Smyth, W.D. Birch, and L.I. Bosma, *Eds.* Geological Society of Australia Abstracts Series, Number 23, p. 295-297.
- Wedepohl, K.H., ed., 1974, *Handbook of geochemistry*: Berlin, Springer-Verlag.
- Wilson, C.J.L., and Tomlinson, K.M., 1988, Structural control on gold mineralization at Walhalla, Victoria. *In Bicentennial Gold 88*. A.D.T. Goode, E.L. Smyth, W.D. Birch, and L.I. Bosma, *Eds.* Geological Society of Australia Abstracts Series, Number 23, p.298-299.
- Wheeler, J.O., 1963, Rogers Pass map area, British Columbia and Alberta: Geological Survey of Canada, Paper 62-32.
- Woberg, A.C., 1986, Sedimentology of the Lower Cambrian Gog Group, British Columbia: An early Cambrian tidal deposit: M. Sc. thesis, University of Alberta, 199 p.
- Young, F.G., 1979, The lowermost Paleozoic McNaughton Formation and equivalent Caribou Group of eastern British Columbia: Piedmont and tidal complex: Geological Survey of Canada, Bulletin 288.

## CHAPTER 4

### Origins of Metamorphogenic Lode Gold Deposits: Implications of Stable Isotope Data From the Central Rocky Mountains, Canada.

#### Introduction

The origins of hydrothermal fluids which generated mesothermal gold-quartz mineralization in low-grade meta-sedimentary ± plutonic domains ("Turbidite-Hosted gold deposits", Keppie *et al.*, 1986; Hutchinson, 1987, Nesbitt, in press) have, in recent years, become a subject of renewed controversy (*eg.* Nesbitt *et al.*, 1986, 1987; Goldfarb, *et al.*, 1987; Kerrich, 1987). The root of much of this controversy stems from the definition of the isotopic (O-H) signatures of naturally occurring waters (Craig, 1961; Taylor, 1974, 1979), and from the increased application of stable isotope (O-H-C-S) systematics to the study of this mineral deposit type. It is becoming increasingly evident through integrated geological-geochemical studies (*e.g.* Mitchell *et al.*, 1981; Nesbitt *et al.*, 1986; Weir and Kerrick, 1987; Shelton *et al.*, 1988) that isotopically evolved waters of meteoric origin may play a significant role in what, based upon field-petrographic relationships, and often cursory geochemical (fluid inclusion, trace element, and/or isotopic) studies, has traditionally been considered a "metamorphogenic" style of gold mineralization (Boyle, 1979; Nesbitt, in press).

The stable isotope relationships of gold-bearing quartz veins recently discovered at Athabasca Pass, in the Canadian Rocky Mountains, provide a new insight into the genesis of gold-quartz veins in low-grade meta-sedimentary domains.

## The Gold-Bearing Quartz Veins of the Athabasca Pass

### *Regional setting*

The Athabasca Pass is located 65 km south-southwest of Jasper, Alberta, in the Main Ranges of the central Canadian Rocky Mountain thrust and fold belt (Fig. 4-1). This lithotectonic domain, physiographically bound by the Rocky Mountain-Tintina Trench system to the West, and by the Foothills and Interior Plains region to the east, consists almost entirely of clastic and carbonate strata. Metamorphic grade decreases from amphibolite grade in the west to low-grade burial metamorphic facies east of the deformation front. Igneous rocks are rare in the Main Ranges. Mid-Cretaceous to Early Tertiary Cordilleran deformation in the Main Ranges caused the northeastward translation and thrust-stacking of parautochthonous miogeoclinal strata derived from the North American craton to the east, onto the western flank of the craton (Price and Mountjoy, 1970; Price *et al.*, 1985). The geologic structure of the region is dominated by complex folds and by widely-spaced thrust faults. Penetrative deformation is pronounced in the western Main Ranges, and less pervasive to absent in the east (Price and Mountjoy, 1970).

Information on lode-gold deposits in the Main Ranges, and in the Canadian Rocky Mountains in general, is sparse. The mineral occurrences and metallogeny of this region have been reviewed by Hedley (1954), Little *et al.* (1976), and by Sinclair *et al.* (1978). Principal deposit-types occurring to the south of the Athabasca Pass include stratiform lead-zinc ( $\pm$ silver) replacement bodies in Middle Cambrian carbonates, and small, quartz-carbonate vein systems containing a variety of base-metal sulfide

assemblages (dominantly galena-sphalerite-pyrite-chalcopyrite). Gold production has not been reported from these occurrences. Brief mention of placer gold occurrences in the Main Ranges was made by Mathews (1944), Sorenson (1955), and by Boyle (1979).

### *Local geology*

Aspects of the geology and geochemistry of the Athabasca Pass gold-quartz lodes have been discussed in detail in Chapters 2 and 3. These mineral occurrences consist of numerous 0.5 cm- to 1 m-thick auriferous, bedding-parallel quartz veins contained within an 800 m-thick, folded and thrust-faulted section of Lower Cambrian quartzite with minor pelite, and quartz-pebble conglomerate known as the McNaughton Formation (Fig. 4-1). This is the lowermost formation of the Gog Group, a regionally extensive stratigraphic unit in excess of 1 km thick throughout much of the Main Ranges. The area has been metamorphosed to sub-or lowermost greenschist grade. Igneous rocks are not known in the area.

Native gold, accompanied by minor pyrite and galena, was deposited late during prolonged, syn-tectonic, syn- to post-metamorphic bedding-parallel vein formation. Thin, incompetent, iron-rich pelites provided structural-chemical traps for the localization of hydrothermal fluids and for the precipitation of native gold. Discordant veins which formed penecontemporaneously with gold emplacement cut only competent quartzites and lack gold and sulfides. Hydrothermal alteration adjacent to some veins includes pyrite  $\pm$  ankerite  $\pm$  white mica. However, this alteration assemblage is not uniquely confined to the proximity of veins and is seen widely distributed within the regional metamorphic suite.

Trace element analysis of auriferous veins and unmineralized host rocks revealed distinct enrichment of Pb, As, Ba, and Fe, and marginal enrichment of Ag, Zn, and Cu in veins, with respect to host rocks. When compared with other lode-gold deposits in similar domains, the Athabasca Pass lodes are conspicuously unenriched in all trace elements except gold. This situation has been attributed to the mineralogical maturity of the McNaughton Formation quartzites.

Microthermometric analyses of fluid inclusions in vein quartz indicated gold-stage fluids were aqueous brines containing 2 to 10 wt. % NaCl eq. and up to 12 mole % CO<sub>2</sub> ± CH<sub>4</sub>. Variations in fluid compositional- and total homogenization-data suggest that gradual fluid evolution (decreasing CO<sub>2</sub> and temperature, increasing salinity) accompanied gold mineralization. Gold deposition took place at between 275° and 350°C and 900 to ≥ 1200 bars.

Combined field, petrographic, trace element and fluid inclusion evidence indicates the Athabasca Pass lodes to be typical of mesothermal gold-quartz lodes in meta-sedimentary domains. This evidence implies the relatively local derivation of vein-filling constituents, and it was suggested in Chapter 3 that the lodes may have been derived through devolatilization and deformation processes associated with low-grade regional metamorphism. To evaluate the possible role of metamorphic fluids in the genesis of the Athabasca Pass lodes, stable isotope analyses of vein and country-rock minerals were undertaken.

### **Stable Isotope (S-O-H) Study**

#### ***Experimental techniques***

Sulfur was extracted from hand-picked vein and country-rock sulfides

using the technique of Ueda and Krouse (1986). Oxygen from vein and host-rock silicate minerals was extracted using the  $\text{BrF}_5$  technique of Clayton and Mayeda (1963). Fluid inclusion waters from bedding-parallel and discordant vein quartz were extracted by thermal decrepitation under vacuum at  $1100^\circ\text{C}$ . Production of hydrogen gas from the released waters was accomplished by reaction with zinc metal at  $450^\circ\text{C}$  (Coleman *et al.*, 1982).

Mass spectrometric results are reported in standard  $\delta$  notation relative to the Cañon Diablo Troilite (CDT) standard for sulfur, and the Standard Mean Ocean Water (SMOW) standard for oxygen and hydrogen. Analytical reproducibilities were  $\pm 0.2$  per mil for sulfur,  $\pm 0.2$  per mil for oxygen, and  $\pm 5.0$  per mil for hydrogen.

#### *Sulfur isotope study*

Twenty-nine samples of sulfide-bearing unmineralized country-rock and gold-mineralized quartz vein were selected. Thirty-seven sulfide separates including seven pyrite separates from the Hadrynian Miette Group, seven pyrite separates from the Lower Cambrian McNaughton Formation, 22 separates from mineralized veins within the McNaughton Formation (including 16 pyrites and 6 galenas), and a single pyrite separate from Middle Cambrian strata were obtained. Petrographic studies indicate that pyrite occurring within Miette Group, McNaughton Formation and Middle Cambrian strata is metamorphic in origin, whereas sulfides occurring within mineralized veins in the McNaughton Formation are hydrothermal in origin, and were coeval with gold mineralization.

### *Results*

$\delta^{34}\text{S}$  values for unmineralized country-rock pyrites (Fig 4-2) range from +1.1 to +8.9 per mil and +12.2 to +16.9 per mil for the Miette Group, and the McNaughton Formation separates respectively. The Middle Cambrian separate produced a value of +36.7 per mil. McNaughton Formation vein pyrites produced values ranging from +13.7 to +19.9 per mil (with 14 of 16 samples falling between +14.2 and +16.3‰). Vein galenas returned values ranging from +11.4 to +13.3 per mil.

### *Sulfur isotope geothermometry*

Pyrite and galena have not been observed in physical contact in the McNaughton Formation quartz veins. Thus it is difficult to assign specific pairs for geothermometry. However, based upon their paragenetic associations, these sulfides were interpreted as coeval. The observed  $\delta^{34}\text{S}$ -enrichment of pyrite over galena (Fig. 4-2) indicates that isotopic equilibrium with respect to sulfur was approached (Bachinski, 1969; Kajiwara and Krouse, 1971). Thus it was deemed that useful paleo-temperatures might be derived from pyrite-galena separates. Two pyrite-galena "pairs" have  $\Delta^{34}\text{S}$  (pyrite - galena) values of 2.6 per mil and 3.0 per mil, thus yielding apparent equilibrium isotope paleo-temperatures of  $353 \pm 53^\circ\text{C}$  and  $309 \pm 44^\circ\text{C}$  (Ohmoto and Rye, 1979). Alternatively, as the distribution of  $\delta^{34}\text{S}$  for vein sulfides exhibits relatively narrow ranges, suggestive of contemporaneous precipitation, geothermometric calculations utilizing the arithmetic means for the  $\delta^{34}\text{S}$  values plotted in Figure 4-2 may be useful. Thus, the mean  $\Delta^{34}\text{S}$  (pyrite - galena) becomes 3.1 per mil and a paleo-temperature of  $300 \pm 43^\circ\text{C}$  is derived. Notably all paleo-temperatures

calculated here are in agreement with pressure corrected paleo-temperatures of 275 - 350°C inferred by gold-stage fluid inclusions in quartz.

#### $\delta^{34}\text{S}(\Sigma\text{S})$ of the hydrothermal fluids

In order to estimate  $\delta^{34}\text{S}(\Sigma\text{S})$  of the hydrothermal fluid, and in turn to speculate upon the source of sulfur for the auriferous veins of the McNaughton Formation, the dominant sulfur species in the fluid must be known. Sulfur speciation is controlled by  $f\text{O}_2$ , pH and by temperature. An assumed paleo-temperature of 325°C is reasonable, based upon fluid inclusion- and pyrite-galena- geothermometry. As oxide minerals are absent from the veins, and methane is present in fluid inclusions,  $f\text{O}_2$  was clearly low, and did not vary outside the stability field of pyrite. The pH was likely buffered to near neutral (*ca.* 5.8 at 325°C) as evidenced by the partial replacement of K-feldspar by white mica in the wall rocks, and by the presence of hydrothermal white mica in the auriferous veins. Under such conditions, the dominant sulfur species in solution would have been  $\text{H}_2\text{S}$ , and  $\delta^{34}\text{S}_{\text{H}_2\text{S}} \approx \delta^{34}\text{S}(\Sigma\text{S})$  can be assumed (Ohmoto and Rye, 1979; Ohmoto, 1986). Using isotopic equilibrium constants between sulfide minerals and  $\text{H}_2\text{S}$  given by Ohmoto and Rye (1979), the  $\delta^{34}\text{S}(\Sigma\text{S})$  of the fluid from which vein sulfides precipitated would have been in the range +13 per mil to +16 per mil.

#### *Sulfur source*

Abundant pyrite porphyroblasts occur within the country rocks of the Athabasca Pass. These country-rock pyrites fall within distinct  $\delta^{34}\text{S}$  ranges, characteristic of the stratigraphic horizon in which the pyrites occur (Fig. 4-2). McNaughton Formation vein sulfides exhibit approximately the same



range of  $\delta^{34}\text{S}$  values as their country-rocks (*i.e.* +11.4 to +19.9 per mil and +11.8 to +16.9 per mil respectively). As stated earlier, the  $\delta^{34}\text{S}(\Sigma\text{S})$  of the fluid from which vein sulfides were deposited was +13 to +16 per mil.  $\text{H}_2\text{S}$  in this mineralizing fluid may have been derived through the hydration of country-rock pyrite. Ohmoto (1986) indicates that  $\text{H}_2\text{S}$  generated by such reactions will have a  $\delta^{34}\text{S}$  signature essentially identical to the reactant pyrite. Thus the congruency between  $\delta^{34}\text{S}$  values for McNaughton Formation vein sulfides, mineralizing fluids, and host-rocks implies that sulfur was locally (*i.e.* interformationally) derived, and that the surrounding Miette Group or Middle Cambrian strata did not contribute sulfur to the gold-bearing veins.

#### *Oxygen isotope study*

Thirty samples, representing local McNaughton Formation quartzites and pelites, bedding-parallel quartz veins (including paragenetically early (Type I), and late (Type III) quartz) and unmineralized discordant veins were analysed. Quartzites were sampled proximal to, and distal from both vein types. Pelites were sampled from cataclasts within mineralized veins and as intact, unveined strata.

#### *Results*

$\delta^{18}\text{O}$  of McNaughton Formation quartzites (7 samples) range from +12.0 to +13.5 (averaging +12.9‰, Table 4-1) Values are uniform, regardless of sample proximity to quartz veins. Likewise, pelites (6 samples) exhibit a narrow range in  $\delta^{18}\text{O}$  (+9.5 to +10.5, averaging +10.0 ‰) with the  $\delta^{18}\text{O}$  of veined and unveined pelite being statistically identical. All 17 pre-gold and

gold-stage vein quartz samples returned  $\delta^{18}\text{O}$  values between +13.0 and +15.0 per mil. Early, Type I quartz, late Type III quartz, and discordant vein quartz averaged  $+14.4 \pm 0.9$ ,  $+14.0 \pm 1.0$ , and  $+14.5 \pm 0.5$  per mil respectively.

#### *Temperature of metamorphism*

Oxygen isotope studies of regional metamorphic domains (see Taylor, 1979; Valley, 1986) reveal a tendency toward total isotopic homogenization and equilibration, due to the lengthy time periods involved in regional metamorphism. McNaughton Formation quartzites and pelites exhibit narrow  $\delta^{18}\text{O}$  ranges, independent of their proximity to, or the degree of, quartz veining. Hence it may be assumed that these rocks have approached isotopic homogenization, and have retained their metamorphic  $\delta^{18}\text{O}$  signatures throughout the mineralizing event. An approximate paleo-temperature of metamorphism may therefore be derived utilizing the quartz - muscovite isotopic geothermometer and  $\Delta^{18}\text{O}$  (quartz-white mica) from McNaughton Formation quartzites and pelites (these rock types are essentially monomineralic). Mean  $\delta^{18}\text{O}$  values of +12.9 (quartzites) and +10.0 (pelites) per mil yield a  $\Delta^{18}\text{O}$  value of +2.9 per mil. Equations given by Field and Fifarek (1985) provide an approximate paleo-temperature of 370°C. Retrograde isotopic resetting during cooling is unlikely at moderate temperatures, hence 370°C likely represents near peak-metamorphic conditions. This temperature is in good agreement with the archimetamorphic (sub- to lowermost greenschist facies) regime implied by the metamorphic mineral assemblages, and by deformational microstructures in the McNaughton Formation.

*Interpretation and  $\delta^{18}\text{O}$  of the hydrothermal fluids*

Segregation vein minerals formed during regional metamorphism generally exhibit  $\delta^{18}\text{O}$  values similar to their host-rocks (Taylor, 1979; Kerrich, 1987). The overlap between the  $\delta^{18}\text{O}$  of quartzites (range +12.0 to +13.5 ‰) and bedding-parallel quartz veins (range +13.5 to +15.0 ‰) at Athabasca Pass suggests that the veins were, in part, deposited from fluids which were isotopically- and thermally-equilibrated with the McNaughton Formation. However, the trend toward higher  $\delta^{18}\text{O}$  values for the quartz veins suggests that the deposition of the bulk of the vein material, including gold and sulfides, took place from fluids which were not isotopically equilibrated with their wallrocks, or alternatively, that wall-rock equilibrated fluids cooled somewhat prior to/during vein deposition, hence depositing vein quartz enriched in  $^{18}\text{O}$ . Direct lateral secretion of the vein-forming components during peak metamorphism is precluded by the trend toward higher  $\delta^{18}\text{O}$  values in the veins (Kerrich, 1987).

Deposition from non-equilibrated fluids can be ruled out by observations implying broad chemical-thermal equilibrium between veins and host-rocks (*e.g.* the paucity of wallrock alteration and the mineralogical congruency between the metamorphic suite  $\pm$  alteration and vein assemblages), and by trace-element and fluid inclusion data which suggest the relatively local derivation of the vein-filling constituents. The involvement of additional, externally-derived fluids and fluid mixing is precluded by the narrow range of  $\delta^{18}\text{O}$  values, and by the lack of mixing trends in both the O- and S-isotope data sets.

Alternatively, the cooling of isotopically equilibrated fluids could account for the apparent vein - wall-rock disequilibrium. For example,

utilizing mean-, and maximum- and minimum- $\delta^{18}\text{O}$  values for McNaughton Formation quartzites and pelites, and an approximate paleo-temperature of metamorphism of  $370^{\circ}\text{C}$ , aqueous fluids in equilibrium with wall-rocks would have had a  $\delta^{18}\text{O}$  value of  $+8.1$  ( $\pm 0.9$  ‰ for quartzites,  $\pm 0.5$  ‰ for pelites; Matsuhisa *et. al.*, 1979 (quartz-water); Friedman and O'Neil, 1976 (muscovite-water)). As this fluid cooled toward/during gold stage deposition (*ca.*  $350$ - $300^{\circ}\text{C}$ , based upon fluid inclusion and sulfur isotope geothermometry), quartz exhibiting  $\delta^{18}\text{O}$  values in the range 13 to 15 per mil would be deposited. This interpretation is supported by fluid inclusion data which suggests the gradual cooling of fluids during vein formation, and by structural, vein-textural, and paragenetic evidence which supports progressive late-syn to post-peak metamorphic vein filling. Thus vein deposition from relatively local aqueous fluids which were isotopically equilibrated with their wall-rocks prior to vein formation best accounts for the McNaughton Formation vein - host-rock O-isotope relationships at Athabasca Pass. The ultimate source of these fluids may be indicated by their H-isotope composition.

#### ***Hydrogen-isotope study***

Fluid inclusion extracts from 6 auriferous bedding-parallel vein quartz separates (4 early, Type I, and 2 late Type III) from the McNaughton Formation were analysed. Such fluids represent samples of the fluids from which the vein components were precipitated (Roedder, 1984). Detailed petrographic investigations indicate abundant fluid inclusions in quartz are associated with gold-stage mineralization at Athabasca Pass.

### *Results*

All fluid inclusion fluids exhibited  $\delta D$  values between -105 and -124 per mil (averaging *ca.* -115 ‰, Table 4-1). No systematic differences between Type I and Type III quartz, or discordant vein quartz fluids were noted. Variations outside analytical uncertainty limits may be accounted for by minor fluctuations in the  $\delta D$  value of the mineralizing fluid during the progressive mineralizing event, or by minor contamination by fluids, trapped during late deformation, which were unrelated to vein formation.

### *Interpretation and $\delta D$ of the hydrothermal fluids*

The H- (versus O-) isotope compositions of the Athabasca Pass vein fluids are plotted in Fig. 4-3. The isotopic (O-H) composition of other naturally occurring waters (magmatic, metamorphic, and meteoric) are also shown. It appears that the  $\delta D$  values of the Athabasca Pass fluids lie significantly below the magmatic- and metamorphic-water fields (*ca.* 30-60 ‰ more negative). Hence large, negative  $\delta D$  shifts must be explained if either of these fluid-types played a significant role in the formation of the Athabasca Pass gold-quartz lodes.

The involvement of magmatic fluids in vein formation is precluded by the regional paucity of igneous rocks. In order for fluids of metamorphic derivation to be involved, negative  $\delta D$  shifts of  $\geq 45$  per mil must be invoked. Such large shifts may, under certain circumstances, be attributable to either fluid evolution-, or to fluid mixing- processes. The evolution of fluids as a result of fluid - wall-rock interactions which cause negative  $\delta D$  (fluid) shifts, is unlikely, as most mineral-water fractionation factors for hydrogen are negative (*i.e.* the fluid phase becomes enriched (Field and

Fifarek, 1985)). Other processes such as boiling or fluid unmixing also tend to enrich, not deplete, the fluid phase in D. The mixing of metamorphic fluids with isotopically lighter fluids at Athabasca Pass is precluded by the relatively narrow ranges, and by the lack of mixing trends exhibited by the associated O-, S-, and H-isotope data sets.

Thus the involvement of significant quantities of magmatic or metamorphic fluids in the formation of the auriferous quartz veins at Athabasca Pass cannot be postulated. Rather, the fluid source for these veins must have involved evolved waters of meteoric origin.

Present-day meteoric water from the Athabasca Pass has a  $\delta D$  value of approximately -135 per mil (Craig, 1961; Nesbitt and Muehlenbachs 1989). Assuming the isotopic composition of meteoric water has not shifted significantly during the last 150 Ma (Taylor, 1979), vein fluids averaging -115 per mil at Athabasca Pass record a positive  $\delta D$  (fluid) shift of up to 20 per mil (possibly somewhat less given the uncertainty in the H-composition of ancient meteoric waters (*i.e.*  $\pm 10$  ‰, Taylor, 1979)). Positive H-isotope shifts of this magnitude may be reconciled through either of two processes, namely: 1) the mixing of minor amounts of isotopically-heavy fluids (in this case metamorphic) with isotopically-light meteoric waters. or 2) by fluid - wall-rock isotope exchange reactions at moderate- to low-water to rock (w/r) ratios. The first possibility is precluded by well constrained S-, O-, and H-isotope data, and by the lack of fluid mixing trends. The involvement of minor amounts of metamorphic water however, cannot be ruled out completely, especially during the early stages of vein formation. Alternatively, the second case of fluid - wall-rock isotope exchange reactions, as discussed below, could account for both the H-, and O-isotope

data sets from the Athabasca Pass, without the involvement of metamorphic fluids.

### *Evolution of the hydrothermal fluids*

The generation of O-enriched meteoric waters through isotope exchange reactions with wall-rock minerals during crustal fluid circulation, and the involvement of these fluids in the formation of lode gold deposits has been demonstrated by many authors (see Taylor (1979), Ohmoto (1986), Kerrich (1987), and Nesbitt (in press) for examples). Recently Nesbitt (1988), and Nesbitt and Muehlenbachs (1989) have demonstrated, through the consideration of crustal permeabilities, that meteoric waters may penetrate to great depths in the crust (possibly to the brittle-ductile transition zone), and in this process become greatly enriched in  $^{18}\text{O}$ . Concomitant positive  $\delta\text{D}$ -shifts are generally not as marked (depending on w/r ratio), due to the low hydrogen content of most rocks. Integrated process models involving the deep circulation and isotopic-chemical evolution of meteoric waters, and their involvement in lode gold-forming systems have been given by Nesbitt (1988; and, in press).

As stated, meteoric water at Athabasca Pass has a  $\delta\text{D}$  value of *ca.* -135 per mil. The equilibrium  $\delta^{18}\text{O}$  value in this area is thus about -18 per mil (Craig, 1961; Dansgaard, 1964). Utilizing the  $\delta^{18}\text{O}$  (fluid) value of *ca.* +8 per mil calculated earlier, vein quartz at Athabasca Pass records a  $\delta^{18}\text{O}$  (fluid) shift of *ca.* +26 per mil.  $\delta^{18}\text{O}$  (fluid) shifts of this magnitude can be produced through O-isotope exchange reactions between fluid and wall-rocks under conditions of  $T > 300^\circ\text{C}$ , and with w/r ratios on the order of 0.1 (see Field and Fifarek (1985)). Additionally, under such conditions,

accompanying  $\delta D$  (fluid) shifts would be +15 to +25 per mil; approximately equal to those observed in the Athabasca Pass vein fluids (*i.e.*  $\leq 20$  ‰). A curve depicting the evolution of the fluids which deposited the gold-quartz veins at Athabasca Pass (using  $T \approx 350^\circ\text{C}$  and a  $w/r$  ratio of *ca.* 0.1), is given in Fig. 4-3. Nesbitt and Muehlenbachs (1989) have documented meteoric water O- and H-isotope shifts of this magnitude, under similar conditions, for a large number of quartz vein  $\pm$  gold occurrences in the Canadian Cordillera.

Thus it is evident that a fluid source for the gold-quartz veins at Athabasca Pass is most simply, and most completely explained by invoking the involvement of evolved meteoric waters. Contribution from a metamorphic fluid is not required. These findings may be more broadly applicable to the generation of mesothermal gold-quartz deposits in low-grade meta-sedimentary domains elsewhere in the world.

#### **Implications for metamorphogenic lode gold deposits**

A metamorphic origin for the fluids which generated mesothermal, turbidite hosted (*ca.* greywacke or slate-belt hosted) gold-quartz veins in low-grade meta-sedimentary domains has been proposed by numerous authors in recent years (*e.g.* Norris *et.al.*, 1976; Graves and Zentilli, 1982; Paterson, 1982, 1986; Cox *et.al.*, 1986; Mawer, 1986; Sandiford and Keays, 1986; Tomkinson, 1988; Kontak and Smith, 1989; Seccombe and Hicks, 1989; McKeag *et. al.*, 1989). In general these fluids are considered to have been generated through prograde metamorphic devolatilization reactions and deformational processes. Ore- and gangue constituents are mobilized by ascending fluids through fluid - wall-rock interactions, and the fluids are focussed into structural conduits (*e.g.* fault zones, dilatant bedding-planes,



fold hinges) where mineral deposition takes place. Field relationships suggesting a lack of temporally-related igneous intrusions, gold distribution related to regional metamorphic isograds, the limited development of wall-rock alteration, and fluid overpressuring (hydrofracturing) during vein formation are well documented. Fluid inclusion studies reveal vein-filling at paleo-temperatures of *ca.* 250 to 350°C, from moderately saline fluids ( $\leq 8$  wt % NaCl eq.). The presence of high density  $\text{CO}_2 \pm \text{CH}_4$  suggests ambient pressures of  $\geq 1000$  bars. Augmented by only cursory S- or O-isotope studies and/or trace-element distribution data, these factors are generally considered to be indicative of metamorphogenic processes in lode gold formation. H-isotope analyses however, are conspicuously absent from all of the studies cited above.

With respect to the auriferous quartz lodes at Athabasca Pass, field, petrographic, and fluid inclusion relationships essentially identical to those documented in the studies cited above have been documented. Additionally, mineralogical and trace-element, and S-, and O-isotope evidence supports the relatively local derivation of the vein-filling constituents, and suggest broad chemical- thermal- and isotopic-equilibrium between the country rocks and the mineralizing fluids at Athabasca Pass. Such lines of evidence are all suggestive of a metamorphogenic origin for the Athabasca Pass lodes, and based upon them alone, such an interpretation would seem inescapable. However, as stated, a metamorphogenic origin is clearly incompatible with the H-isotope data presented herein. The formation of such lodes can only be reconciled by a fluid which involved meteoric water. As outlined by Nesbitt (1988; and, in press) models for mesothermal lode gold mineralization involving evolved

meteoric waters versus metamorphic fluids are very similar. The meteoric water model however is consistent with all of the data generally cited in support of the metamorphic model, as well as being in agreement with the  $\delta D$  data.

#### **Concluding statment**

It is now apparent that an accurate evaluation of the potential fluid sources contributing to the formation of mesothermal, turbidite hosted lode gold deposits should not be performed without first acquiring H-isotope data. In the absence of H-isotope data, the involvement of an evolved meteoric water source-fluid cannot be ruled out. Indeed, considering the paucity of H-isotope data pertaining to turbidite hosted gold lodes, such involvement may be much more common than presently recognized. The application of fully integrated O-H-isotope studies, and the critical role of H-isotope data in the evaluation of potential source fluids for turbidite hosted lode gold deposits, is again re-emphasized.

**Table 4-1. Oxygen and hydrogen isotope data for mineralized and unmineralized quartz veins and McNaughton Formation host rocks at Athabasca Pass, B.C., Canada.**

Description & Sample No.	$\delta^{18}\text{O}$ (‰, SMOW)	Average $\xi^{18}\text{O}$ (‰, SMOW)	$\delta^{18}\text{O}_{\text{H}_2\text{O}}$ (‰, SMOW)	$\delta\text{D}_{\text{H}_2\text{O}}$ (‰, SMOW)		
<b>Quartzites</b>						
PBG-A1	12.8	12.9	$8.1 \pm 0.9^\#$			
PBG-A4	13.5					
PBG-A5	13.5					
PB-632	12.9					
PB-633	12.0					
PBM-A1	13.3					
PBM-A2	12.4					
<b>Pelites</b>						
PB-A11-P1	10.4	10.0	$8.1 \pm 0.5^\#$			
PB-A11-P2	9.7					
PB-A16-P1	10.5					
PB-A17-P1	10.0					
PB-A18-P1	10.2					
KEA-P1	9.5					
<b>Bedding-parallel quartz vein (Type I qtz.)</b>						
PB-A4-1	13.5	14.2	$8.2 \pm 1.4^*$	-124		
PB-A8-1	14.3					
PB-A11-1	14.6					
PB-A16-1	13.3					
PB-A17-1	15.0					
PB-A18-1	14.9					
KEA-1	14.8					
Gam-1	14.8					
<b>Bedding-parallel quartz vein (Type III qtz.)</b>						
PB-A4-3	14.4					-109
PB-A8-3	14.3			-109		
PB-A11-3	13.0					
PB-A15-3	13.6					
PB-A16-3	15.0					
PB-A18-3	14.0					
<b>Discordant veins</b>						
PBG-A5-V1	14.7					
PB-V632	14.7					
PB-V633	14.2					

<sup>#</sup> Calculated using a temperature of 370°C derived from quartz - muscovite geothermometry.

<sup>\*</sup> Calculated using a temperature of 325°C derived from fluid inclusion and sulfur isotope geothermometry

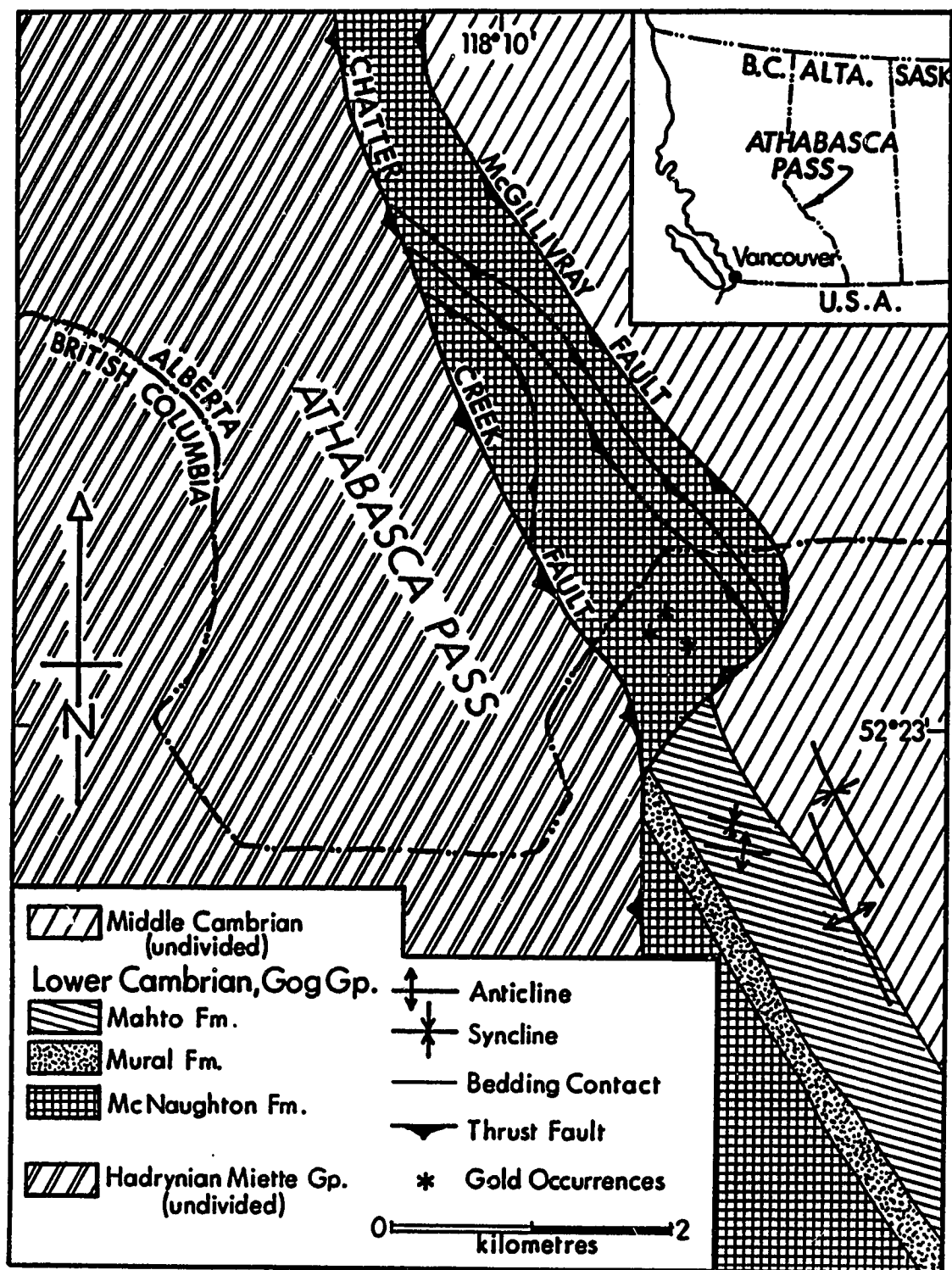


Figure 4-1. Location and general geology of the Athabasca Pass (Modified after Mountjoy and Price, in prep.). Gold occurrences represent clusters of mineralized veins.

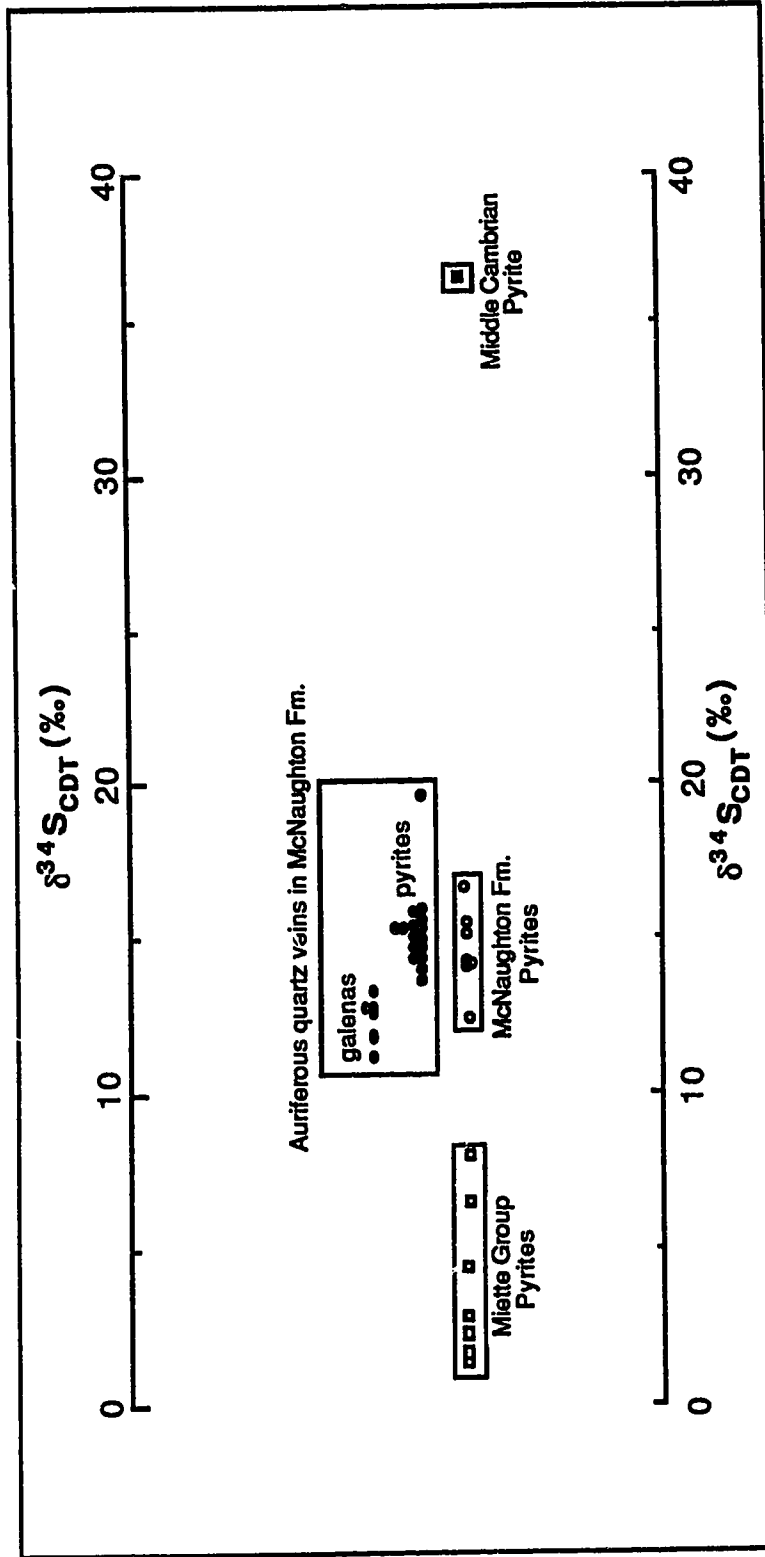


Figure 4-2.  $\delta^{34}\text{S}$  values for sulfides from the various rock types in the Athabasca Pass.

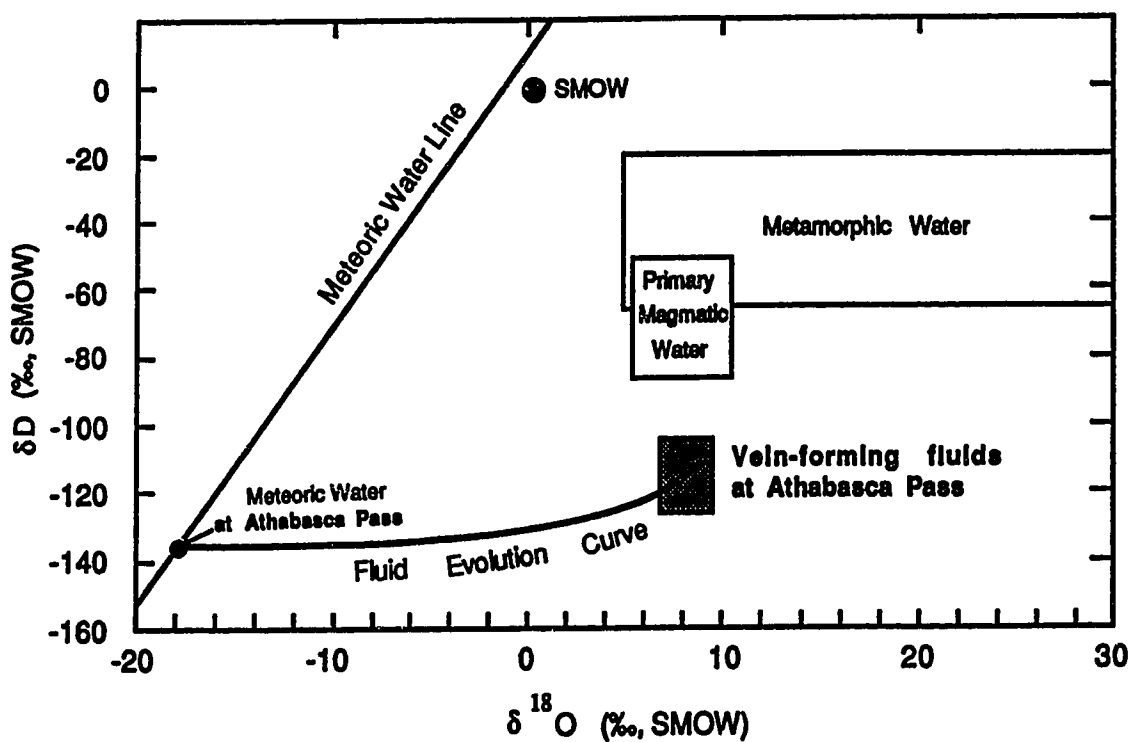


Figure 4-3. Plot of  $\delta D$  vs.  $\delta^{18}O$  of the hydrothermal fluids which generated auriferous quartz veins in the McNaughton Formation at Athabasca Pass. Fluid evolution curve depicts the O- and H-isotope shift of meteoric waters due to water - rock interactions at  $T=350^{\circ}C$  and water to rock ratios of *ca.* 0.1.

## References

- Bachinski, D. 1969 Bond strength and sulphur isotopic fractionation in coexisting sulphides. *Econ. Geol.* 64: 56-65.
- Boyle, R. W. 1979 The geochemistry of gold and its deposits. Geological Survey of Canada, Bulletin 280.
- Clayton, R.N. and Mayeda, T.K. 1963 The use of bromine pentafluoride in the extraction of oxygen from oxides and silicates for isotopic analysis. *Geochimica et Cosmochimica acta.* 27: 43-52.
- Coleman, M.L., Shepherd, T.J., Durham, J.J., Rouse, J.E., and Moore, G.R. 1982 Reduction of water with zinc for hydrogen isotope analysis. *Analytical Chemistry.* 54: 993-555.
- Cox, S.F., Etheridge, M.A., and Wall, V.J. 1986 The role of syn-tectonic mass transport and localization of metamorphic vein-type ore deposits. *Ore Geology Reviews.* 2: 65-86.
- Craig, H. 1961 Isotopic variations in meteoric waters. *Science.* 133: 1702-1703.
- Dansgaard, W. 1964 Stable isotopes in precipitation. *Tellus.* 16: 436-468.
- Field, C.W. and Fifarek, R.H. 1985 Light stable isotope systematics in the epithermal environment. *In Geology and Geochemistry of Epithermal Systems*, B.R. Berger and P.M. Bethke, *Eds.* Reviews in Economic Geology Volume 2: 99-128.
- Friedman, I. and O'Neil, J.R. 1976 Compilation of stable isotope fractionation factors of geochemical interest. *In Data of Geochemistry*, Sixth Edition, M. Fleischer, *Ed.* U.S. Geological Survey, Professional Paper 440-KK: KK1-KK12.
- Graves, M.C. and Zentilli, M. 1982 A review of the geology of gold in Nova Scotia. *In Geology of Canadian gold deposits*, R.W. Hodder and W. Petrak *Eds.* Canadian Institute of Mining and Metallurgy, Special Volume 24: 233-242.

- Hedley, M.S. 1954 Mineral deposits in the southern Canadian Rocky Mountains of Canada. Alberta Society of Petroleum Geologists, Fourth Annual Field Conference Guide Book: 110-118.
- Henley, R.W., Norris, R.J., and Patterson, C.J. 1976 Multistage ore genesis in the New Zealand Geosyncline, a history of post-metamorphic lode emplacement. *Mineralium Deposita*. 11: 180-196.
- Hutchinson, R.W. 1987 Metallogeny of Precambrian gold deposits: space and time relationships. *Econ. Geol.* 82: 1993-2007.
- Keppie, D.J., Boyle, R.W., and Haynes, S.J., *Eds.* 1986 Turbidite-hosted gold deposits. Geological Association of Canada, Special Paper 32.
- Kajiwara, Y and Krouse, H. R, 1971 Sulfur isotope partitioning in metallic sulfide systems. *Can. J. Earth Sci.* 8: 1397-1408.
- Kerrick, R. 1987 The stable isotope geochemistry of Au-Ag vein deposits in metamorphic rocks. *In Short Course in Stable Isotope Geochemistry of Low Temperature Fluids*, T.K. Kyser, *Ed.* Mineralogical Association of Canada. 13: 287-326.
- Kontak, D.J. and Smith, P.K. 1989 Sulphur isotopic composition of sulphides from the Beaver Dam and other Meguma-Group-hosted gold deposits, Nova Scotia: implications for genetic models. *Can. J. Earth Sci.* 26: 1617-1629.
- Little, H.W., Belyea, R., Stott, D. F., Latour, B. A., and Douglas, R. J. W. 1976 Economic minerals of western Canada. *In Geology and economic minerals of Canada*. R. J. W. Douglas, *Ed.* 489-546. Geological Survey of Canada, Economic Geology Report No. 1: 489-546.
- Matsuhisa, Y., Goldsmith, J.R., and Clayton, R.N. 1979 Oxygen isotope fractionation in the system quartz-albite-anorthite-water. *Geochimica et Cosmochimica Acta*. 43.: 1131-1140.
- Mathews, W.H. 1944 Lode-gold deposits: Southeastern British Columbia. British Columbia Department of Mines, Bulletin No. 20, Part 2.



- Mawer, C. K. 1986 The bedding-concordant gold-quartz veins of the Meguma Group, Nova Scotia. *In* Turbidite-Hosted Gold Deposits, J.D. Keppie, R.W. Boyle, and S.J. Haynes, *Eds.* Geological Association of Canada, Special Paper 32:135-148.
- McKeag, S.A., Craw, D., and Norris, R.J. 1989 Origin and deposition of a schist-hosted metamorphogenic Au-W deposit, East Otago, New Zealand. *Mineralium Deposita.* 24: 124-131.
- Mitchell, P.A., Silberman, M.L., and O'Neil, J.R. 1981 Genesis of gold mineralization in an Upper Cretaceous turbidite sequence, Hope-Sunrise District, southern Alaska. U.S. Geological Survey Open-File Report 81-355, p. 34-49.
- Mountjoy, E.W., and Price, R.A. in preparation Athabasca Pass (83D/8) geological map and cross-sections. Geological Survey of Canada.
- Nesbitt, B.E., Murowchick, J.B., and Muehlenbachs K. 1986 Dual origins of lode gold deposits in the Canadian Cordillera. *Geology.* 14: 506-509.
- Nesbitt, B.E. 1988 Gold deposit continuum: A genetic model for lode gold mineralization in the continental crust. *Geology.* 16: 1044-1048.
- Nesbitt, B.E. and Muehlenbachs, K. 1989 Origins and movements of fluids during deformation and metamorphism in the Canadian Cordillera. *Science.* 245: 733-736.
- Nesbitt, B.E. in press Phanerozoic gold deposits in tectonically active continental margins. *In* Gold Metallogeny and Exploration, R.P. Foster *Ed.* Blackie and Sons Ltd. Glasgow.
- Paterson, C.J. 1982 Oxygen isotope evidence for the origin and evolution of a scheelite ore-forming fluid, Glenorchy, New Zealand. *Econ. Geol.* 77: 1672-1687.
- Paterson, C. J. 1986 Controls on gold and tungsten mineralization in metamorphic-hydrothermal systems, Otago, New Zealand. *In* Turbidite-Hosted Gold Deposits, J.D. Keppie, R.W. Boyle, and S.J.

- Haynes, *Eds.* Geological Association of Canada, Special Paper 32: 25-39.
- Price, R.A., and Mountjoy, E.W. 1970 Geological structure of the Canadian Rocky Mountains between Bow and Athabasca Rivers - a progress report. *In* Structure of the Southern Canadian Cordillera, J.O. Wheeler, *Ed.* Geological Association of Canada, Special Paper 6: 7-25.
- Price, R. A., Monger, J. W. H., and Roddick, J. A. 1985 *In* Field Guides to Geology and Mineral Resources in the Southern Canadian Cordillera, D. Templeman-Kluit, *Ed.* Geological Society of America Cordillern Section, Annual Meeting, Vancouver.
- Ohmoto, H. 1986 Stable isotope geochemistry of ore deposits. *In* Stable Isotopes in High Temperature Geologic Processes, J.W. Valley, H. P. Taylor, and J.R. O'Neil, *Eds.* Reviews in Mineralogy. 16: 491-559.
- Ohmoto, H. and Rye, R.O. 1979 Isotopes of sulfur and carbon. *In* Geochemistry of Hydrothermal Ore Deposits, H. L. Barnes, *Ed.* John Wiley and Sons, New York: 509-567.
- Roedder, E. 1984 Fluid Inclusions. Mineralogical Society of America, Reviews in Mineralogy, Volume 12.
- Sandiford, M. and Keays, R.R. 1986 Structural and tectonic constraints on the origin of gold deposits in the Ballarat Slate Belt, Victoria. *In* Turbidite-Hosted Gold Deposits, J.D. Keppie, R.W. Boyle, and S.J. Haynes, *Eds.* Geological Association of Canada, Special Paper 32: 15-24.
- Seccombe, P.K. and Hicks, M.N. 1989 The Hill End goldfield, NSW, Australia - Early metamorphic deposition of auriferous quartz veins. *Mineralogy and Petrology.* 40: 257-273.
- Shelton, K.L. So, C.S., and Chang, J.S. 1987 Gold rich mesothermal vein deposits of the Republic of Korea: geochemical studies of the

- Jungwon gold area. *Econ. Geol.* 83: 1221-1237.
- Sinclair, A.J., Wynne-Edwards, H.R., and Sutherland-Brown, A. 1978 An analysis of distribution of mineral occurrences in British Columbia. British Columbia Ministry of Mines and Petroleum Resources, Bulletin 68.
- Sorensen, M. K. 1955 Some observations on the geology of the Rocky Mountain Trench between latitudes 53° and 53° 30'. Alberta Society of Petroleum Geologists, Fifth Annual Field Conference Guide Book: 53-68.
- Taylor, H.P., Jr. 1979 Oxygen and hydrogen isotope relationships in hydrothermal mineral deposits. *In* *Geochemistry of Hydrothermal Ore Deposits*, H. L. Barnes, *Ed.* New York: John Wiley and Sons: 236-277.
- Tomkinson, M.J. 1988 Gold mineralization in phyllonites at the Haile Mine, South Carolina. *Econ. Geol.* 83: 1392-1400.
- Ueda, A. and Krouse, H. R. 1986 Direct conversion of sulphide and sulphate minerals to SO<sub>2</sub> for isotope analysis. *Geochemical Journal.* 20: 209-212.
- Valley, J.W. 1986 Stable isotope geochemistry of metamorphic rocks. *In* *Stable Isotopes in High Temperature Geologic Processes*, J.W. Valley, H. P. Taylor, and J.R. O'Neil, *Eds.* *Reviews in Mineralogy.* 16: 445-490.
- Weir, H.R. Jr. and Kerrick, D.M. 1987 Fluid inclusion and stable isotope study of several gold mines in the Mother Lode, Tuolumne and Mariposa Counties, California. *Econ. Geol.* 82: 328-344.

## CHAPTER 5

### Concluding Statement

In the preceding chapters, it has been demonstrated that the auriferous veins at Athabasca Pass are typical cases of mesothermal, gold-quartz mineralization in low-grade meta-sedimentary domains. It is evident that a combination of regional- and local-scale controls have contributed to the genesis of these gold-bearing veins. All of these controls will not be reiterated here. However, because of its ubiquitous nature, the role of meteoric water, its involvement in, and implications for, lode gold formation in the Main Ranges of the Rocky Mountains will here be considered further.

As discussed, (Chapters 3 and 4), the marked chemical-isotopic evolution of meteoric waters (*i.e.* addition of dissolved salts, CO<sub>2</sub>, metal-complexes *etc.*) must take place prior to/during mesothermal gold mineralization. Such evolution is the result of fluid - rock interactions, at moderately deep crustal levels, and moderate water to rock ratios. The structural, mineralogical and temporal relationships at Athabasca Pass place some constraints on these processes in the Main Ranges.

It has been established (Chapter 2) that the formation of the Athabasca Pass lodes post-dated both penetrative deformation and peak metamorphism in the Main Ranges. Hence, two major structural-metamorphic events pre-dated mineralization, namely 1) the formation of the large, pre-metamorphic thrust faults which underlie the Main Ranges, and 2) the pre- to syn-metamorphic rise of major antiformal culminations such as the Porcupine Creek Anticlinorium. These earlier events are

considered important as they would have provided a regional scale plumbing system for the pre-metamorphic influx, and subsequent syn- to post-metamorphic chemical (thermal-isotopic) evolution of meteoric waters prior to gold mineralization. During these events, meteoric waters could have penetrated to intermediate crustal levels. Localized equilibration of these fluids with their wall-rocks, and the scavenging of vein components could have taken place as metamorphism progressed. The structural initiation of fluid conduits could also have been induced at this time.

Post-dating metamorphism, structures associated with the development of late, out-of -sequence thrust faults such as the Chatter Creek thrust (*i.e.* dilatant bedding planes, *en echelon* tension fractures, incipient thrust faults) would have provided localized reservoirs for the previously evolved fluids. Other local controls, such as the availability of gold and sulfur, the presence of effective chemical-structural trapping mechanisms, and the existence of temperature -pressure -  $fO_2$  - pH *etc.* conditions conducive to gold precipitation would determine whether or not those veins were auriferous.

Thus, in the broadest sense, the involvement of meteoric waters in lode gold genesis at Athabasca Pass suggests that gold lodes in the Main Ranges may be more widespread than presently recognized. The stratigraphic - structural - lithochemical - and mineralogical controls on gold mineralization at Athabasca Pass, which have been recognized during the course of this study, provide some discriminating guide parameters which may aid in the future exploration for other gold-quartz lodes in the Main Ranges and elsewhere in the Canadian Rocky Mountains.

## **APPENDICES**

**Appendix 1. Results of ICPES multielement analyses of various rock types from the Athabasca Pass**

Sample #	Classification	Au	Ag	As	Pb	Zn	Cu	Ba	Fe(%)	
027	Unmineralized quartzite/conglomerate	*10	0.2	15	4	3	<1	35	0.29	
081		*80	<0.2	<5	<2	2	3	20	0.34	
084		*5	<0.2	<5	<2	3	2	45	0.31	
086		*40	0.2	<5	2	2	3	160	0.48	
105		*15	0.2	5	8	4	2	45	2.46	
603		*5	<0.2	<5	2	4	2	56	0.39	
604		*5	<0.2	<5	2	3	1	60	0.35	
629		*10	0.2	<5	2	4	3	5	0.54	
640		Unmineralized pelite	*85	0.2	<5	8	5	<1	25	2.78
834			*20	<0.2	<5	<2	2	1	35	0.35
601	*5		<0.2	<5	2	10	3	47	3.69	
522	Highly anomalous bedding-parallel veins	26.2	0.4	20	58	4	2	245	1.05	
523		124.8	0.4	20	42	4	3	85	1.27	
524		573.7	8.8	20	42	3	3	250	1.01	
877		41.9	0.2	15	10	3	3	180	1.79	
878		15.8	0.2	5	6	4	2	160	1.86	
906		71.5	0.4	20	28	4	2	25	0.78	
599		14.9	<0.2	<5	21	147	5	21	0.58	
527	Moderately anomalous bedding-parallel veins	*570	0.2	<5	10	2	3	30	0.75	
767		*480	0.2	5	24	1	3	40	0.74	
880		2.9	0.2	15	28	4	2	185	1.60	
907		*440	0.2	20	18	4	2	60	1.17	
908	Brecciated pelitic bedding-parallel vein	*170	<0.2	20	6	4	1	80	1.16	
600		*45	<0.2	5	19	125	1	79	1.76	
602	Discordant vein	*1	<0.2	5	16	20	3	31	0.79	
632		*55	0.2	<5	4	2	3	35	0.42	

All data recorded in parts per million (ppm) except where indicated.  
 \* Indicates parts per billion (ppb).  
 Fe = % total iron.

**Appendix 2. Instrumental neutron activation elemental analysis of vein and country-rock pyrite separates from the Athabasca Pass area: Sample descriptions and results.**

<b>Sample number</b>	<b>Description</b>
PB-A1	Pyrite from auriferous quartz vein on McGillivray Ridge.
PB-A4	Pyrite from auriferous quartz vein on McGillivray Ridge.
PB-A11	Pyrite from auriferous quartz vein on McGillivray Ridge.
PB-A16	Pyrite from auriferous quartz vein on McGillivray Ridge.
PB-A16	Pyrite contained within pelite fragment from auriferous quartz vein on McGillivray Ridge.
PB-A5	Metamorphic pyrite contained within McNaughton Formation quartzite from McGillivray Ridge.
PB-A6	Metamorphic pyrite contained within McNaughton Formation quartzite from McGillivray Ridge.
MB17-A26	Metamorphic pyrite contained within Miette Group grit from Mount Brown.
MB9-A24	Metamorphic pyrite contained within Miette Group pelite from Mount Brown.

**Results**

Sample number	Element		
	Au (ppm)	Ag (ppm)	As (ppm)
PB-A1	93.30	<8	990
PB-A4	16.30	<12	1100
PB-A11	551.00	<13	740
PB-A16	1.95	<14	1800
PB-A16	3.82	<11	2200
PB-A5	2.02	<9	80
PB-A6	0.15	<10	490
MB17-A26	<0.02	<8	550
MB9-A24	0.08	<7	870

Analyses performed by Dr. E.L. Hoffman, Activation Laboratories, Branford, Ontario.



**Appendix 3. Gold content of unmineralized, quartz-dominated McNaughton Fm. rock types of McGillivray Ridge, Athabasca Pass, B.C.**

Sample #	Quartz <sup>1</sup> (%)	White Mica <sup>1</sup> (%)	K-Feldspar <sup>1</sup> (%)	Au <sup>2</sup> (ppb)
026	85-90	10-15	3-5	10
027	95-99	<5	<1	15
028	80-85	15-20	<3	<5
029	90-95	5-10	<3	5
030	65-70	30-35	3-5	5
031	65-70	30-35	3-5	10
032	90-95	5-10	<3	<5
033	45-50	45-50	<3	<5
034	90-95	5-10	3-5	<5
035	95-99	<5	<1	20
036	65-70	30-35	<3	<5
037	50-60	40-50	<3	<5
038	85-90	10-15	<3	<5
039	75-80	20-25	5-10	<5
040	90-95	5-10	<3	<5
041	75-80	20-25	3-5	15
042	75-80	20-25	5-10	5
043	85-90	10-15	<3	10
044	75-80	20-25	5-10	35
045	90-95	5-10	<3	5
046	90-95	5-10	<3	<5
047	90-95	5-10	3-5	5
048	85-90	10-15	3-5	5
049	75-80	20-25	5-7	10
050	80-85	15-20	3-5	10
051	85-90	10-15	3-5	5
052	90-95	5-10	<3	<5
053	85-90	10-15	5-7	<5
054	85-90	10-15	<3	15
055	90-95	5-10	<3	10
076	70-75	25-30	5-10	<5
077	70-75	25-30	<3	<5
078	90-95	5-10	3-5	<5
079	85-90	10-15	<1	75

(Cont)

## Appendix 3. (con't)

Sample #	Quartz <sup>1</sup> (%)	White Mica <sup>1</sup> (%)	K-Feldspar <sup>1</sup> (%)	Au <sup>2</sup> (ppb)
080	75-80	20-25	5-10	<5
081	80-85	15-20	<3	80
082	70-75	25-30	<3	10
083	95-99	<5	<1	10
084	90-95	5-10	3-5	<5
085	80-85	15-20	3-5	15
086	80-85	15-20	3-5	40
087	80-85	15-20	<3	10
088	80-85	15-20	3-5	5
089	90-95	5-10	<3	<5
090	60-65	35-40	5-7	25
091	85-90	10-15	3-5	5
092	85-90	10-15	<3	5
093	90-95	5-10	<3	5
094	75-80	20-25	<3	10
096	70-75	25-30	10-15	20
097	50-60	40-50	<3	25
098	85-90	10-15	3-5	30
099	70-75	25-30	<3	25
100	80-85	15-20	3-5	115
101	75-80	20-25	10-15	10
102	75-80	20-25	5-7	10
103	80-90	10-20	3-5	10
104	90-95	5-10	<3	20
105	85-90	10-15	3-5	15
106	75-80	20-25	3-5	30

<sup>1</sup> Estimated modal percentage of mineral observed in hand specimen.

<sup>2</sup> Determined by atomic absorption spectrometry, detection limit 5 ppb Au.

**Appendix 4. Microthermometric data for Type A fluid inclusions in quartz from auriferous veins on McGillivray Ridge, Athabasca Pass, B.C.**

Sample #	Quartz type	Tm CO2 (°C)	Tm ice (°C)	Wt. % NaCl eq. (Tm ice)	Tm Clath. (°C)	Wt. % NaCl eq. (Tm Clath.)	Th CO2 (°C)	T decrep. (°C)	Th total (°C)	
PB-A2	I	-	-	-	7.9	4.1	-	-	360	
		-	-	-	7.9	4.1	-	-	350	
		-	-5.8	8.9	-	-	-	-	-	251
		-	-4.3	6.9	-	-	-	-	-	205
		-	-4.3	6.9	-	-	-	-	-	280
		-	-4.1	6.6	8.6	2.8	-	-	-	187
		-	-3.8	6.1	8.8	2.4	-	-	-	187
		-	-	-	8.6	2.8	-	-	-	197
		-	-4.5	7.2	8.6	2.8	-	-	-	207
		-	-4.8	7.6	8.6	2.8	-	-	-	215
		-	-3.8	6.1	-	-	-	-	-	233
		-	-4.3	6.9	-	-	-	-	-	253
		-	-	-	-	-	-	-	-	266
		-	-3.3	5.4	8.5	3.0	-	-	-	194
		-	-	-	7.7	4.5	-	281	-	-
PB-A3	I	-	-5.6	8.7	-	-	-	-	320	
		-	-3.8	6.1	-	-	-	-	300	
		-	-3.6	5.8	-	-	-	-	289	
		-	-5.5	8.5	-	-	-	-	304	
PB-A4	I	-	-4.2	6.7	-	-	-	-	235	
		-	-5.1	8.0	-	-	-	-	206	
		-	-5.1	8.0	-	-	-	-	227	
		-	-5.1	8.0	-	-	-	-	225	
		-	-	-	-	-	-	-	222	
		-	-4.2	6.7	8	3.9	-	-	-	-
		-	-3.8	6.1	-	-	-	-	-	225
		-	-5.1	8.0	-	-	-	-	-	244
		-	-4.5	7.2	-	-	-	-	-	231
		-	-4.1	6.6	-	-	-	-	-	251
		-	-	-	-	-	-	-	315	282
		-	-	-	-	-	-	-	315	-
		-	-	-	-	-	-	-	-	307
		-	-5.0	7.9	-	-	-	-	-	315
		-	-7.0	10.5	-	-	-	-	-	283
-	-	-	-	-	-	-	-	287		
-	-5.5	8.5	-	-	-	-	-	287		
PB-A11	III	-	-	-	-	-	-	-	251	
		-	-	-	-	-	-	-	252	
		-	-	-	-	-	-	-	262	
		-	-3.8	5.8	7.5	4.9	-	-	-	308
		-	-5.4	8.4	-	-	-	-	-	281
		-	-3.6	5.8	6.9	5.9	-	-	-	293
		-	-	-	-	-	-	-	215	-
		-	-	-	-	-	-	-	238	-
		-	-	-	7.6	4.7	-	-	-	285
		-	-5.6	8.7	8.2	3.6	20.8	-	-	-
		-	-5.2	8.1	8.3	3.4	-	-	-	-
		-	-5.2	8.1	-	-	-	-	-	-
		-	-4.2	6.7	8.1	3.8	-	-	-	-
		-	-4.7	7.4	-	-	-	-	-	253
		-	-58	-	8.3	3.4	-	177	-	-
PB-A11	I	-	-5.2	8.1	8.3	3.4	-	220	-	
		-	-	-	9.0	2.0	22.1	d	-	
		-	-	-	-	-	-	-	-	

(Con't)

## Appendix 4.(con't)

Sample #	Quartz type	Tm CO2 (°C)	Tm ice (°C)	Wt. % NaCl eq. (Tm ice)	Tm Clath. (°C)	Wt. % NaCl eq. (Tm Clath.)	Th CO2 (°C)	T decrep. (°C)	Th total (°C)
PB-A11 I	-	-5.0	7.9	-	-	-	-	-	241
	-	-4.3	6.9	-	-	-	-	-	257
	-	-4.8	7.6	-	-	-	-	-	264
	-	-4.8	7.6	-	-	-	-	-	305
	-	-	-	-	8.8	2.4	-	-	163
	-	-	-	-	8.1	3.8	-	-	292
	-	-4.8	7.6	-	-	-	-	-	259
	-	-6.0	9.2	-	-	-	-	-	276
	-	-	-	-	3.6	11.2	-	d	-
	-	-	-	-	8.1	3.8	-	-	266
	-	-5.0	7.9	-	-	-	-	248	-
PB-A17 I	-	-4.2	6.7	-	-	-	-	306	-
	-	-4.8	7.8	-	-	-	-	282	-
	-	-	-	-	7.6	4.7	-	176	-
	-	-3.8	6.1	-	-	-	-	196	-
	-	-4.0	6.4	-	-	-	-	228	-
	-	-5.3	8.3	-	-	-	-	-	245
	-	-	-	-	-	-	-	-	250
	-	-5.5	8.5	-	-	-	-	-	252
	-	-5.7	8.8	-	-	-	-	-	-
	-	-5.6	8.7	-	-	-	-	245	-
	-	-5.6	8.7	-	-	-	-	234	-
	-	-6.8	10.2	-	-	-	-	-	250
	-	-6.4	9.7	-	-	-	-	-	265
	-	-	-	-	6.9	5.9	-	-	265
	-	-5.6	8.7	-	8.6	2.8	-	-	270
	-	-5.6	8.7	-	-	-	-	-	267
	-	-5.7	8.8	-	8.1	3.8	-	190	-
	-	-5.8	8.9	-	8.1	3.8	15.7	190	-
	-	-4.8	7.6	-	-	-	-	-	172
PB-30 I	-	-	-	-	-	-	-	-	161
	-	-	-	-	8.1	3.8	-	-	160
	-	-5.3	8.3	-	8.4	3.2	-	190	-
	-	-6.2	9.5	-	7.9	4.1	-	270	-
PB-A31 III	-	-	-	-	7.9	4.1	-	-	258
	-	-5.9	9.1	-	7.8	4.3	-	-	267
	-	-4.1	6.6	-	8.7	2.6	-	-	280
	-	-2.1	3.5	-	8.7	2.6	-	-	223
	-	-4.1	6.6	-	8.2	3.6	-	-	220
	-	-4.2	6.7	-	8.1	3.8	-	-	-
	-	-4.2	6.7	-	8.1	3.8	-	-	-
	-	-3.8	6.1	-	-	-	-	-	245
	-	-	-	-	-	-	-	-	205
	-	-3.4	5.5	-	-	-	-	-	222
	-	-3.2	5.2	-	-	-	-	-	225
	-	-4.1	6.6	-	-	-	-	-	229
	-	-3.7	6.0	-	-	-	-	-	237
	-	-4.1	6.6	-	-	-	-	-	221

d=decrepitated

**Appendix 5. Sulfur-isotope data for country rock and vein sulfide minerals from the Athabasca Pass area, B.C.**

Sample number	Mineral analysed	* Host lithology	$\delta^{34}\text{S}$ ‰, CDT
<b>COUNTRY ROCKS</b>			
PBG-A4	pyrite	McN quartzite	15.3
PBG-A5	pyrite	McN quartzite	12.4
PBG-A5r	pyrite	McN quartzite	11.4
PBG-A5r	pyrite	McN quartzite	12.2
PBG-A5r	pyrite	McN quartzite	12.4
PBG-A5r	pyrite	McN quartzite	11.8
PBG-A5r	pyrite	McN quartzite	11.8
PBG-A6	pyrite	McN quartzite	14.1
PB-A15	pyrite	McN pelite	14.2
PBM-A20	pyrite	McN pelite	14.0
PBP-A3	pyrite	McN pelite	16.9
PBP-A7	pyrite	McN pelite	15.3
PBE-A14	pyrite	MC dolomite	36.7
MBG-A12a	pyrite	MG pelite	3.0
MBG-A12b	pyrite	MG pelite	2.8
MBG-A9	pyrite	MG pelite	1.1
MBG-A16	pyrite	MG pelite	1.5
MBG-A17	pyrite	MG grit	8.9
MBG-A18	pyrite	MG grit	4.3
MBG-A13	pyrite	MG grit	7.1
<b>VEIN SULFIDES from the McNAUGHTON FORMATION</b>			
PBM-A1	pyrite	Type III qtz.	19.9
PBM-A2a	galena	Type I qtz.	12.8
PBM-A2b	pyrite	Type I qtz.	15.8
PBM-A3	galena	Type I qtz.	11.4
PBM-A4	pyrite	Type III qtz.	15.2
PBM-A7	pyrite	Type III qtz.	16.6
PBM-A8	pyrite	Type III qtz.	15.7
PBM-A9	galena	Type I qtz.	12.8
PBM-A10a	pyrite	Type III qtz.	15.1
PBM-A10b	pyrite	Type I qtz.	16.3
PBM-A11a	galena	Type I qtz.	12.8
PBM-A11b	pyrite	Type I qtz.	14.4
PBM-A11c	pyrite	Type III qtz.	15.4
PBM-A12a	pyrite	Type I qtz.	14.7
PBM-A12ar	pyrite	Type I qtz.	15.3
(Cont)			

## Appendix 5 (con't).

Sample number	Mineral analysed	* Host lithology	$\delta^{34}\text{S}$ ‰, CDT
PBM-A16a	pyrite	Type III qtz.	16.3
PBM-A16ar	pyrite	Type III qtz.	15.1
PBM-A16ar	pyrite	Type III qtz.	15.5
PBM-A16b	galena	Type I qtz.	13.3
PBM-A16br	galena	Type I qtz.	14.2
PBM-A16c	galena	Type I qtz.	11.6
PBM-A17a	pyrite	Type II qtz.	14.8
PBM-A17b	pyrite	Type I qtz.	15.0
PBM-A17br	pyrite	Type I qtz.	15.3
PBM-A18a	pyrite	Type III qtz.	15.1
PBM-A18b	pyrite	Type III qtz.	15.0
PBM-A18br	pyrite	Type III qtz.	15.3
PBM-A19	pyrite	Type III qtz.	16.3
PBM-A22	pyrite	Type III qtz.	13.7

**\*Lithologic Abbreviations:**

McN = McNaughton Formation

MC = Middle Cambrian strata

MG = Hadrynian Miette Group strata

Type I qtz. = Paragenetically early bedding-parallel vein quartz

Type II qtz. = Paragenetically late bedding-parallel vein quartz

## APPENDIX 6

## Formulae Used for Fluid Inclusion and Stable Isotope Calculations

## Chapter 2

*Fluid inclusion study*

Calculation of salinity for H<sub>2</sub>O - NaCl-bearing fluid inclusions (Potter *et al.*, 1978):

$$W_s = 0.00 + 1.76958 \theta - 4.2384 \times 10^{-2} \theta^2 + 5.2778 \times 10^{-4} \theta^3 (\pm 0.028)$$

Where;

$W_s$  = weight percent NaCl in solution.

$\theta$  = the freezing point depression of ice, in °C.

Calculation of salinity for H<sub>2</sub>O - NaCl - CO<sub>2</sub>-bearing fluid inclusions (Bozzo *et al.*, 1973):

$$W_s = 15.52023 - 1.02342 (T_{m_{clath}}) - 0.05286 (T_{m_{clath}})^2$$

Where;

$W_s$  = weight percent NaCl in solution.

$T_{m_{clath}}$  = Final melting temperature of clathrate in °C.

## Chapter 3

*Sulfur isotope study*

Sulfur isotope (pyrite - galena) geothermometry (Ohmoto and Rye, 1979):

$$T = ((1.01 \pm 0.04) \times 10^3) + \Delta^{1/2} (\pm 25^\circ)$$

Where;

T = temperature in °Kelvin.

$\Delta$  =  $\delta^{34}\text{S}$  (pyrite) -  $\delta^{34}\text{S}$  (galena).

Calculation of fluid (H<sub>2</sub>S) - pyrite sulfur isotope fractionation (Ohmoto and Rye, 1979):

$$\delta^{34}\text{S} (\text{pyrite}) - \delta^{34}\text{S} (\text{H}_2\text{S}) = ((0.40 \pm 0.08) + T^2) \times 10^6$$

Where;

T = temperature in °Kelvin.

## APPENDIX 6 (con't)

***Oxygen isotope study***

Oxygen isotope (quartz - white mica) geothermometry (Field and Ficarek, 1985):

$$T (^{\circ}\text{K}) = (0.98 \times 10^3) + (\Delta - 0.58)^{1/2}$$

Where;

$$\Delta = \delta^{18}\text{O} (\text{quartz}) - \delta^{18}\text{O} (\text{white mica}).$$

Calculation of fluid - mineral oxygen isotope fractionation:

***Quartz - H<sub>2</sub>O:***

$$\delta^{18}\text{O} (\text{quartz}) - \delta^{18}\text{O} (\text{H}_2\text{O}) = ((3.34 \times 10^6) + T^2) - 3.31 \text{ (Matsuhisa et. al., 1979).}$$

***Muscovite - H<sub>2</sub>O:***

$$\delta^{18}\text{O} (\text{muscovite}) - \delta^{18}\text{O} (\text{H}_2\text{O}) = ((2.38 \times 10^6) + T^2) - 3.89 \text{ (Friedman and O'Neil,}$$

1976).

Where;

$$T = \text{Temperature } (^{\circ}\text{K})$$